



THESIS  
2  
2000



This is to certify that the  
dissertation entitled


**ANALYSIS AND DESIGN OF CLASSES OF TWO-TIME-SCALE  
MULTI-PORT MODELS WITH DERIVATIVE CAUSALITY**

presented by

*Ahmed Abdelaziz Omara*

has been accepted towards fulfillment  
of the requirements for

PhD                      Mechanical Engineering  
\_\_\_\_\_ degree in \_\_\_\_\_

  
Major professor

Date 8/28/00

**PLACE IN RETURN BOX** to remove this checkout from your record.  
**TO AVOID FINES** return on or before date due.  
**MAY BE RECALLED** with earlier due date if requested.

DATE DUE	DATE DUE	DATE DUE

**ANALYSIS AND DESIGN OF CLASSES OF TWO-TIME-SCALE  
MULTI-PORT MODELS WITH DERIVATIVE CAUSALITY**

By

**Ahmed Abdelaziz Omara**

**A DISSERTATION**

Submitted to  
Michigan State University  
in partial fulfillment of the requirements  
for the degree of

**DOCTOR OF PHILOSOPHY**

Department of Mechanical Engineering

2000



## **ABSTRACT**

### **ANALYSIS AND DESIGN OF CLASSES OF TWO-TIME-SCALE MULTI-PORT MODELS WITH DERIVATIVE CAUSALITY**

By

Ahmed Abdelaziz Omara

Eliminating derivative causality by inserting parasitic elements produces modified systems that are two-time-scale. The computational accuracy and simulation efficiency of the solution of the modified systems are strongly influenced by the choice of the inserted parasitic element parameters. Computational accuracy can be traded off with simulation efficiency. Some important aspects of the nature and behavior of the modified two-time-scale systems have not been investigated. In addition, there is no known method that shows how to choose the values of the parasitic parameters to achieve certain desired accuracy at a highly efficient computational price. Tools based on the singular perturbation method, on physical systems modeling, and on numerical simulation are used in this research to analyze and design some classes of these two-time-scale modified systems.

Analysis revealed some important aspects of the nature and behavior of the systems under investigation. Understanding those aspects is extremely important for the general understanding of these systems. A choice for the perturbation parameter  $\varepsilon$  that helps to reveal the time-scale properties of the modified system is given; a suggested preferred standard singular perturbation

form (PSSPF) is shown; a systematic method to transform the modified systems to the PSSPF is derived; models of the fast sub-systems are obtained and validated; and proof of stability of such a modified system is shown.

The results of the analysis efforts are used to set procedures to design the fast sub-systems. The design objective is to achieve certain desired accuracy at highly efficient computational efforts. The validated models of the fast sub-systems are used in the design procedures. Examples that demonstrate the usefulness of these procedures are presented. Analysis and design work shown here include classes from both linear and nonlinear systems.

**To my parents**

## **ACKNOWLEDGEMENTS**

For my parents, completing this degree comes in partial return on the many investments they have made down a long road; and in partial fulfillment of some of their dreams. Their relentless support and dreams contributed a major thrust to my drive throughout my life.

I would like to acknowledge the continuous support I received from Dr. Ron Rosenberg, the chairman of my Ph. D. committee, since I joined MSU. In particular, I indeed appreciate the quality time and thoughts that he regularly shared with me. It is a fact that my main motive to join MSU was joining Dr. Rosenberg's program. The other important and necessary role for shaping and guiding these research efforts was Dr. Hassan Khalil's. I am indebted to him for the help he has given to these research efforts. He has never hesitated to assign a slot from his time to strengthen these efforts. If there were a co-chairman post for my Ph. D. committee he would have earned it without any doubt. Between him and Dr. Rosenberg, I enjoyed a very precious access to some unique blend of expertise. I would also like to thank my other committee members, Dr. Mukherjee, Dr. Newhouse, Dr. Rohde, and Dr. Radcliffe for their important role in guiding and sharpening these research efforts.

Last but not least, I would like to thank my wife, Manal, for her patience and understanding during some extremely busy times.

## TABLE OF CONTENTS

<b>CHAPTER 1</b>	
<b>INTRODUCTION .....</b>	<b>1</b>
1.1 Mathematical Modeling of Mechatronic Systems .....	1
1.2 Multiport Modeling of Mechatronic Systems .....	2
1.3 Some Equation Formulation Issues in Mechatronic Modeling .....	7
1.4 Problem Statement and Research Objectives .....	9
1.5 Dissertation Outline.....	11
 <b>CHAPTER 2</b>	
<b>ANALYSIS OF A CLASS OF TWO-TIME-SCALE MULTIPORT MODELS .....</b>	<b>13</b>
2.1 Singular Perturbation Method and Two-Time-Scale Systems.....	13
2.1.1 Some Important Issues Related to Using the SP Method .....	13
2.1.2 Additional Remarks on the Standard SP Form.....	16
2.2 Classes of Bond Graph Models Under Investigation .....	17
2.3 Related Work .....	20
2.3.1 The Algorithm Under Investigation .....	20
2.3.2 Other Related Work.....	23
2.4 Determining the Appropriate Perturbation Parameter.....	25
2.4.1 Physical-System-Modeling-Based Analysis .....	26
2.4.2 Simulation-Based Analysis.....	28
2.5 Finding the Standard Singular Perturbation Form.....	37
2.5.1 Using Transformation Procedures to Obtain PSSPF.....	38
2.5.2 A Transformation to Obtain the PSSPF.....	50
2.5.2.1 Derivation and Proof of Existence.....	53
2.5.2.2 Example of Using the Transformation Matrix.....	55
 <b>CHAPTER 3</b>	
<b>DESIGN OF A CLASS OF TWO-TIME-SCALE MULTIPORT MODELS .....</b>	<b>61</b>
3.1 Introduction .....	61
3.2 A Model for the Fast Sub-System and Proof of Stability .....	61
3.3 Validating the Fast Sub-System Model .....	66
3.3.1 Accuracy of Slow and Fast Poles Locations.....	67
3.3.2 Conditions of Two Critically Damped Fast Poles.....	75
3.3.2.1 Advantages of Critically Damped Fast Poles.....	79
3.3.3 Effect of Selected Dependent Element Value on Model Performance	81
3.4 An Algorithm to Improve the Model Performance .....	84
3.5 Design Procedures for the Fast Sub-System .....	88
 <b>CHAPTER 4</b>	
<b>ANALYSIS AND DESIGN OF A CLASS OF TWO-TIME-SCALE NONLINER MULTIPORT MODELS.....</b>	<b>96</b>
4.1 Introduction .....	96

4.2 Class of Nonlinear Systems Under Investigation .....	96
4.3 Obtaining the PSSPF .....	98
4.4. A Model for the Fast Sub-System and Proof of Stability .....	102
4.5 Effect of Inaccurate Effective Field Value on Model Performance .....	106
4.6 Design Procedures for the Fast Sub-System.....	111
4.7 An Example .....	114
CHAPTER 5	
CONCLUSIONS .....	123
5.1 Summary of Main Contributions.....	123
5.2 Suggested Directions for Future Research .....	126
5.2.1 More than One Dependent Element.....	126
5.2.2 Analysis and Design for Eliminating Algebraic Loops.....	127
REFERENCES .....	128

# **CHAPTER 1**

## **INTRODUCTION**

### **1.1 Mathematical Modeling of Mechatronic Systems**

Mathematical modeling is becoming more and more an important step in design, analysis and development of engineering systems. See, for example, Chang and Rohde, 1996. There are two main reasons for this phenomenon. (1) Global competition produced a need to reduce time-cycle and related cost of product design and development. (2) The continuous improvement of computer support, in terms of both the cost and the capability, makes CAE more effective. Therefore, mathematical modeling is increasingly perceived in the industry as an investment that is necessary to survive in a competitive environment. There are many research and development efforts focused on developing new tools to aid engineers in the abstraction, mathematical formulation, and analysis processes of product design.

Engineering systems have become increasingly complex and interdisciplinary. Typically, a variety of components are linked together, including control sub-systems and imbedded "intelligence" to form a system. In 1967 Yasakawa Electric America (a Japanese company) coined the term "mechatronics" to refer to systems that combine mechanisms, electronics, and control (Tomkinson et al. 1996). The term was coined by combining the words "mechanics" and "electronics" (Auslander et al. 1996). Currently there are

several common definitions for the term, with perhaps more underway. However, there is a common understanding that continues to be associated the term. It is the interaction among different physical sub-systems such as mechanical, electrical, magnetic, hydraulic, pneumatic, and thermal, with electronics, control, and imbedded intelligence. For such systems, the multiport approach is seen as a suitable modeling environment (Cellier, 1992; Cellier 1995; Karnopp et al., 2000).

## **1.2 Multiport Modeling of Mechatronic Systems**

Physical sub-systems with one or more ports are called multiports (Karnopp et al. 2000). Ports are places at which power can flow among the sub-systems. As indicated above, mechatronic systems include signal coupling in addition to the power coupling. Bond graph is a modeling environment that consists of elements/sub-systems linked together by power bonds. A bond graph shows power coupling and describes the exchange of energy in a system. Each bond in a bond graph, in general, implies the existence of a pair of signals flowing in opposite directions. The two signals are the flow signal and the effort signal. As multiports essentially transmit finite power when interconnected, which requires the existence of a flow variable and an effort variable, bond graph is a very efficient way to model multiports. Figure 1.1 shows a simple hydraulic system and its bond graph model (from Rosenberg et al. 1983). On the other



hand, block diagrams are efficient in modeling signal coupling. Therefore, block diagram can be combined with bond graph to model mechatronic systems.

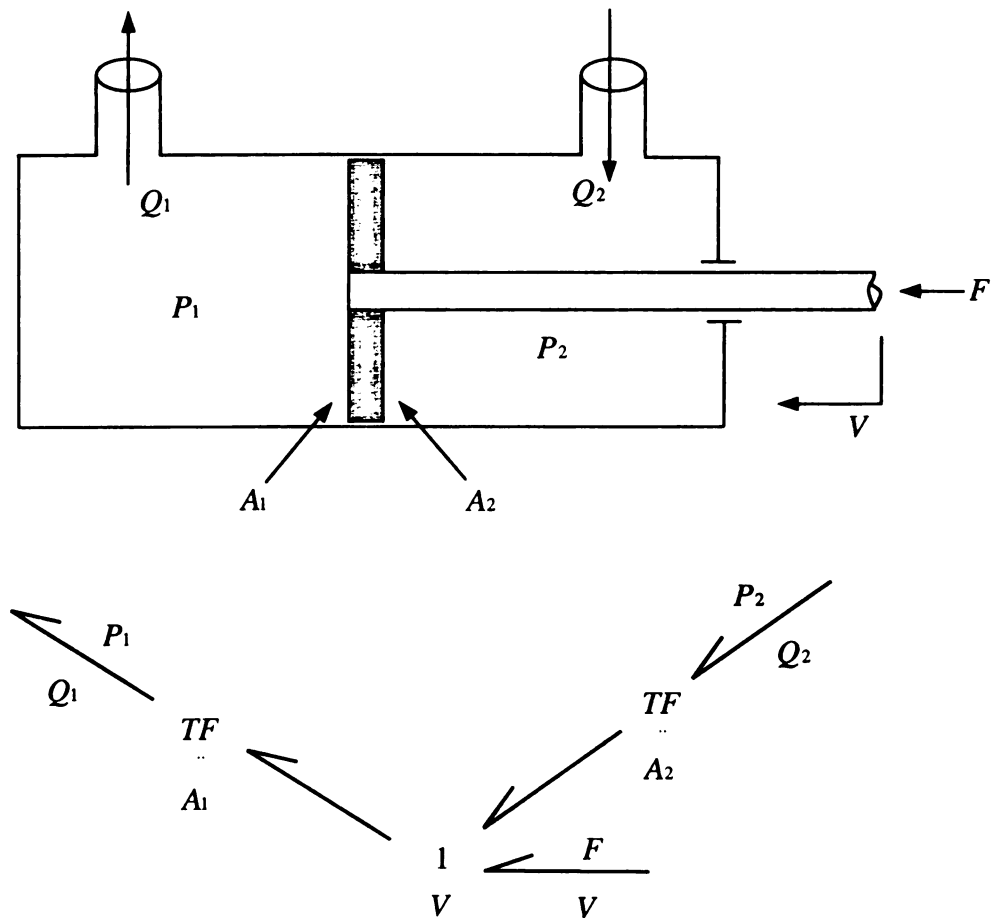


Figure 1.1. A hydraulic cylinder and its bond graph model

The main reasons why the bond graph is valuable as a modeling environment for mechatronic systems are

- 1) It provides a unified graphical representation for multiport modeling regardless of the physical domain type. This makes the bond graph especially valuable for systems containing transducers.
- 2) It provides tools to perform graphical analysis that provide insight to the user efficiently.
- 3) It enables algorithmic equation formulation that is suitable for computer implementation. This leads to an efficient and error-free formulation of system equations for large and complex models (Rosenberg et al., 1983; Cellier, 1992; Cellier 1995; Karnopp et al., 2000).

The literature includes many examples of using bond graphs to gain insight into the dynamics of systems and to reveal some of their structural properties. To mention a few examples, Sueur and Dauphin-Tanguy (1989, 1991) present necessary and sufficient conditions for structural controllability/observability of linear systems represented by bond graphs. Rosenberg and Zhou (1988) proposed a power-based tool for visualizing the dynamic response of engineering systems in bond graph form. They showed that the power response of dynamic systems could be used as a basis for model order reduction under some conditions. In particular, they used the RMS power levels in a bond graph model to determine the weakest power connections in the model. These bonds became candidates for elimination to reduce the model order. The tool is suitable for handling both linear and nonlinear systems. Rosenberg (1987) discusses several applications of causality in understanding

the dynamic structure of models, such as revealing the presence of algebraic couplings. Zeid and Rosenberg (1986) show that, by transforming a bond graph model of a linear time invariant system to a canonical form, the gyrobondgraph, inspection of the resulting graph structure reveals various properties of the system eigenvalue spectrum. Dauphin-Tanguy and Borne (1985) show that the fast and slow dynamics of bond graph models can be estimated by determination of causal loop-gains. They used this result in model order reduction of multi-time-scale systems. The powerful analysis tools, great insight, and the computer-aided enabling environment offered by the bond graph give it a decisive advantage as an engineering modeling environment. Consequently, numerous research efforts are devoted to addressing issues that arise in the bond graph environment. This effort is among them; it is dedicated to addressing the derivative causality issue.

The literature also provides many examples of algorithmic formulation of system equations from bond graph models. A variety of algorithms to obtain formulations for different physical domains have been proposed (Karnopp et al., 1990). That includes obtaining the preferred formulation for certain classes of problems such as the Lagrange Formulation for non-linear mechanics (Karnopp 1977, 1978). One can proceed algorithmically from a bond graph model to a set of *fundamental equations* or to different sets of *secondary equations*. A set of equations representing a system is called a fundamental set if it preserves all of the structural information about the system. Otherwise, the set of equations is

called a secondary set. Structural information depends only on the system's topology and the nature of its components. Structural information does not depend on the numerical values of the parameters of the system elements. As an example, consider an electrical circuit. A set of fundamental equations is obtained by applying the volt-current relation for every element in the circuit, Kirchhoff's current law, and Kirchhoff's voltage law. The state equations, the nodal equations, and the mesh equations are three different sets of secondary equations. While it is usually straightforward to proceed from a set of fundamental equations to different sets of secondary equations, the case is different if you try to proceed from a set of secondary equations to another set of secondary equations. Karnopp (1983) points out that the bond graph is unique in providing a mechanism for demonstrating causal interactions among different components and sub-models; therefore, studying alternative equation formulations becomes easier. He describes how different causal patterns can lead to different equation formulations for the same dynamic system. Because the procedures offered in the bond graph environment are algorithmic, they can be computerized. ENPORT is one example of a software package that implements bond graph procedures (Rosenberg and Karnopp 1983). The author views the bond graph as a basic physical model representation that can lead to a variety of equation formulations and analysis methods.

### 1.3 Some Equation Formulation Issues in Mechatronic Modeling

A typical equation formulation goal is to obtain the standard explicit state space form

$$\frac{dX}{dt} = f(X, U, t) \quad (1.1)$$

Where,  $X$  is the vector of independent state variables,  $t$  is time, and  $U$  is the input vector. However, systems could have two different types of couplings effects that may prevent this form from being attainable. The first is the so-called “algebraic coupling.” The resulting equations have the general (functional) form

$$\frac{dX}{dt} = f(X, H, U, t) \quad (1.2)$$

$$0 = g(X, H, U, t) \quad (1.3)$$

where  $H$  is the coupling vector. The second type of coupling that may prevent the realization of the explicit state space form is “energy-variable coupling.” The resulting equations have the general (functional) form

$$\frac{dX_i}{dt} = f(X_i, \frac{dX_d}{dt}, U, t) \quad (1.4)$$

$$X_d = \bar{\varphi}(X_i, U, t) \quad (1.5)$$

Where,  $X_i$  is the vector of independent state variables,  $X_d$  is the vector of dependent state variables. Of course it is possible for both types of couplings to exist in the same model. The energy-variable coupling is known as “derivative causality” in bond graph terms (Rosenberg et al. 1983). This research effort is

related to alleviating the effect of the derivative causality for some classes of dynamic systems. A definition for these classes will be provided later; equations (1.4) and (1.5) define only a functional form.

Equations (1.2) and (1.3) and equations (1.4) and (1.5) are two implicit sets of differential equations. They can be converted to explicit sets by algebraic manipulation if the system is linear. If the number of coupled elements is greater than two or three, the algebra may become cumbersome. If the system is nonlinear the algebraic manipulation might be very difficult or even impossible (Rosenberg et al., 1983; Karnopp et al., 2000). When one applies an integration formula to a set of differential equations, the result will be an explicit set of difference equations only if both the integration formula and the set of differential equations are explicit. Otherwise, the result will be an implicit set of difference equations. Therefore, integrating an implicit set of equations such as the set given by equations (1.4) and (1.5), is an implicit-integration problem, regardless of the type of the integration formula used. Implicit integrators are generally computationally more involved than explicit integrators (Bennett, 1995). However, the computational cost is not the major reason why we usually do not prefer the presence of derivative causality. The following section includes a summary on why we do not prefer the presence of derivative causality.

## **1.4 Problem Statement and Research Objectives**

As stated above, bond graph models with derivative causality produce mathematical models with algebraically coupled derivative terms. Some times it is preferable to eliminate the derivative causality, and consequently to enable an algorithmic derivation of an explicit ordinary differential equations (ODEs) model.

The main reasons for preferring explicit ODEs are:

- 1) to take advantage of many control algorithms that are available for systems expressed in the explicit ODEs form (Turner & Zeid, 93; Krishnaswami, 93);
- 2) to take advantage of the standard CAD control packages that can algorithmically linearize, analyze, and synthesize controllers for dynamic systems (Turner & Zeid, 93; Krishnaswami, 93);
- 3) to take advantage of easy and error-free automated formulation of dynamic multiport equations (Rosenberg, 71; Karnopp, 79; Zeid, 88);
- 4) to obtain a more parallelizable set of equations, for computation on parallel processors (Turner & Zeid, 93; Krishnaswami, 93).

In addition, this work shows that the derived set of explicit ODEs might require less computational effort to integrate, compared with the original implicit set, even if the explicit state-space order is increased as compared to the original model.

There are two common ways to eliminate the effect of the derivative causality. The first is to obtain an equivalent expression for the behavior of the variables. This approach guarantees that all responses' behavior match exactly those of the original model; except for the internal details of the coupled subsystem. This approach needs some algebraic manipulation that might be difficult or impossible if the system is nonlinear. For these cases where the algebraic manipulation is not preferable/possible the second way becomes an attractive option. In the second way, some parasitic elements are inserted to break the coupling, and consequently eliminate the derivative causality.

Karnopp and Margolis (1979) showed a method to eliminate derivative causality in bond graph models. It breaks the coupling between the coupled energy storing elements by inserting parasitic elements into the original model. Consequently, a modified model that approximates the original model is produced. This modified model is supposed to be a two-time-scale (stiff) model so that the dynamic behavior of the original state variables would not be greatly affected (Karnopp et al., 1979; Zeid, 1988; Zeid, 1989). This approach is the approach being investigated in this research work. The choices of the inserted parasitic elements' values directly affect both computational efficiency and approximation accuracy; approximation accuracy can be traded off with the system stiffness. In general, there are some important aspects of the nature and the behavior the modified two-time-scale system that have not been investigated in detail. In addition, there is no known method or algorithm to show the user



how to choose the values of the inserted parasitic parameters to achieve high computational efficiency while satisfying certain desired accuracy.

This research work has two main objectives:

- 1) Analyze the class of two-time-scale modified systems that results from using the above-mentioned approach to eliminate the derivative causality. The purpose of this analysis is to better understand the important two-time-scale properties of that class of two-time-scale systems.
- 2) Formalize the above-mentioned approach of using parasitic elements to eliminate the derivative causality in a design context. The purpose of this formalization is to enable the user to achieve the greatest possible simulation efficiency for specified approximation accuracy, by making the appropriate choices for the values of the parasitic elements parameters.

A description of the classes of dynamic systems for which this research effort will be conducted will be defined later.

## **1.5 Dissertation Outline**

CHAPTER 2 starts by briefly discussing the usefulness of the singular perturbation method for analysis and design of two-time-scale systems. Then, the classes of bond graph models for which these research efforts will be conducted are defined. This is followed by a brief review of related work with more emphasis on the bond-graph-based methods for eliminating derivative

causality. The last two sections of CHAPTER 2 show how to determine the appropriate perturbation parameter  $\varepsilon$  for the classes of modified systems under investigation; and how to use this perturbation parameter to transform them to the standard singular perturbation form. A preferred standard singular perturbation form (PSSPF) is shown and the transformation needed to obtain it directly from the modified systems equations is derived. CHAPTER 3 carries on the results of CHAPTER 2, and shows some procedures to design the fast sub-system. First a model for the fast sub-system is derived and validated; and the stability of the modified system is demonstrated. An algorithm to improve the model performance is shown, before the design procedures are given. An example demonstrating the usefulness of the design procedures is included. Nonlinear systems are studied in CHAPTER 4. Therein, a class of nonlinear systems is defined. Then, obtaining the PSSPF is shown and a model of the fast sub-system is derived. Stability of the modified system is also proved. The chapter concludes by giving some procedures to design the fast sub-system of the class of nonlinear systems under investigation, with an example demonstrating the usefulness of the design procedures. CHAPTER 5 gives a summary of the main contributions and suggests some future research directions.

## **CHAPTER 2**

### **ANALYSIS OF A CLASS OF TWO-TIME-SCALE MULTI-PORT MODELS**

#### **2.1 Singular Perturbation Method and Two-Time-Scale Systems**

It was stated in CHAPTER 1 that the algorithm, for eliminating the derivative causality, under investigation breaks the coupling between the coupled energy storing elements by inserting parasitic elements into the original model. It was also stated that a modified model that approximates the original model is produced; and that this modified model is supposed to be a two-time-scale (stiff) model so that the dynamic behavior of the original state variables would not be greatly affected (Karnopp et al., 1979; Zeid, 1988; Zeid, 1989). The singular perturbation method has proved to be very useful in analysis and design of multi-time-scale dynamic systems (Kokotovic et al., 1976; Khalil, 1986; Kokotovic et al., 1986). It decomposes a two-time-scale system into a slow and a fast sub-systems by assuming a small singular perturbation parameter approaching zero. Tools to analyze the slow and the fast sub-models and the interrelation between them are available. For these reasons the singular perturbation (SP) method will be used (among other tools) in this research work.

### 2.1.1 Some Important Issues Related to Using the SP Method

There are two important issues related to the use of SP method. These two issues can be defined as (1) the determination of the “appropriate” perturbation parameter ( $\varepsilon$ ). (2) Transforming a singularly perturbed model to the standard singular perturbation form. Solving the first issue is a pre-request for solving the second one. This sub-section will briefly discuss these issues; later in this chapter, they will be dealt with so that the singular perturbation method can be of useful use to the problem under investigation.

Although the singular perturbation theory has seen significant developments, and has many applications; theory users have a major concern. The time-scale separation is not always, easily detectable. In many situations, a good understanding of the physical process is needed to detect the separation, and to choose the perturbation parameter(s) (Kokotovic et al., 1986) and (Sueur, 1991). Choosing the “appropriate” perturbation parameter is usually crucial to the usefulness of singular perturbation analysis. This task becomes more difficult when the system involved is complex. In addition, the perturbation parameter of a two-time-scale system does not have to be unique; there might be several possible perturbation parameters.

The general form of the standard singular perturbation model is

$$\dot{X} = f(X, Z, \varepsilon, t), \quad X(t_0) = X^0, \quad X \in R^n, \quad (2.1)$$

$$\varepsilon \dot{Z} = g(X, Z, \varepsilon, t), \quad Z(t_0) = Z^0, \quad Z \in R^m \quad (2.2)$$

where;  $\varepsilon$  is a small positive scalar; a superscript dot denotes a time derivative; and  $f$  and  $g$  are functions that are assumed to be sufficiently several times continuously differentiable. This model is the most studied SP model in the literature and the first one to be used in control and systems theory (Kokotovic et al., 1986). Consequently, numerous analysis and design tools are available for two-time-scale systems that are in the standard form (2.1) and (2.2). Of course, expressing the model in the standard form is not going to change any thing in the system's time-scale properties; but it is going to reveal them. In contrast, a singularly perturbed model that is not in the standard form might hide its time-scale properties. Even though, there are procedures to help transform a two-time-scale system from a non-standard form to the standard form; these procedures are general and their outcome is not unique.

Zeid (1988 and 1989) suggested that the modified systems that result from removing derivative causality by inserting parasitic elements could be transformed to a standard singular perturbation form. He also noticed that once a standard form is reached the singular perturbation theory tools could be conveniently used. However, there was no method defined to show how to transform the system and consequently, there was no attempt made to use the singular perturbation analysis tools.

The objectives of the work reported in this chapter are

- (1) To introduce a choice for the singular perturbation parameter ( $\varepsilon$ ) that helps reveal the two-time-scale properties of the class of modified systems under investigation.
- (2) To show how the general procedure outlined in Kokotovic et al. (1986) for transforming singularly perturbed models to the standard form can be used to obtain a preferred standard singular perturbation form (PSSPF) and to gain insight into the problem under investigation.
- (3) To define the transformation needed to obtain that PSSPF.

### 2.1.2 Additional Remarks on the Standard SP Form

When  $\varepsilon$  is set to zero, equation (2.2) reduces/degenerate to the algebraic equation

$$0 = g(\bar{X}, \bar{Z}, 0, t) \quad (2.3)$$

The bar in  $\bar{X}$  and  $\bar{Z}$  indicates that the variables belong to a system with  $\varepsilon = 0$ .

Model (2.1) and (2.2) will be said to be in the standard form iff (2.3) has  $k \geq 1$  distinct real roots

$$\bar{Z} = \bar{\phi}_i(\bar{X}, t), \quad i = 1, 2, \dots, k. \quad (2.4)$$

This assumption ensures that each root of (2.4) will correspond to a well-defined n-dimensional reduced model that can be obtained by substituting (2.4) into (2.1).

The  $i$ th reduced model would be

$$\dot{\bar{X}} = f(\bar{X}, \bar{\phi}_i(\bar{X}, t), 0, t), \quad \bar{X}(t=0) = X(t=0) \quad (2.5)$$

Notice that the initial conditions of  $\bar{X}$  are the same as those of  $X$ . The model (2.5) is called a quasi steady state model because when  $\varepsilon$  is small  $Z$  will converge rapidly to the solution of (2.3), (Kokotovic et al., 1986). It has been shown in the literature (Kokotovic et al., 1986; Khalil, 1986; Kokotovic et al., 1976) that, for a small  $\varepsilon$  and a stable system

$$X(t) - \bar{X}(t) = O(\varepsilon), \quad t \geq 0 \quad (2.6)$$

and, in addition,

$$Z(t) - \bar{Z}(t) = O(\varepsilon), \quad t > 0 \quad (2.7)$$

## 2.2 Classes of Bond Graph Models Under Investigation

The classes of bond graph models under investigation in this research effort are the classes that can be represented using the basic bond graph set  $S_1 = \{\underline{C}, \underline{I}, \underline{R}, S_e, S_f, TF, GY, 0, 1\}$ . The basic set  $S_1$  includes multiport capacitances, multiport inertances, multiport dissipations, sources of effort, sources of flow, displacement-modulated transformers, displacement-modulated gyrators, 0-junctions, and 1-junctions. The general homogeneous mathematical form for the derivative causality that occurs in these classes of bond-graph models can be expressed in equations (2.8) to (2.11). This form assumes that the model does not include algebraic loops that are not separable from the derivative causality.

$$\dot{X}_i = J_{ii}(X_i) * Z_i + J_{id}(X_i) * \dot{X}_d \quad (2.8)$$

$$Z_d = J_{di}(X_i) * Z_i \quad (2.9)$$

$$Z_i = \varphi_1(X_i) \quad (2.10)$$

$$X_d = \varphi_2(Z_d) \quad (2.11)$$

Where, the  $J$  matrices are the constraints imposed by the junction structure between sets of ports; they are in general nonlinear.  $X_i$  is the independent energy variables vector,  $X_d$  is the dependent energy variables vector,  $Z_i$  and  $Z_d$  are the coenergy vectors for  $X_i$  and  $X_d$  respectively,  $U$  is the sources input vector; and  $\varphi_1$  and  $\varphi_2$  are generally nonlinear functions, Rosenberg (1971), van Dijk (1994). Throughout this document the dimension of  $X_d$  will be one. The above general formulation allows non-linearity in both the fields and junction structure. If the fields and junction structure are both linear, the fields' relations and the junction structure matrices will become linear. Consequently, the junction matrices will no longer be function of the independent state vector  $X_i$ . The general mathematical form of these classes of linear systems can be written as follows.

$$\dot{X}_i = J_{ii} * Z_i + J_{id} * \dot{X}_d \quad (2.12)$$

$$Z_d = J_{di} * Z_i \quad (2.13)$$

$$Z_i = S_i * X_i \quad (2.14)$$

$$X_d = S_d^{-1} * Z_d \quad (2.15)$$



Rosenberg (1971) has also shown that  $J_{id}$  and  $J_{di}$  are one another's negative transpose. If  $Z_d$  and  $Z_i$  are eliminated, the linear general mathematical form will simplify to

$$\dot{X}_i = J_{ii} * S_i * X_i + J_{id} * \dot{X}_d \quad (2.16)$$

$$S_d * X_d = J_{di} * S_i * X_i \quad (2.17)$$

Zeid's proposed algorithm is supposed to be implemented in the bond graph environment. Actually, facilitating the automated derivation of an explicit set of equations is one of the main reasons for using his algorithm. However, since this work includes analysis and design of the modified systems that are produced from this algorithm, it is necessary to show the general mathematical form for these modified systems. If the original system is in the form (2.16) and (2.17) the homogeneous modified system will be in the general form (2.18) to (2.20).

$$\dot{X}_i = J_{ii} * S_i * X_i + J_{id} * (K_p * q + R * (J_{di} * S_i * X_i - S_d * X_d)) \quad (2.18)$$

$$\dot{X}_d = K_p * q + R * (J_{di} * S_i * X_i - S_d * X_d) \quad (2.19)$$

$$\dot{q} = J_{di} * S_i * X_i - S_d * X_d \quad (2.20)$$

Where,  $K_p$  and  $R$  are the inserted parasitic stiffness and resistance respectively;  $q$  is the flow variable in the inserted parasitic elements. In these research efforts we will study systems with one derivative causality per storage field. Of course using the algorithm is not limited to linear systems only. First linear systems that can be expressed in the general form (2.16) and (2.17) and whose modified systems are in the general explicit form (2.18) to (2.20) will be studied. Then, in CHAPTER 4, a class of nonlinear systems will be studied.

## **2.3 Related Work**

Because the method of eliminating the derivative causality under investigation here is bond-graph-based, this section will discuss only the bond-graph-based methods to eliminate the derivative causality. Examples of the other methods include the kinematics-based work of Allen (1981) to obtain explicit ODEs; the work of Gordon et al. (1998) to convert systems of ADEs to ODEs; and the work of Borutzky and Cellier (1996a and 1996b) which partition (tear) the resultant ADEs from the bond graph using symbolic manipulation for a more efficient solution. Presentations of the bond-graph-based methods will be very brief except for the method that is under investigation in this research work.

### **2.3.1 The Algorithm Under Investigation**

This research work is a continuation of the method for eliminating derivative causality demonstrated by Karnopp-Margolis (1979) and generalized and automated by Zeid (1988). In 1979 Karnopp and Margolis demonstrated a method to eliminate the derivative causality in bond graph models of planar mechanisms. The method eliminates the derivative causality by inserting parasitic damping and parasitic stiffness. Zeid (1988) showed an algorithm to generalize and automate the method demonstrated by Karnopp and Margolis. Zeid summarized his proposed algorithm as shown in Figure 2.1 to Figure 2.4.

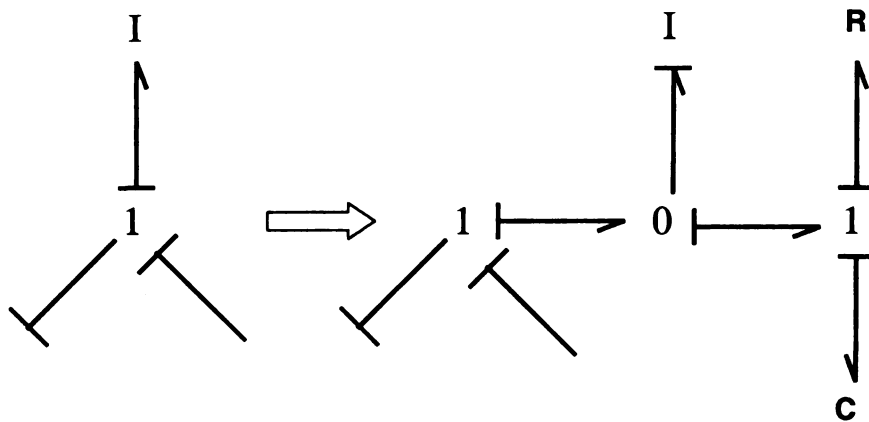


Figure 2.1. Handling an inductance that is attached to a 1-junction

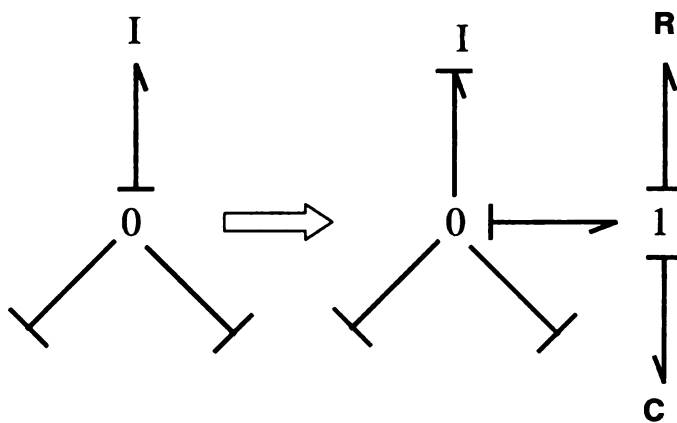


Figure 2.2. Handling an inductance that is attached to a 0-junction

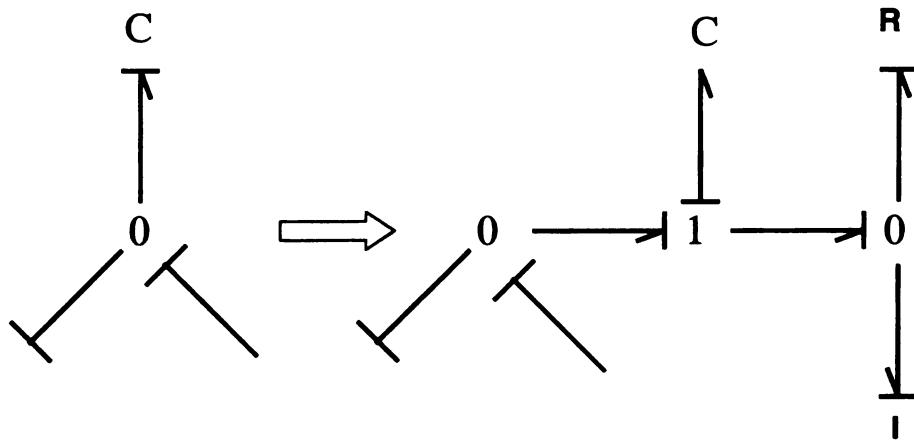


Figure 2.3. Handling a capacitance that is attached to a 0-junction

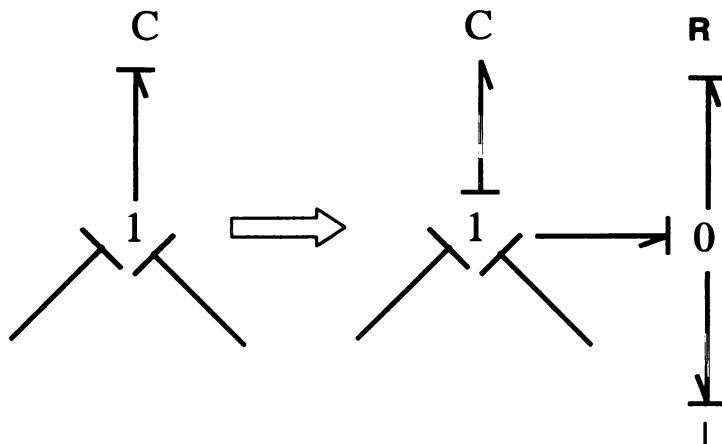


Figure 2.4. Handling a capacitance that is attached to a 1-junction

As the figures above indicate, a dependent inertia is treated by adding a parasitic damping and a parasitic stiffness; the parasitic elements are in series with respect to one another, and they are both in parallel with respect to the dependent inertia. On the other hand a dependent stiffness is treated by adding

a parasitic damping and a parasitic inertia; the parasitic elements are in parallel with respect to one another, and they are both in series with respect to the dependent inertia. The dependent stiffness problem and the dependent inertia problem are the dual of one another. Therefore, it is sufficient to analyze only one of them. It has been decided to do the dependent inertia problem.

### **2.3.2 Other Related Work**

Joseph et al. (1974) presents a method for causality assignment (relaxed causality) for nonlinear systems with algebraic loops and/or derivative causality. The method will still produce a set of ADEs for systems with algebraic loops and/or derivative causality. However, he claims that it is more suitable for computerized formulation of nonlinear systems than the widely used Sequential Causality Assignment Procedures (due to Karnopp and Rosenberg).

Granda (1984) shows different alternatives to deal with derivative causality and algebraic loops. The proposed alternatives can be summarized as being deleting elements from the original model, adding elements to the original model, or algebraic manipulation. Each of these alternatives could be the right choice, depending on the problem under investigation and depending on the objective of the process. He emphasized the importance of alternatives that can be implemented on a computer.

Bos et al. (1985) describes a method that uses formula manipulation to remove differential causality from mechanical systems. It states that the computational demand of the formula manipulation is “excessively large.”

Karnopp (1992) proposed another approach to eliminate derivative causality in bond graph models of mechanical systems. The approach defines an I-field or an IC-field using generalized momenta or generalized coordinates similar to those used in Lagrange’s equations. Karnopp (1992) showed that this method would require a matrix inversion, at each time step if nonlinear constraints such as modulated transformers were involved. In addition, this method would be more difficult to automate compared with the method under investigation in this research.

Margolis (1993) acknowledges that when the goal of analysis is to simulate the system's transient response, the derivative causality issue has to be dealt with; and shows a way to derive input/output transfer functions for bond graph models with derivative causality.

Edstrom (1999) shows that by inserting a parasitic resistance into a class of bond graph models with derivative causality; then deriving the explicit set of equations for the modified system; and setting the parasitic resistance to zero (or infinite); a set of explicit ODEs can be obtained for the original system that contained a derivative causality. Results were proved for a very limited class of

linear bond graph models that did not include transformers, gyrators, or multi-port elements. The main importance of this paper is highlighting the relationship between mathematical models derived from bond graphs with derivative causality and the standard singular perturbation model; although it was addressing a less general (compared to the modifications under investigation in this work) type of modifications and no details have been investigated.

## **2.4 Determining the Appropriate Perturbation Parameter**

As stated earlier, there might be more than one possible perturbation parameter for a two-time-scale system. In addition, there is no systematic way to identify the most "appropriate" one for a problem under investigation. Some insight into the problem under investigation is needed to enable the user to acquire this information. The objective of this section is to gain that insight and to determine the appropriate perturbation parameter  $\varepsilon$  for the problem under investigation. To the author's knowledge, there are no published efforts that discuss this issue in detail. Zeid (1988) suggested (without analysis) using two different perturbation parameters,  $C$  and  $R$  with  $C$  being "very small" and  $R$  being "very big". This suggests that  $RC$  is  $O(1)$ . On the other hand, some simulation results, which were obtained within this research work and will be shown later, show that the modified system can include two fast poles. These results showed also that the separation between the slow and the fast sub-systems increases as  $RC$  decreases. This suggests using  $RC$  as the

perturbation parameter. This section will show another possible choice for the perturbation parameter; later it will be demonstrated that this choice helps reveal the time-scale properties of the systems under investigation.

### 2.4.1 Analysis Based on Physical System Modeling

Figure 2.5 shows the simplest version of the problem under investigation. It shows a case in which the original system consists of only two “coupled” masses,  $I_1$  and  $I_2$ .

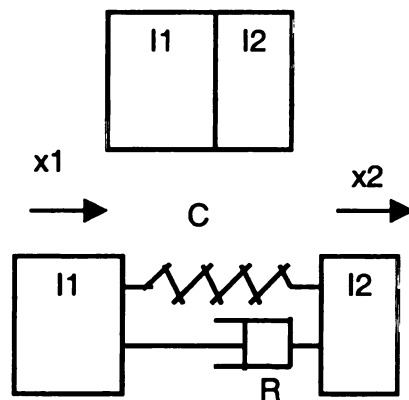


Figure 2.5 A local problem

Let us assume that these two coupled masses are decoupled by inserting a parasitic spring, whose compliance is  $C$  and a parasitic damper whose resistance is  $R$ . This is exactly equivalent to using the method under investigation to eliminate the derivative causality. Assume that the translation of



the two masses are  $x_1$  and  $x_2$  respectively. The equations of the modified system can be written as

$$\ddot{x}_1 = \frac{1}{I_1 C} (x_2 - x_1) + \frac{R}{I_1} (\dot{x}_2 - \dot{x}_1)$$

$$\ddot{x}_2 = -\frac{1}{I_2 C} (x_2 - x_1) - \frac{R}{I_2} (\dot{x}_2 - \dot{x}_1)$$

$$\delta = (x_1 - x_2)$$

This system can be written in the state space form with the state vector

$$X = \begin{bmatrix} \dot{x}_1 \\ \dot{x}_2 \\ \delta \end{bmatrix} \text{ and system matrix } A = \begin{bmatrix} \frac{-R}{I_1} & \frac{R}{I_1} & \frac{-1}{CI_1} \\ \frac{R}{I_2} & \frac{-R}{I_2} & \frac{1}{CI_2} \\ 1 & -1 & 0 \end{bmatrix}$$

It can be shown that the characteristic equation of this system is

$$\lambda \left\{ \lambda^2 + \lambda \left( \frac{R}{I_1} + \frac{R}{I_2} \right) + \frac{1}{C} \left( \frac{1}{I_1} + \frac{1}{I_2} \right) \right\} = 0$$

where,  $\lambda$  is a root of the characteristic equation; and  $\lambda = 0$  root represents the slow “original system” eigenvalue. To find the eigenvector that corresponds to  $\lambda = 0$ , set  $\lambda = 0$  in the equation

$$AV = \lambda V$$

Where,  $V$  is the eigenvector that corresponds to  $\lambda$ . It is easy to show that for  $\lambda = 0$ ,

$$V = \begin{bmatrix} V_1 \\ V_1 \\ 0 \end{bmatrix}$$

This mode represents a solid body mode in which the two masses have the same velocities; this is an accurate description of the original system.

The other two eigenvalues of the modified system are the eigenvalues of the fast sub-system and they are the solution of

$$\lambda^2 + \lambda \left( \frac{R}{I1} + \frac{R}{I2} \right) + \frac{1}{C} \left( \frac{1}{I1} + \frac{1}{I2} \right) = 0 \quad (2.21)$$

As the best separation will occur when the two fast poles are equally fast which means that the sluggishness of neither of them would dominate. We examine here the condition at which the two fast poles of (2.21) are critically damped. It is easy to show here that for roots of (2.21) to be critically damped, the following condition (2.22) must be satisfied

$$RRC = \frac{4}{\frac{1}{I1} + \frac{1}{I2}} \quad (2.22)$$

Equation (2.22) will be examined subsequently, together with the results from the next sub-section.

### 2.4.2 Simulation-Based Analysis

In another effort to discover the appropriate perturbation parameter for the problem under investigation, simulations of some simplified versions of the problem were conducted. In one attempt, Example 1 was used; Figure 2.6 shows a schematic diagram and a bond graph of the original system of Example 1. Where, the *original system* refers to the system with the derivative causality.

As shown, the original system includes two inertances,  $L1$  and  $L2$ , that are coupled through a transformer,  $TF$ , whose modulus is  $m$ . Figure 2.7 shows a schematic and bond graph model for modified system of Example 1. Where, the *modified system* refers to the original system after inserting parasitic elements into it to eliminate the derivative causality. The terms original system and modified system will be used throughout this thesis to convey the above-mentioned meanings.

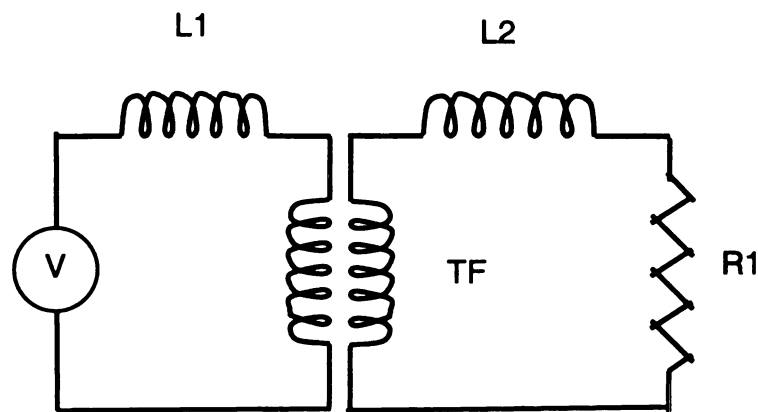


Figure 2.6 (a). Schematic diagram for the original system of Example 1

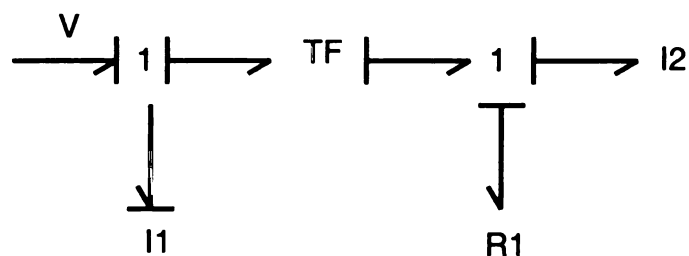


Figure 2.6 (b). Bond graph model for the original system of Example 1

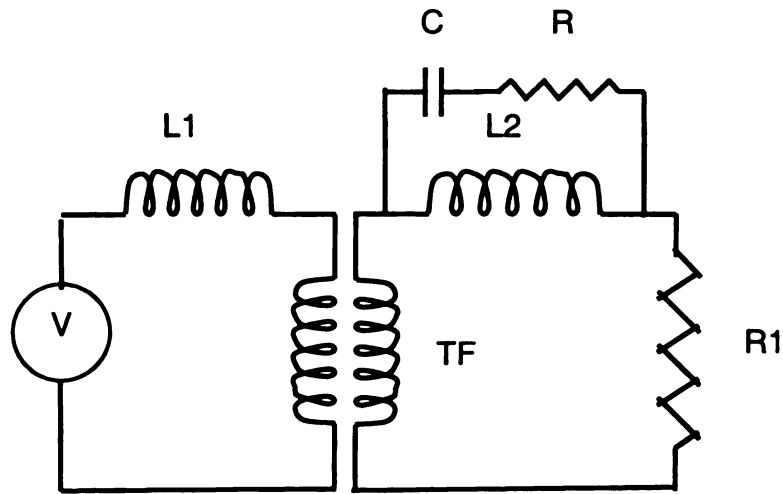


Figure 2.7 (a). Schematic diagram for the modified system of Example 1

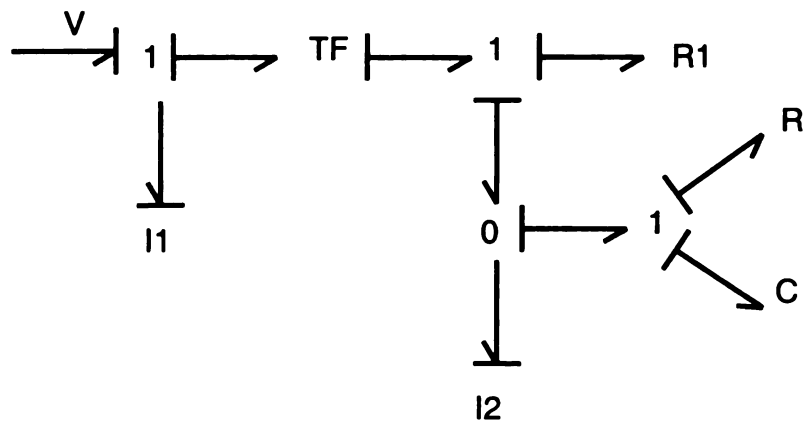


Figure 2.7 (b). Bond graph model of the modified system of Example 1

The following set of parameters was used for Example 1 in this attempt:

$$I1 = I2 = 2000$$

$$R1 = 2000$$

$$m = 1$$

Eigenvalues of the modified system were calculated at different values of the product  $RC$  that were chosen. For every chosen value of  $RC$ , the values of  $R$

and  $C$  were changed till a pair of two critically damped poles for the fast sub-system are obtained. For these values of  $R$  and  $C$  for which two critically damped fast poles occur, the product  $R^2C$  was recorded vs. its corresponding value of  $RC$ . Again, the critically damped condition was chosen because it was thought to provide the best separation between the fast sub-system and the slow sub-system. To obtain suitable values for the fast poles some trial and error alongside with knowing, that generally reducing  $RC$  will produce faster poles in the fast sub-system were used. Figure 2.8 summarizes the results of this investigation for Example 1. The horizontal axis in Figure 2.8 is the product  $RC$  and the vertical axis is  $R^2C$  normalized by dividing it by the right hand side of equation (2.22).

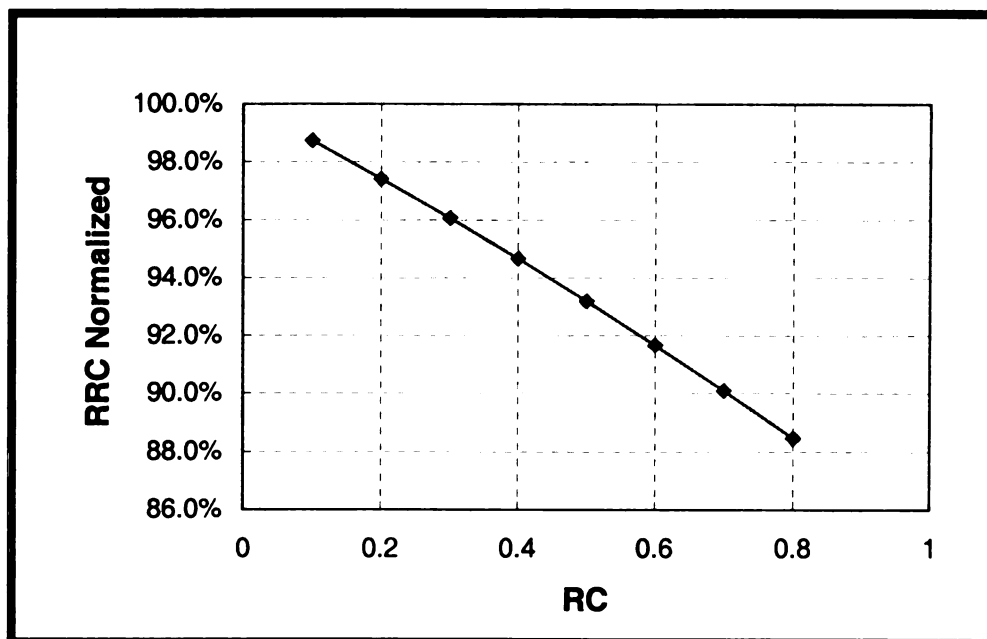


Figure 2.8 Relation between normalized RRC and  $RC$ , Example 1

To further the understanding of the results shown in Figure 2.8 the procedure described above in this section were implemented again for another example (Example 2). Figure 2.9 shows a schematic diagram and a bond graph model of the original system of Example 2; and Figure 2.10 shows a schematic diagram and a bond graph model of the modified system of Example 2. The difference between Example 1 and Example 2 is that Example 2 has an additional energy-storing element (capacitor,  $C1$ ). Consequently, Example 2 is more general than Example 1 and its order is higher than that of Example 1 by one.

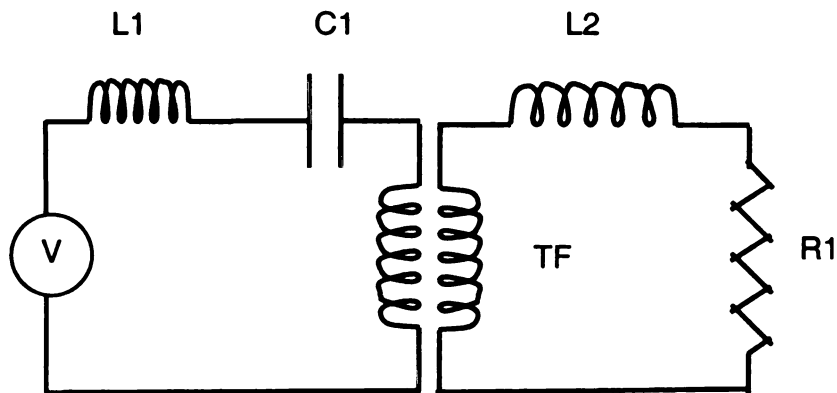


Figure 2.9 (a). Schematic diagram for the original system of Example 2

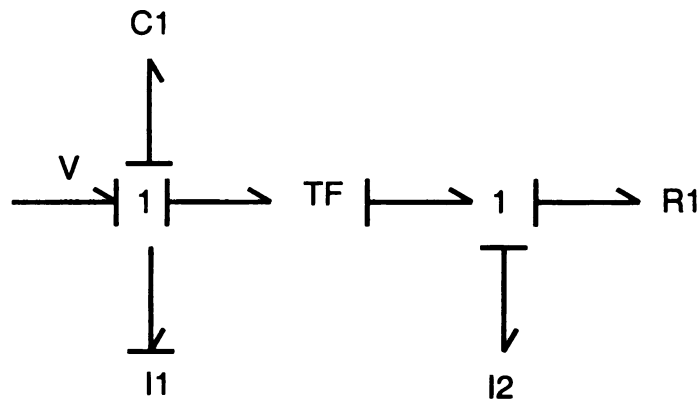


Figure 2.9 (b). Bond graph model for the original system of Example 2

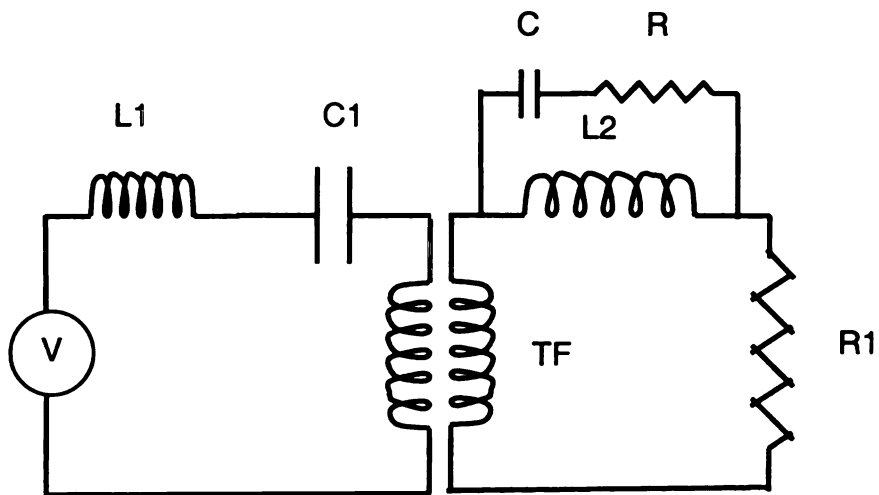


Figure 2.10 (a). Schematic diagram for the modified system of Example 2

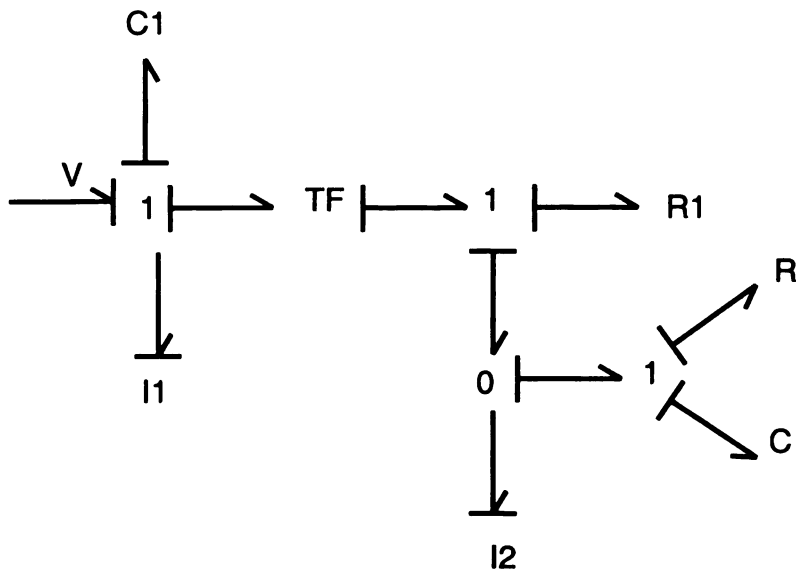


Figure 2.10 (b). Bond graph model for the modified system of Example 2

The same procedure described above for Example 1 was applied for Example 2 for three different cases; every case had a different set of original system parameter values. The three different sets of parameters were chosen such that:

- 1) One set produces an over damped original system, one set produces a critically damped original system, and one set produces an under damped original system.
- 2) The real part of the fastest pole in all cases is equal to  $-0.25$ . This will make comparing the three different cases with one another and with Example 1 easier and more meaningful.

The used three different sets of original system parameters along side with their corresponding eigenvalues are as follows:



**Case one:**

$$C1 = 0.0107$$

$$I1 = I2 = 1250$$

$$R1 = 1000$$

$$\lambda1 = -0.25$$

$$\lambda2 = -0.15$$

$$m = 1$$

**Case two:**

$$C1 = 0.008$$

$$I1 = I2 = 1000$$

$$R1 = 1000$$

$$\lambda1 = -0.25$$

$$\lambda2 = -0.25$$

$$m = 1$$

**Case three:**

$$C1 = 0.004$$

$$I1 = I2 = 1000$$

$$R1 = 1000$$

$$\lambda1 = -0.25 + i0.2501 \quad \lambda2 = -0.25 - i0.2501$$

$$m = 1$$

The results of these three cases are summarized in Figure 2.11

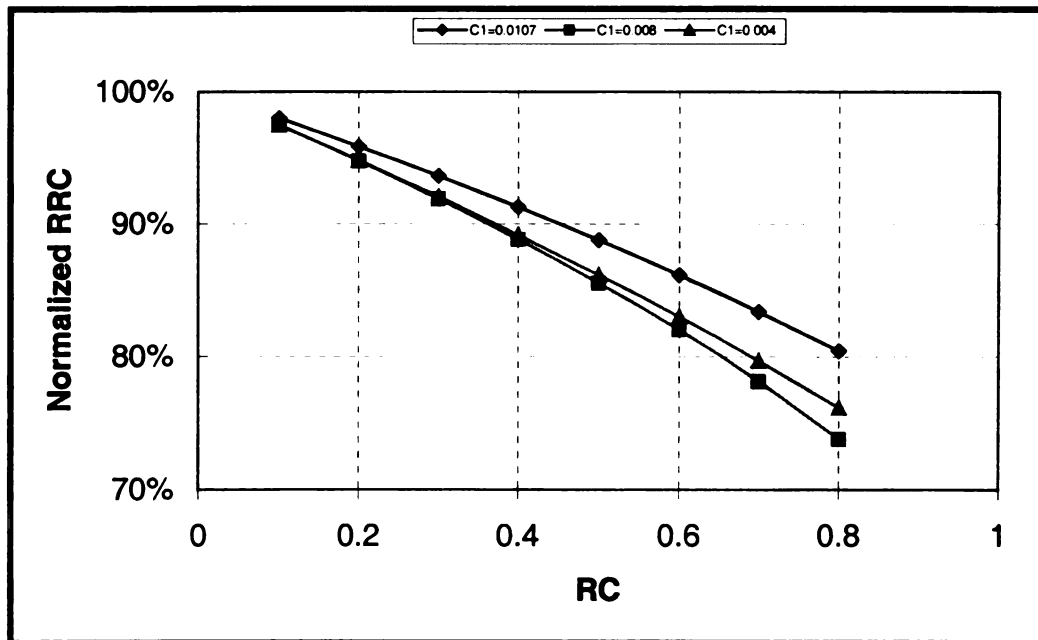


Figure 2.11 Relation between normalized RRC and RC, Example 2

Figure 2.8 and Figure 2.11 indicate that the product  $R^2C$  converges to a constant as  $RC$  gets smaller. In other words,  $R^2C$  converges to a constant as the time-scale separation between the slow sub-system (original system) and the fast sub-system increases. Moreover, Figure 2.8 and Figure 2.11 indicate that the constant (to which  $R^2C$  converges) could be related to the original system parameters only. These conclusions agree with and perhaps explain equation (2.22) that was derived for the two coupled masses example. After examining Figure 2.8 and Figure 2.11 it is easier to understand that equation (2.22) was obtained because the original system had a zero eigenvalue; therefore any value for the two critically damped fast eigenvalues will provide enough time-scale separation between the original sub-system and the fast sub-system for  $R^2C$  to converge to  $\frac{4}{\frac{1}{I_1} + \frac{1}{I_2}}$ . The observation that  $R^2C$  converges to a constant as  $\varepsilon$  tends to zero means that there is another option for choosing  $\varepsilon$  in addition to  $\varepsilon = RC$ ; it is  $\varepsilon = \frac{1}{R}$ . These results will aid the efforts to find the standard singularly perturbed model for the class of systems under investigation. These efforts are reported in the next section.

Although examples used in this section are somewhat restricted, they were useful in demonstrating some important aspects of the general problem for these reasons:

- 1) They contain the important aspects of the problem under investigation; they contain a coupling between two energy-storing elements in the original system; and they contain the same structural modifications under investigation in this work. The modifications do not depend on the details of the original system.
- 2) As the time-scale separation between the slow sub-system and the fast sub-system in modified system increases; most of the details of the slow sub-system (the original system) are not going to affect the fast-sub-system. Later, it will be shown that, only the inertia field will affect the fast sub-system as the time-scale separation increases.
- 3) As the time-scale separation between the slow sub-system and the fast sub-system in the modified system increases; the effect of the fast sub-system on the slow sub-system tends to vanish.

## 2.5 Finding the Standard Singular Perturbation Form

The results obtained from section 2.4 are more of clues that provide insight, which is typically needed before being able to use the singular perturbation method effectively. In addition, until this point of this presentation, it has not been confirmed yet that choosing  $\varepsilon = \frac{1}{R}$  and assuming that  $R^2C$  converges to a constant as  $\varepsilon$  tends to zero, will be a better option for the problem under investigation. A subsequent analysis based on these results will prove their usefulness. An important part of this analysis is formulating the

modified system in the standard singular perturbation form. This issue is investigated in this section.

### 2.5.1 Using Transformation Procedures to Obtain PSSPF

Even though there are some general procedures to help transform a two-time-scale singularly perturbed model from a non-standard form to the standard form (Kokotovic et al. 1986), the result of these procedures are not unique; and you have to decide what  $\varepsilon$  is and put the model in a required form before you can start using those procedures. This section shows how the transformation procedure outlined in Kokotovic et al. (1986) can be best used for the classes of models under investigation. It demonstrates that by showing how to use the procedure in transforming two simple examples; then it characterizes the preferred standard singular perturbation form (PSSPF).

This procedure assumes that the systems are linear; they can be summarized in three steps as follows:

#### Step 1:

Put the system in the form

$$\varepsilon \dot{v} = F(\varepsilon)v, \quad v \in R^{n+m} \quad (2.23)$$

Where,  $n$  is the order of the slow sub-system and  $m$  is the order of the fast sub-system.

$$\text{Let } F(\varepsilon) = F_0 + \varepsilon F_1(\varepsilon)$$

For two or more time-scales to appear we should have  $\det F(0) = 0$ .  
 If  $\det F(0) \neq 0$  then all the components of  $v$  would be fast. Assume that the dimension of the null space (N) of  $F_0$  is equal to  $n$ . To be able to find the transformation, rank of  $F_0$  must equal to the number of the fast variables. The null space (N) of  $F_0$  is defined as

$$N(F_0) = \left\{ y \in R^{n+m} \mid F_0 y = 0 \right\}$$

**Step 2:**

To select a fast variable vector  $\eta$  choose  $m$  linearly independent vectors in  $R^{n+m}$  orthogonal to the null-space  $N(F_0)$  and arrange them as the rows of an  $m \times (n+m)$  matrix  $Q$ .

**Step 3:**

To select a slow variables vector  $x$ , find  $P$  (the left null space of  $F_0$ ) such that

$$PF_0 = 0$$

The change of coordinates

$$x = Pv, \quad \eta = Qv; \quad T = \begin{bmatrix} P \\ Q \end{bmatrix} \quad (2.24)$$

will transform the system (2.23) into the standard form

$$\dot{x} = A_{11}(\varepsilon)x + A_{12}(\varepsilon)\eta \quad (2.25)$$

$$\varepsilon \dot{\eta} = \varepsilon A_{21}(\varepsilon)x + A_{22}(\varepsilon)\eta \quad (2.26)$$

as long as the transformation matrix  $T$  is nonsingular. In addition, as  $\varepsilon$  becomes small,  $A_{11}(0)$  will contain the  $n$  slow eigenvalues and  $\frac{1}{\varepsilon}A_{22}(0)$  will contain the  $m$  fast eigenvalues in the original time-scale  $t$  (vs. the fast time-scale  $\tau = \frac{t}{\varepsilon}$ ), Kokotovic et al. (1986). The next paragraphs will demonstrate how to use this general procedure by explaining how to apply them to two simple examples.

Following the Sequential Causality Assignment Procedures (Rosenberg et al. 1983) it can be shown that the homogeneous original system of Example 1 can be written as

$$\frac{dp1}{dt} = -m \left( mR1 \frac{p1}{I1} + \frac{dp2}{dt} \right) \quad (2.27)$$

$$\frac{p2}{I2} = m \frac{p1}{I1} \quad (2.28)$$

and that its homogeneous modified system can be written as

$$\frac{dp1}{dt} = -\frac{m^2(R + R1)}{I1} p1 + \frac{mR}{I2} p2 - \frac{m}{C} q \quad (2.29)$$

$$\frac{dp2}{dt} = \frac{mR}{I1} p1 - \frac{R}{I2} p2 + \frac{1}{C} q \quad (2.30)$$

$$\frac{dq}{dt} = \frac{m}{I1} p1 - \frac{1}{I2} p2 \quad (2.31)$$

Where  $i1$  and  $i2$  are the currents in the inductors  $L1$  and  $L2$  respectively;  $q$  is the charge in the parasitic capacitor;  $p1 = I1i1$ ;  $p2 = I2i2$ . Next we will apply the transformation procedure to convert the modified system to the standard form.

First, the modified system equations (2.29) - (2.31) can be expressed in the matrix form

$$\frac{d}{dt} \begin{bmatrix} p1 \\ p2 \\ q \end{bmatrix} = \begin{bmatrix} \frac{-m^2(R+R1)}{I1} & \frac{mR}{I2} & \frac{-m}{C} \\ \frac{Rm}{I1} & \frac{-R}{I2} & \frac{1}{C} \\ \frac{m}{I1} & \frac{-1}{I2} & 0 \end{bmatrix} \quad (2.32)$$

Inspecting equation (2.32) shows if we proceed from here to calculate  $F_0$ , the rank of  $F_0$  would equal to one. Since it was stated above that the number of fast variables should be equal to the rank of  $F_0$ , and we already decided that there should be two fast variables; this indicates a potential inconsistency, and means that some scaling is needed to avoid this potential inconsistency. Knowing that  $\varepsilon = \frac{1}{R}$ , and that  $R^2C$  becomes constant as  $\varepsilon$  becomes small; an experienced observer can notice that he/she needs to scale the variable  $q$  to  $Rq$  to be able to proceed correctly. As  $R$  is equal to  $\frac{1}{\varepsilon}$ , this scaling is an  $\varepsilon$ -based scaling, which is exercised only to avoid potential inconsistency such as the one detected above. Implementing this scaling and substituting  $\alpha$  for  $R^2C$  will produce

$$\frac{d}{dt} \begin{bmatrix} p1 \\ p2 \\ Rq \end{bmatrix} = \begin{bmatrix} \frac{-m^2(R+R1)}{I1} & \frac{mR}{I2} & \frac{-mR}{\alpha} \\ \frac{Rm}{I1} & \frac{-R}{I2} & \frac{R}{\alpha} \\ \frac{mR}{I1} & \frac{-R}{I2} & 0 \end{bmatrix} \quad (2.33)$$

Consequently, we can obtain

$$\varepsilon \frac{d}{dt} \begin{bmatrix} p1 \\ p2 \\ Rq \end{bmatrix} = \begin{bmatrix} \frac{-m^2(1+\varepsilon R1)}{I1} & \frac{m}{I2} & \frac{-m}{\alpha} \\ \frac{m}{I1} & \frac{-1}{I2} & \frac{1}{\alpha} \\ \frac{m}{I1} & \frac{-1}{I2} & 0 \end{bmatrix} \quad (2.34)$$

Comparing (2.23) and (2.34), we can see that

$$F_0 = \begin{bmatrix} \frac{-m^2}{I1} & \frac{m}{I2} & \frac{-m}{\alpha} \\ \frac{m}{I1} & \frac{-1}{I2} & \frac{1}{\alpha} \\ \frac{m}{I1} & \frac{-1}{I2} & 0 \end{bmatrix} \quad (2.35)$$

and that the rank of  $F_0$  is two, which is the correct rank.

In the second step, to select the fast variables, find the right null space ( $y$ ) of

$F_0$ . Calculating  $y$  from  $F_0 y = 0$  leads to

$$y = \begin{bmatrix} y1 \\ \frac{mI2}{I1} y1 \\ 0 \end{bmatrix}$$

where  $y1$  is an arbitrary constant. Notice that the dimension of this null space is one, which is equal to the number of the slow variables. The next step is to choose two linearly independent vectors that are orthogonal to  $y$ . Obviously, the choices of these vectors are not unique. This research work recommends choosing the two orthogonal vectors to be



$$\begin{bmatrix} \frac{m}{I1} \\ -\frac{1}{I2} \\ 0 \end{bmatrix} \quad \text{and} \quad \begin{bmatrix} 0 \\ 0 \\ 1 \end{bmatrix} \quad (2.36)$$

This choice is recommended because the two fast variables this choice is going to produce are physically meaningful and moreover, understanding and characterizing their behaviors are useful to this research work. With this recommended choice the two fast variables are

$$\frac{m}{I1} p1 - \frac{1}{I2} p2 \quad (2.37)$$

$$Rq \quad (2.38)$$

The first fast variable  $(\frac{m}{I1} p1 - \frac{1}{I2} p2)$  can be seen as the error introduced into the second equation (2.28) of the original system model due to inserting the parasitic elements. The second variable  $(Rq)$  is a scaling of the charge in the parasitic capacitance; it is basically, the integral of the first fast variable. From design perspective, it is important to design the modified system such that these two variables are fast; so that the effect of the parasitic elements on the original system behavior will vanish quickly. Therefore, these two variables are of particular importance to this investigation.

In the third step, to select the slow variables, find  $P$  (the left null space of  $F_0$ ) such that  $PF_0 = 0$ . This will produce

$$P = [P1 \quad mP1 \quad 0] \quad (2.39)$$

where,  $P1$  is an arbitrary constant, it will be chosen to equal to one; so that

$$P = \begin{bmatrix} 1 & m & 0 \end{bmatrix} \quad (2.40)$$

With this choice, the slow variable in this example is going to be

$$p_1 + mp_2 \quad (2.41)$$

This slow variable has a physical meaning. If we were to algebraically manipulate the original system equation (2.27) to sum the coupled derivative terms together, this algebraic manipulation would have produced the derivative of this variable (2.41) as the sum. With  $P$  and  $Q$  available, the transformation matrix  $T$  can be written as

$$T = \begin{bmatrix} P \\ Q \end{bmatrix} = \begin{bmatrix} 1 & m & 0 \\ m & -1 & 0 \\ \frac{I_1}{0} & \frac{I_2}{0} & 1 \end{bmatrix} \quad (2.42)$$

Consequently, the system matrix of the transformed system is

$$\tilde{A} = T \begin{bmatrix} \frac{-m^2(R+R_1)}{I_1} & \frac{mR}{I_2} & \frac{-mR}{\alpha} \\ \frac{mR}{I_1} & \frac{-R}{I_2} & \frac{R}{\alpha} \\ \frac{mR}{I_1} & \frac{-R}{I_2} & 0 \end{bmatrix} T^{-1}, \text{ or}$$

$$\tilde{A} = \begin{bmatrix} \frac{-m^2 R_1}{(I_1 + m^2 I_2)} & \frac{-m^3 I_2 R_1}{(I_1 + m^2 I_2)} & 0 \\ \frac{-m^3 R_1}{I_1(I_1 + m^2 I_2)} & \frac{-m^4 I_2^2 R_1}{I_1 I_2 (I_1 + m^2 I_2)} - R \left[ \frac{m^2}{I_1} + \frac{1}{I_2} \right] & -\frac{R}{\alpha} \left[ \frac{m^2}{I_1} + \frac{1}{I_2} \right] \\ 0 & R & 0 \end{bmatrix}$$

Therefore, this system can be written in the standard singular perturbation form

$$\dot{x} = A_{11}(\varepsilon)x + A_{12}(\varepsilon)\eta \quad (2.25)$$

$$\varepsilon \dot{\eta} = \varepsilon A_{21}(\varepsilon)x + A_{22}(\varepsilon)\eta \quad (2.26)$$

with

$$x = p_1 + m p_2, \quad \eta = \begin{bmatrix} \frac{m}{I_1} p_1 - \frac{1}{I_2} p_2 \\ Rq \end{bmatrix},$$

$$A_{11} = \begin{bmatrix} \frac{-m^2 R_1}{(I_1 + m^2 I_2)} \end{bmatrix}, \quad A_{12} = \begin{bmatrix} \frac{-m^3 I_2 R_1}{(I_1 + m^2 I_2)} & 0 \end{bmatrix},$$

$$A_{21} = \begin{bmatrix} \frac{-m^3 R_1}{I_1(I_1 + m^2 I_2)} \\ 0 \end{bmatrix}, \text{ and } A_{22} = \begin{bmatrix} \frac{-m^4 I_2^2 R_1 \varepsilon}{I_1 I_2 (I_1 + m^2 I_2)} - \left[ \frac{m^2}{I_1} + \frac{1}{I_2} \right] & -\frac{1}{\alpha} \left[ \frac{m^2}{I_1} + \frac{1}{I_2} \right] \\ 1 & 0 \end{bmatrix}$$

Examining the eigenvalues of the original system shows that it is really equal to the one indicated by  $A_{11}$  as it was stated. It was also stated above that

$\frac{1}{\varepsilon} A_{22}(0)$  contains the eigenvalues of the fast sub-system as  $\varepsilon$  gets small.

$$A_{22}(0) = \begin{bmatrix} -\left[ \frac{m^2}{I_1} + \frac{1}{I_2} \right] & -\frac{1}{\alpha} \left[ \frac{m^2}{I_1} + \frac{1}{I_2} \right] \\ 1 & 0 \end{bmatrix} \quad (2.43)$$

Using equation (2.43), the eigenvalues ( $\lambda$ ) of the fast sub-system, as  $\varepsilon$  gets small, can be calculated from

$$\left( \lambda + \left( \frac{m^2}{I_1} + \frac{1}{I_2} \right) R \right) \lambda + \frac{1}{\alpha} \left( \frac{m^2}{I_1} + \frac{1}{I_2} \right) R^2 = 0 \quad (2.44)$$

Next we will demonstrate how to apply the procedure to Example 2. Example 2 is more complex than Example 1; its original and modified systems were given above in Figure 2.4.5 and Figure 2.4.6 respectively. Following the

SCAP (Rosenberg et al. 1983), the homogeneous original system of Example 2 can be formulated as

$$\frac{dq1}{dt} = \frac{p1}{I1} \quad (2.45)$$

$$\frac{dp1}{dt} = -\frac{1}{C1}q1 - m\left(mR1\frac{p1}{I1} + \frac{dp2}{dt}\right) \quad (2.46)$$

$$\frac{p2}{I2} = m\frac{p1}{I1} \quad (2.47)$$

and its homogeneous modified system can be written as

$$\frac{dq1}{dt} = \frac{p1}{I1} \quad (2.48)$$

$$\frac{dp1}{dt} = -\frac{1}{C1}q1 - \frac{m^2(R+R1)}{I1}p1 + \frac{mR}{I2}p2 - \frac{m}{C}q \quad (2.49)$$

$$\frac{dp2}{dt} = \frac{mR}{I1}p1 - \frac{R}{I2}p2 + \frac{1}{C}q \quad (2.50)$$

$$\frac{dq}{dt} = \frac{m}{I1}p1 - \frac{1}{I2}p2 \quad (2.51)$$

1) After scaling  $q$  to  $Rq$ , this system can be written in the matrix form as

$$\frac{d}{dt} \begin{bmatrix} q1 \\ p1 \\ p2 \\ Rq \end{bmatrix} = \begin{bmatrix} 0 & \frac{1}{I1} & 0 & 0 \\ -\frac{1}{C1} & -\frac{m^2(R+R1)}{I1} & \frac{mR}{I2} & -\frac{mR}{C} \\ 0 & \frac{mR}{I1} & -\frac{R}{I2} & \frac{R}{C} \\ 0 & \frac{mR}{I1} & -\frac{R}{I2} & 0 \end{bmatrix} \quad (2.52)$$

Therefore,

$$F_0 = \begin{bmatrix} 0 & 0 & 0 & 0 \\ 0 & \frac{-m^2}{I1} & \frac{m}{I2} & \frac{-m}{\alpha} \\ 0 & \frac{m}{I1} & \frac{-1}{I2} & \frac{1}{\alpha} \\ 0 & \frac{m}{I1} & \frac{-1}{I2} & 0 \end{bmatrix} \quad (2.53)$$

2) To select the fast variables, find the right null space (  $y$  ) of  $F_0$  . Calculating  $y$

from  $F_0 y = 0$  leads to

$$y = \begin{bmatrix} y1 \\ y2 \\ \frac{mI2}{I1} y2 \\ 0 \end{bmatrix} = y1 \begin{bmatrix} 1 \\ 0 \\ 0 \\ 0 \end{bmatrix} + y2 \begin{bmatrix} 0 \\ 1 \\ \frac{mI2}{I1} \\ 0 \end{bmatrix} \quad (2.54)$$

Where  $y1$  and  $y2$  are arbitrary constants. Notice that the dimension of this null space is two, which is equal to the number of the slow variables. To select the same meaningful fast variables we selected for Example 1 the two vectors that are orthogonal to the right null space should be selected as

$$\begin{bmatrix} 0 \\ \frac{m}{I1} \\ \frac{-1}{I2} \\ 0 \end{bmatrix} \quad \text{and} \quad \begin{bmatrix} 0 \\ 0 \\ 0 \\ 1 \end{bmatrix} \quad (2.55)$$

Therefore, the two fast variables remains to be

$$\frac{m}{I1} p1 - \frac{1}{I2} p2 \quad (2.56)$$

$$Rq \quad (2.57)$$

3) To select the slow variables, find  $P$  (the left null space of  $F_0$ ) such that  $PF_0 = 0$ . This will produce

$$P = \begin{bmatrix} P_{11} & P_{12} & mP_{12} & 0 \\ P_{21} & P_{22} & mP_{22} & 0 \end{bmatrix} \quad (2.58)$$

Where,  $P_{11}$ ,  $P_{12}$ ,  $P_{21}$ , and  $P_{22}$  are arbitrary constants to be chosen so that the transformation matrix is not singular. We still desire to get the meaningful slow variable that was obtained in Example 1. To do that select

$$P_{21} = 0, \quad P_{22} = 1 \quad (2.59)$$

This will select one of the two slow variables as

$$p_1 + mp_2 \quad (2.60)$$

The other meaningful slow variable would be the state ( $q_1$ ) in the original system. To select it select

$$P_{11} = 1, \quad P_{12} = 0 \quad (2.61)$$

With  $P$  and  $Q$  available, the transformation matrix  $T$  can be written as

$$T = \begin{bmatrix} P \\ Q \end{bmatrix} = \begin{bmatrix} 1 & 0 & 0 & 0 \\ 0 & 1 & m & 0 \\ 0 & \frac{m}{I_1} & \frac{-1}{I_2} & 0 \\ 0 & 0 & 0 & 1 \end{bmatrix} \quad (2.62)$$

One can easily notice that the lower right 3x3 sub-matrix in the transformation matrix of Example 2 (2.62) is the same as the transformation matrix of Example 1 (2.42). The system matrix of the transformed system is

$$\tilde{A} = T \begin{bmatrix} 0 & \frac{1}{I1} & 0 & 0 \\ -1 & \frac{-m^2(R+R1)}{I1} & \frac{mR}{I2} & \frac{-mR}{\alpha} \\ 0 & \frac{mR}{I1} & \frac{-R}{I2} & \frac{R}{\alpha} \\ 0 & \frac{mR}{I1} & \frac{-R}{I2} & 0 \end{bmatrix} T^{-1}, \text{ or}$$

$$\tilde{A} = \begin{bmatrix} 0 & \frac{1}{I1+m^2I2} & \frac{mI2}{I1+m^2I2} & 0 \\ -1 & \frac{-m^2R1}{I1+m^2I2} & \frac{-m^3I2R1}{I1+m^2I2} & 0 \\ \frac{-m}{I1C1} & \frac{-m^3R1}{I1(I1+m^2I2)} & \frac{-m^4I2R1}{I1(I1+m^2I2)} - R \left[ \frac{m^2}{I1} + \frac{1}{I2} \right] & \frac{-R}{\alpha} \left[ \frac{m^2}{I1} + \frac{1}{I2} \right] \\ 0 & 0 & R & 0 \end{bmatrix},$$

$$x = \begin{bmatrix} q1 \\ p1+mp2 \end{bmatrix},$$

$$\eta = \begin{bmatrix} \frac{m}{I1} p1 - \frac{1}{I2} p2 \\ Rq \end{bmatrix}, \text{ and}$$

$$A_{22}(\varepsilon) = \begin{bmatrix} \frac{-m^4I2R1\varepsilon}{I1(I1+m^2I2)} - \left[ \frac{m^2}{I1} + \frac{1}{I2} \right] & \frac{-1}{\alpha} \left[ \frac{m^2}{I1} + \frac{1}{I2} \right] \\ 1 & 0 \end{bmatrix} \quad (2.63)$$

Consequently,

$$A_{22}(0) = \begin{bmatrix} -\left[ \frac{m^2}{I1} + \frac{1}{I2} \right] & \frac{-1}{\alpha} \left[ \frac{m^2}{I1} + \frac{1}{I2} \right] \\ 1 & 0 \end{bmatrix} \quad (2.64)$$

It is remarkable that  $A_{22}(0)$  for Example 1 (2.43) is the same as that for Example 2 (2.64). In other words, the fast sub-systems in both examples will become same as  $\varepsilon$  decreases. More details will be given on that in CHAPTER 3.

As explained while demonstrating how to use the procedure on the two examples, there are some variables that are preferable, to be states in the transformed standard form, to others. The standard form that includes these preferred variables will be called the preferable standard singular perturbation form (PSSPF). This PSSPF has the following characteristics:

- 1) The slow variables consist of the states that are not part of the coupled field in the original system, and the variables whose sum of derivatives are obtained if we were to sum the coupled derivatives (in an equation-by-equation basis) in the original system as shown in the examples.
- 2) One of the fast variables is the error introduced into the original system's algebraic equation due to inserting the parasitic elements.
- 3) The other fast variable is a scaling of the charge ( $Rq$ ) in the inserted parasitic capacitance.

### **2.5.2 A Transformation to Obtain the PSSPF**

This section derives the transformation matrix needed to transform a general modified system from the class of systems under investigation to the PSSPF and proves its existence.

Assume that a linear system includes a coupled energy field together with some other energy storing elements that are not coupled with the field. Assume



that the vector of the states that are not among the coupled field is  $X_r$  and its dimension is  $r$ . One way to recognize the elements of the coupled field is by the appearance of their parameters in  $J_{di}$ . Further, assume that the coupled field includes only one dependent energy-storing element. Based on general form for the coupled field given in equations (2.16) and (2.17), the general form of this class of original systems can be written as

$$\dot{X}_r = A_{rr}X_r + A_{ri}X_i \quad (2.65)$$

$$\dot{X}_i = J_{ii} * S_i * X_i + J_{id} * \dot{X}_d \quad (2.66)$$

$$S_d * X_d = J_{di} * S_i * X_i \quad (2.67)$$

Consequently, the general form of the modified systems of this class, and based on the general form given in equations (2.18) to (2.20), can be written as

$$\frac{d}{dt} \begin{bmatrix} X_r \\ X_i \\ X_d \\ q \end{bmatrix} = \begin{bmatrix} A_{rr} & A_{ri} & 0 & 0 \\ A_{ir} & J_{ii}S_i + RJ_{id}J_{di}S_i & -RJ_{id}S_d & \frac{1}{C}J_{id} \\ 0 & RJ_{di}S_i & -RS_d & \frac{1}{C} \\ 0 & J_{di}S_i & -S_d & 0 \end{bmatrix} \begin{bmatrix} X_r \\ X_i \\ X_d \\ q \end{bmatrix} \quad (2.68)$$

Where,  $\frac{1}{C} = K_p$ . The transformation matrix that transforms this modified system

to the PSSPF is

$$T = \begin{bmatrix} I_r & 0 & 0 & 0 \\ 0 & I_i & -J_{id} & 0 \\ 0 & J_{di}S_i & -S_d & 0 \\ 0 & 0 & 0 & R \end{bmatrix} \quad (2.69)$$

If the modified system is in the explicit form

$$\dot{X} = AX + BU$$

then, the transformed modified system will be

$$\dot{Z} = TAT^{-1}Z + TBU, \quad Z = TX$$

Where  $I_i$  is a square unit matrix whose dimension is the same as that of  $X_i$  and  $I_r$  is a square unit matrix whose dimension is the same as that of  $X_r$ . Notice that because there is only one dependent energy-storing element, the dimension of  $S_d$  is one by one and the dimension of  $X_d$  is one. Further notice that one does not have to formulate the original system to be able to formulate the modified system and transform it to the PSSPF. To obtain the transformation matrix given in (2.69) one needs to know  $J_{id}$ ,  $S_i$ , and  $S_d$ . The matrix  $J_{di} = -J_{id}^T$  which relates the flows (velocities) of the dependent and independent energy storing elements can easily be obtained from the original system bond graph; and  $S_i$  and  $S_d$  are inverse inertia matrices that are parts of the original system parameters.

### 2.5.2.1 Derivation and Proof of Existence

To derive equation (2.69), we will start from the general form for the modified systems given in equation (2.68). This form is rewritten again here in equation (2.70).

$$\frac{d}{dt} \begin{bmatrix} X_r \\ X_i \\ X_d \\ q \end{bmatrix} = \begin{bmatrix} A_{rr} & A_{ri} & 0 & 0 \\ A_{ir} & J_{ii}S_i + RJ_{id}J_{di}S_i & -RJ_{id}S_d & \frac{1}{C}J_{id} \\ 0 & RJ_{di}S_i & -RS_d & \frac{1}{C} \\ 0 & J_{di}S_i & -S_d & 0 \end{bmatrix} \begin{bmatrix} X_r \\ X_i \\ X_d \\ q \end{bmatrix} \quad (2.70)$$

Changing  $q$  to  $Rq$  and substituting  $\alpha$  for  $R^2C$  in equation (2.70) will lead to

$$\frac{d}{dt} \begin{bmatrix} X_r \\ X_i \\ X_d \\ Rq \end{bmatrix} = \begin{bmatrix} A_{rr} & A_{ri} & 0 & 0 \\ A_{ir} & J_{ii}S_i + RJ_{id}J_{di}S_i & -RJ_{id}S_d & \frac{R}{\alpha}J_{id} \\ 0 & RJ_{di}S_i & -RS_d & \frac{R}{\alpha} \\ 0 & RJ_{di}S_i & -RS_d & 0 \end{bmatrix} \begin{bmatrix} X_r \\ X_i \\ X_d \\ Rq \end{bmatrix} \quad (2.71)$$

Equation (2.71) means that

$$F_0 = \begin{bmatrix} 0 & 0 & 0 & 0 \\ 0 & J_{id}J_{di}S_i & -J_{id}S_d & \frac{1}{\alpha}J_{id} \\ 0 & J_{di}S_i & -S_d & \frac{1}{\alpha} \\ 0 & J_{di}S_i & -S_d & 0 \end{bmatrix} \quad (2.72)$$

This means that the null space of  $F_0$  is

$$Y = \begin{bmatrix} Y_r \\ Y_i \\ \frac{J_{di}S_i}{S_d}Y_i \\ 0 \end{bmatrix}$$

and that the two orthogonal vectors to the null space can be chosen as

$$\begin{bmatrix} 0 \\ (J_{di}S_i)^T \\ -S_d \\ 0 \end{bmatrix} \text{ and } \begin{bmatrix} 0 \\ 0 \\ 0 \\ 1 \end{bmatrix}$$

This means that the  $Q$  matrix can be written as

$$Q = \begin{bmatrix} 0 & J_{di}S_i & -S_d & 0 \\ 0 & 0 & 0 & 1 \end{bmatrix} \quad (2.73)$$

To select the slow variables, find  $P$  (the left null space of  $F_0$ ) such that  $PF_0 = 0$ .

This will produce

$$P = \begin{bmatrix} P_{rr} & P_{ri} & -P_{ri}J_{id} & 0 \\ P_{ir} & P_{ii} & -P_{ii}J_{id} & 0 \end{bmatrix} \quad (2.74)$$

Where,  $P_{rr}$ ,  $P_{ri}$ ,  $P_{ir}$ , and  $P_{ii}$  are arbitrarily chosen so that the transformation matrix is nonsingular. To get the meaningful slow variables that we want (as explained in the examples above), select

$$P_{ir} = 0, \quad P_{ii} = I_i \quad (2.75)$$

$$P_{rr} = I_r, \quad P_{ri} = 0 \quad (2.76)$$

combining the change of variable  $q$  to  $Rq$  with  $P$  and  $Q$ , we can get the transformation matrix  $T$  as in equation (2.69) to be applied directly to the general form (2.70).

Next we will show that the transformation matrix given in equation (2.69) is always nonsingular.

$$\det (T) = R \det (I_r) \det (I_i) \det (-S_d + J_{di} S_i I_i^{-1} J_{id})$$

$$= \pm R \det (S_d + J_{id}^T S_i J_{id})$$

Since  $S_i$  and  $S_d$  are inertia matrices, they must be positive definite. Therefore,

$$S_d > 0, \text{ and}$$

$$J_{id}^T S_i J_{id} \geq 0, \text{ with the inequality satisfied when } J_{id} \text{ is nonsingular.}$$

This proves that  $\det (T) \neq 0$  which means that the transformation exists.

### 2.5.2.2 Example of Using the Transformation Matrix

This sub-section shows an example of using the transformation matrix defined above to transform a modified system to the PSSPF. Figure 2.12 and Figure 2.13 shows a schematic diagram of a fluid pipe system and its bond graph model respectively. Figure 2.14 shows a bond graph model for the modified system.

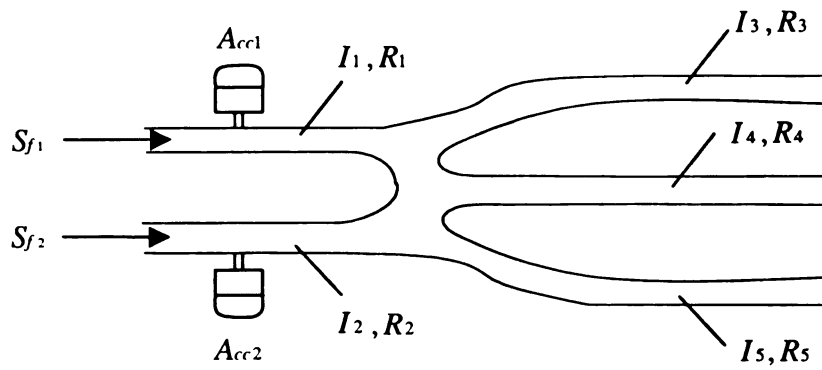


Figure 2.12. Schematic diagram of the fluid pipe system

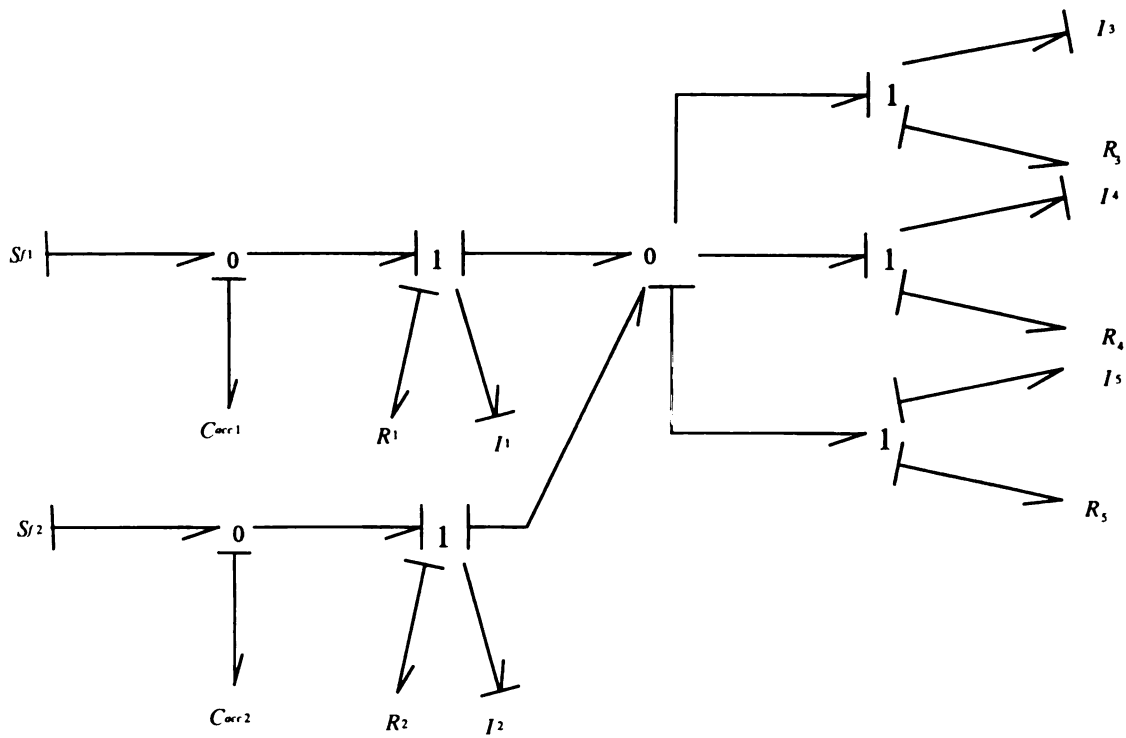


Figure 2.13. Bond graph for the original fluid pipe system

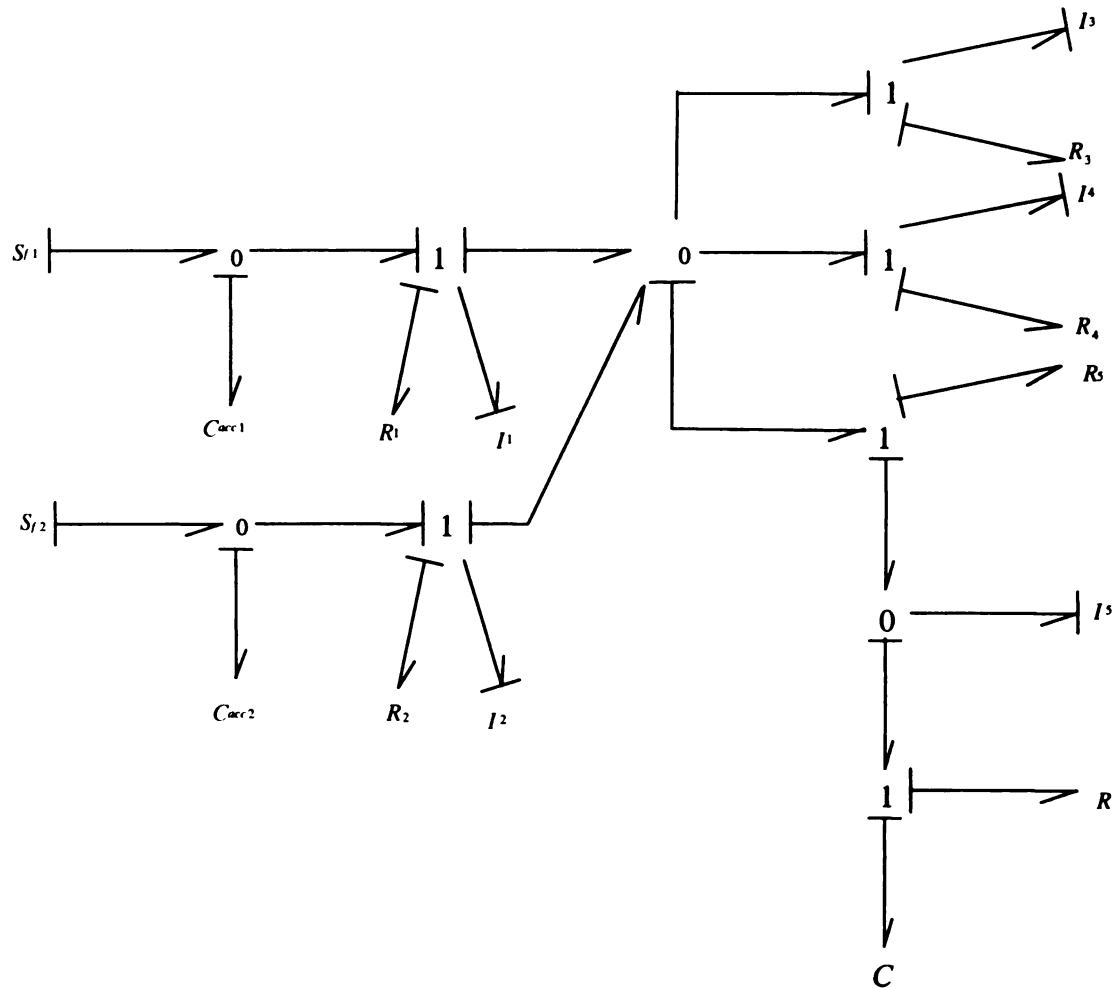


Figure 2.14. Bond graph for the modified fluid pipe system model

For this system

$$X_i = \begin{bmatrix} p1 \\ p2 \\ p3 \\ p4 \end{bmatrix},$$

$$X_d = [p5],$$

$$X_r = \begin{bmatrix} q1 \\ q2 \end{bmatrix},$$

$$S_i = \begin{bmatrix} \frac{1}{I_1} & & & \\ & \frac{1}{I_2} & & \\ & & \frac{1}{I_3} & \\ & & & \frac{1}{I_4} \end{bmatrix}, \quad S_d = \begin{bmatrix} \frac{1}{I_5} \end{bmatrix}, \quad J_{di} = [1 \quad 1 \quad -1 \quad -1]$$

Using the SCAP, the modified system can be written as

$$\frac{dq_1}{dt} = S_{f1} - \frac{p_1}{I_1}$$

$$\frac{dq_2}{dt} = S_{f2} - \frac{p_2}{I_2}$$

$$\frac{dp_1}{dt} = \frac{1}{C_{acc1}} q_1 - R_1 \frac{p_1}{I_1} - \frac{1}{C} q - R \left( \frac{p_1}{I_1} + \frac{p_2}{I_2} - \frac{p_3}{I_3} - \frac{p_4}{I_4} - \frac{p_5}{I_5} \right) - R_5 \left( \frac{p_1}{I_1} + \frac{p_2}{I_2} - \frac{p_3}{I_3} - \frac{p_4}{I_4} \right)$$

$$\frac{dp_2}{dt} = \frac{1}{C_{acc2}} q_2 - R_2 \frac{p_2}{I_2} - \frac{1}{C} q - R \left( \frac{p_1}{I_1} + \frac{p_2}{I_2} - \frac{p_3}{I_3} - \frac{p_4}{I_4} - \frac{p_5}{I_5} \right) - R_5 \left( \frac{p_1}{I_1} + \frac{p_2}{I_2} - \frac{p_3}{I_3} - \frac{p_4}{I_4} \right)$$

$$\frac{dp_3}{dt} = \frac{1}{C} q + R \left( \frac{p_1}{I_1} + \frac{p_2}{I_2} - \frac{p_3}{I_3} - \frac{p_4}{I_4} - \frac{p_5}{I_5} \right) + R_5 \left( \frac{p_1}{I_1} + \frac{p_2}{I_2} - \frac{p_3}{I_3} - \frac{p_4}{I_4} \right) - R_3 \frac{p_3}{I_3}$$

$$\frac{dp_4}{dt} = \frac{1}{C} q + R \left( \frac{p_1}{I_1} + \frac{p_2}{I_2} - \frac{p_3}{I_3} - \frac{p_4}{I_4} - \frac{p_5}{I_5} \right) + R_5 \left( \frac{p_1}{I_1} + \frac{p_2}{I_2} - \frac{p_3}{I_3} - \frac{p_4}{I_4} \right) - R_4 \frac{p_4}{I_4}$$

$$\frac{dp_5}{dt} = \frac{1}{C} q + R \left( \frac{p_1}{I_1} + \frac{p_2}{I_2} - \frac{p_3}{I_3} - \frac{p_4}{I_4} - \frac{p_5}{I_5} \right)$$

$$\frac{dq}{dt} = \frac{p_1}{I_1} + \frac{p_2}{I_2} - \frac{p_3}{I_3} - \frac{p_4}{I_4} - \frac{p_5}{I_5}$$

Consequently, the modified homogeneous system can be written in the matrix form as



$$\frac{d}{dt} \begin{bmatrix} q^1 \\ q^2 \\ p^1 \\ p^2 \\ p^3 \\ p^4 \\ p^5 \\ q \end{bmatrix} = \begin{bmatrix} 0 & 0 & -\frac{1}{I_1} & 0 & 0 & 0 & 0 & 0 \\ 0 & 0 & 0 & -\frac{1}{I_2} & 0 & 0 & 0 & 0 \\ \frac{1}{C_1} & 0 & -\frac{R+R_1+R_5}{I_1} & -\frac{I_2}{R+R_5} & \frac{R+R_5}{I_3} & \frac{R+R_5}{I_4} & \frac{R}{I_5} & -\frac{1}{C} \\ 0 & \frac{1}{C_2} & -\frac{I_1}{R+R_5} & -\frac{I_2}{R+R_2+R_5} & \frac{I_3}{R+R_5} & \frac{I_4}{R+R_5} & \frac{R}{I_5} & -\frac{1}{C} \\ 0 & 0 & \frac{I_1}{R+R_5} & \frac{I_2}{R+R_5} & -\frac{I_3}{R+R_3+R_5} & -\frac{I_4}{R+R_5} & -\frac{R}{I_5} & \frac{1}{C} \\ 0 & 0 & \frac{I_1}{R+R_5} & \frac{I_2}{R+R_5} & -\frac{I_3}{R+R_5} & -\frac{I_4}{R+R_4+R_5} & -\frac{R}{I_5} & \frac{1}{C} \\ 0 & 0 & \frac{I_1}{R} & \frac{I_2}{R} & -\frac{I_3}{R} & -\frac{I_4}{R} & -\frac{I_5}{R} & \frac{1}{C} \\ 0 & 0 & \frac{1}{I_1} & \frac{1}{I_2} & -\frac{1}{I_3} & -\frac{1}{I_4} & -\frac{1}{I_5} & 0 \end{bmatrix}$$

Using equation (2.69) the transformation matrix can be written as

$$T = \begin{bmatrix} 1 & 0 & 0 & 0 & 0 & 0 & 0 & 0 \\ 0 & 1 & 0 & 0 & 0 & 0 & 0 & 0 \\ 0 & 0 & 1 & 0 & 0 & 0 & 1 & 0 \\ 0 & 0 & 0 & 1 & 0 & 0 & 1 & 0 \\ 0 & 0 & 0 & 0 & 1 & 0 & -1 & 0 \\ 0 & 0 & 0 & 0 & 0 & 1 & -1 & 0 \\ 0 & 0 & \frac{1}{I_1} & \frac{1}{I_2} & -\frac{1}{I_3} & -\frac{1}{I_4} & -\frac{1}{I_5} & 0 \\ 0 & 0 & 0 & 0 & 0 & 0 & 0 & R \end{bmatrix}$$

With this transformation, the states of the transformed modified system are

$$\begin{bmatrix} q^1 \\ q^2 \\ p^1 + p^5 \\ p^2 + p^5 \\ p^3 - p^5 \\ p^4 - p^5 \\ \frac{p^1}{I_1} + \frac{p^2}{I_2} - \frac{p^3}{I_3} - \frac{p^4}{I_4} - \frac{p^5}{I_5} \\ Rq \end{bmatrix}$$

Notice that the original system equations are the following algebraic differential equations

$$\frac{dq_1}{dt} = S_{f1} - \frac{P_1}{I_1}$$

$$\frac{dq_2}{dt} = S_{f2} - \frac{P_2}{I_2}$$

$$\frac{dP_1}{dt} = \frac{1}{C_1} q_1 - R_1 \frac{P_1}{I_1} - \frac{dP_5}{dt} - R_5 \left( \frac{P_1}{I_1} + \frac{P_2}{I_2} - \frac{P_3}{I_3} - \frac{P_4}{I_4} \right)$$

$$\frac{dP_2}{dt} = \frac{1}{C_2} q_2 - R_2 \frac{P_2}{I_2} - \frac{dP_5}{dt} - R_5 \left( \frac{P_1}{I_1} + \frac{P_2}{I_2} - \frac{P_3}{I_3} - \frac{P_4}{I_4} \right)$$

$$\frac{dP_3}{dt} = \frac{dP_5}{dt} + R_5 \left( \frac{P_1}{I_1} + \frac{P_2}{I_2} - \frac{P_3}{I_3} - \frac{P_4}{I_4} \right) - R_3 \frac{P_3}{I_3}$$

$$\frac{dP_4}{dt} = \frac{dP_5}{dt} + R_5 \left( \frac{P_1}{I_1} + \frac{P_2}{I_2} - \frac{P_3}{I_3} - \frac{P_4}{I_4} \right) - R_4 \frac{P_4}{I_4}$$

$$\frac{P_5}{I_5} = \frac{P_1}{I_1} + \frac{P_2}{I_2} - \frac{P_3}{I_3} - \frac{P_4}{I_4}$$

## **CHAPTER 3**

### **DESIGN OF A CLASS OF TWO-TIME-SCALE MULTIPOINT MODELS**

#### **3.1 Introduction**

Analysis carried out in CHAPTER 2 gave insight into the problem under investigation; and showed how to transform a modified system from the class of systems under investigation to the PSSPF. This sets the stage for taking advantage of several tools that are provided by the singular perturbation method. CHAPTER 3 will take advantage of some of these tools, together with some other tools, to design the class of systems under investigation. The design objective, which is the same as the chapter objective, is to achieve the greatest possible simulation efficiency for a specified approximation accuracy by making the appropriate choices for the values of the parasitic element parameters. As explained earlier, the computational efficiency and the approximation accuracy of the modified systems can be traded off together.

#### **3.2 A Model for the Fast Sub-System and Proof of Stability**

As indicated earlier, if the modified system is correctly designed, it should be a two-time-scale system, so that the modifications would not greatly affect the behavior of the original system's variables. This two-time-scale system should contain two sub-systems; the slow sub-system and the fast sub-system. The slow sub-system represents the original system, which is known and there is an

obvious interest in not altering its behavior. The fast sub-system results from inserting the parasitic parameters. It is well understood that the fast sub-system will affect the behavior of the slow (original) one. Unfortunately, there is not much known about the fast sub-system. Particularly, there is no published work that characterizes or models it. Therefore, the first step in this effort of designing the fast sub-system is to model it. This section will carry on some of the results obtained in CHAPTER 2 to achieve this task. In addition, the results obtained in this section directly address the stability of the fast sub-system and consequently, of the whole modified system.

Work presented in CHAPTER 2 derived a general form for the transformation matrix  $T$  and the matrix  $F_0$  that is used to select the fast and slow variables, so that a modified system in the general form (3.1) can be transformed to the standard form (3.2) and (3.3). These general forms are rewritten again here, for the reader's convenience.

$$\frac{d}{dt} \begin{bmatrix} X_r \\ X_i \\ X_d \\ q \end{bmatrix} = \begin{bmatrix} A_{rr} & A_{ri} & 0 & 0 \\ A_{ir} & J_{ii}S_i + RJ_{id}J_{di}S_i & -RJ_{id}S_d & \frac{1}{C}J_{id} \\ 0 & RJ_{di}S_i & -RS_d & \frac{1}{C} \\ 0 & J_{di}S_i & -S_d & 0 \end{bmatrix} \begin{bmatrix} X_r \\ X_i \\ X_d \\ q \end{bmatrix} \quad (3.1)$$

$$\dot{x} = A_{11}(\varepsilon)x + A_{12}(\varepsilon)\eta \quad (3.2)$$

$$\varepsilon\dot{\eta} = \varepsilon A_{21}(\varepsilon)x + A_{22}(\varepsilon)\eta \quad (3.3)$$

$$F_0 = \begin{bmatrix} 0 & 0 & 0 & 0 \\ 0 & J_{id}J_{di}S_i & -J_{id}S_d & \frac{1}{\alpha}J_{id} \\ 0 & J_{di}S_i & -S_d & \frac{1}{\alpha} \\ 0 & J_{di}S_i & -S_d & 0 \end{bmatrix} \quad (3.4)$$

$$T = \begin{bmatrix} P \\ Q \end{bmatrix} = \begin{bmatrix} I_r & 0 & 0 & 0 \\ 0 & I_i & -J_{id} & 0 \\ 0 & J_{di}S_i & -S_d & 0 \\ 0 & 0 & 0 & 1 \end{bmatrix} \quad (3.5)$$

Kokotovic et al. (1986) showed that

$$A_{22}(0) = QF_0W \quad (3.6)$$

where,

$$T^{-1} = [V \quad W] \quad (3.7)$$

As the general form for both  $F_0$  and  $Q$  have been derived in CHAPTER 2 (they are rewritten above as (3.4) and (3.5)), the only remaining piece that is needed to calculate  $A_{22}(0)$  from equation (3.6) is  $W$ . To find  $W$ , we will derive  $T^{-1}$  using equation (3.5), and then use equation (3.7) to find  $W$ . From equation (3.5)

$$T^{-1} = \begin{bmatrix} I_r^{-1} & 0 & 0 \\ 0 & G^{-1} & 0 \\ 0 & 0 & 1 \end{bmatrix} \text{ where, } G = \begin{bmatrix} I_i & -J_{id} \\ J_{di}S_i & -S_d \end{bmatrix}$$

Using an inverse block matrices formula (see for example Kailath 1980), it can be shown that

$$G^{-1} = \begin{bmatrix} I_i^{-1} - \frac{J_{id} J_{di} S_i}{S_d - J_{di} S_i J_{id}} & \frac{J_{id}}{-S_d + J_{di} S_i J_{id}} \\ \frac{J_{di} S_i}{S_d - J_{di} S_i J_{id}} & \frac{1}{-S_d + J_{di} S_i J_{id}} \end{bmatrix} \text{ and consequently, it can be}$$

shown that

$$W = \begin{bmatrix} 0 & 0 \\ \frac{J_{id}}{-S_d + J_{di} S_i J_{id}} & 0 \\ \frac{1}{-S_d + J_{di} S_i J_{id}} & 0 \\ 0 & 1 \end{bmatrix}$$

Therefore, using equation (3.6) it can be shown that

$$A_{22}(0) = QF_0 W = \begin{bmatrix} -(S_d + J_{id}^T S_i J_{id}) & \frac{-1}{\alpha} (S_d + J_{id}^T S_i J_{id}) \\ 1 & 0 \end{bmatrix} \quad (3.8)$$

and consequently, as  $\varepsilon$  becomes small, the fast sub-system dynamics can be written as

$$\frac{1}{\varepsilon} A_{22}(0) = \begin{bmatrix} -R(S_d + J_{id}^T S_i J_{id}) & \frac{-R}{\alpha} (S_d + J_{id}^T S_i J_{id}) \\ R & 0 \end{bmatrix} \quad (3.9)$$

Assuming that  $\varepsilon$  is small enough, equation (3.9) models the fast sub-system.

The term

$$\frac{1}{(S_d + J_{id}^T S_i J_{id})} \equiv I_{eq} \quad (3.10)$$

is the equivalent of the inertia field evaluated at (reflected on) the dependent energy-storing element. Therefore, equation (3.9) can be written as

$$A_f = \begin{bmatrix} -\frac{R}{I_{eq}} & \frac{-R}{R^2 C I_{eq}} \\ R & 0 \end{bmatrix} \quad (3.11)$$

where  $A_f$  refers to the fast sub-system dynamics, and  $I_{eq}$  refers to the equivalent of the inertia field evaluated at (reflected on) the dependent energy-storing element. Using equation (3.11), the characteristic equation of  $A_f$  can be written as

$$\lambda^2 + \frac{R}{I_{eq}} \lambda + \frac{1}{C I_{eq}} = 0 \quad (3.12)$$

Equation (3.12) is the characteristic equation of a series R-L-C circuit, with the term  $I_{eq}$  as the inductance of L. This result shows that, as  $\varepsilon$  gets small, the fast sub-system can be approximated by the parasitic capacitance, the parasitic resistance, and  $I_{eq}$  connected in series. This model should be very useful for any design work for the two-time-scale modified system; and it will be used in the design algorithm to be presented later in this chapter. The condition, of having a small enough  $\varepsilon$ , imposed on the validity of this model is not detrimental at all for our framework, because it is the same condition that applies for any useful modified system. Equation (3.12) also proves the stability of the fast sub-system for a small enough  $\varepsilon$ , which means that the whole two-time-scale modified system will be stable, if the original system is stable (Kokotovic et al. 1986). The model of the fast sub-system described above can be shown in a graphical form. Figure 3.1 shows a bond graph model of the fast sub-system.

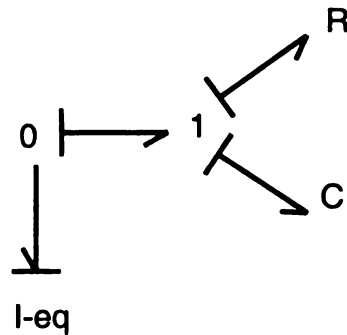


Figure 3.1. A bond graph model of the fast sub-system

Notice that the parasitic elements  $R$  and  $C$  are linear by choice. The model given in Figure 3.1 is derived for linear systems; however, it will be useful for nonlinear systems too. That will be shown later in CHAPTER 4.

### 3.3 Validating the Fast Sub-System Model

The model of equation (3.11) for the fast sub-system is very important; but it should be validated before it is used. As the model is an approximation that is good when  $\varepsilon$  is "small enough," this validation should also help us to get an idea of what "small enough  $\varepsilon$ " means.



### 3.3.1 Accuracy of Slow and Fast Poles Locations

In this sub-section we examine the accuracy of the fast and slow poles of the modified system after using the fast sub-system model to choose the values of the parasitic elements to place the fast poles at certain specified locations. The first example used is the electrical circuit that was introduced as Example 2 in CHAPTER 2. The homogeneous original system of Example 2 that was given in equations (2.45) to (2.47); and its homogeneous modified system that was given in equations (2.48) to (2.51) are rewritten here again for the reader's convenience.

$$\frac{dq_1}{dt} = \frac{p_1}{I_1} \quad (2.45)$$

$$\frac{dp_1}{dt} = -\frac{1}{C_1}q_1 - m\left(mR_1\frac{p_1}{I_1} + \frac{dp_2}{dt}\right) \quad (2.46)$$

$$\frac{p_2}{I_2} = m\frac{p_1}{I_1} \quad (2.47)$$

$$\frac{dq_1}{dt} = \frac{p_1}{I_1} \quad (2.48)$$

$$\frac{dp_1}{dt} = -\frac{1}{C_1}q_1 - \frac{m^2(R + R_1)}{I_1}p_1 + \frac{mR}{I_2}p_2 - \frac{m}{C}q \quad (2.49)$$

$$\frac{dp_2}{dt} = \frac{mR}{I_1}p_1 - \frac{R}{I_2}p_2 + \frac{1}{C}q \quad (2.50)$$

$$\frac{dq}{dt} = \frac{m}{I_1}p_1 - \frac{1}{I_2}p_2 \quad (2.51)$$

Three different cases of Example 2 were examined in this validation work; every case had a different set of original system parameters values. The three different sets of parameters were chosen such that:

- 1) One set produces an over damped original system, one set produces a critically damped original system, and one set produces an under damped original system.
- 2) The real part of the fastest pole in all cases is equal to  $-0.25$ , to make comparing the three different cases with one another easier and more meaningful.

The used three different sets of original system parameters along side with their corresponding eigenvalues are as follows.

**Case one:**

$$\begin{array}{llll} C1 = 0.0107 & I1 = I2 = 1250 & R1 = 1000 & m = 1 \\ \lambda_1 = -0.25 & \lambda_2 = -0.15 & & \end{array}$$

**Case two:**

$$\begin{array}{llll} C1 = 0.008 & I1 = I2 = 1000 & R1 = 1000 & m = 1 \\ \lambda_1 = -0.25 & \lambda_2 = -0.25 & & \end{array}$$

**Case three:**

$$\begin{array}{llll} C1 = 0.004 & I1 = I2 = 1000 & R1 = 1000 & m = 1 \\ \lambda_1 = -0.25 + i0.2501 & \lambda_2 = -0.25 - i0.2501 & & \end{array}$$

We assume that we desire the two fast poles to be critically damped and to be at a certain desired pole location (DPL). Then, equation (3.12) is used to calculate the values of the parasitic parameters that will place the fast poles at the desired

location. These values of the calculated parasitic parameters are used in the modified model and subsequently, the eigenvalues of the modified model are calculated to examine how close the fast poles to the specified desired ones and how close the slow poles to the original system poles. Notice to use equation (3.12) to calculate the values of the parasitic parameters, we need to know  $I_{eq}$ , in addition to the two desired location of the poles.  $I_{eq}$  Can be calculated using equation (3.10); it can be shown it is, for this example, equal to

$$\frac{1}{\frac{1}{I_1} + \frac{1}{I_2}}$$

Tables 3.1 to 3.3 show the calculated eigenvalues from the modified system (as described above) for every desired pole location (DPL) that was examined; the three different cases of the example are shown. The first column in every table lists the eigenvalues of the original system. PR is the ratio between the used desired pole location and the real part of fastest pole in the original system.

Orig	DPL=-1.25	DPL=-2.5	DPL=-5	DPL=-7.5	DPL=-12.5	DPL=-17.5	DPL=-25
	PR=5	PR=10	PR=20	PR=30	PR=50	PR=70	PR=100
	-2.2744	-3.7827	-6.6724	-9.4794	-14.9726	-20.3766	-28.3881
	-0.5709	-1.6101	-3.7261	-5.9199	-10.4271	-15.0233	-22.0119
-0.25	-0.3093	-0.2592	-0.2529	-0.2519	-0.2514	-0.2513	-0.2512
-0.15	-0.1454	-0.148	-0.1486	-0.1488	-0.1488	-0.1488	-0.1488

Table 3.1 Validating the fast sub-system model against Example 2, case 1

Orig	DPL=-1.25	DPL=-2.5	DPL=-5	DPL=-7.5	DPL=-12.5	DPL=-17.5	DPL=-25
	PR=5	PR=10	PR=20	PR=30	PR=50	PR=70	PR=100
	-2.4509	-3.9817	-6.9112	-9.7517	-15.3003	-20.7505	-28.821
	-0.4201	-1.5041	-3.5859	-5.7471	-10.1993	-14.7493	-21.6789
-0.25	0.1194i	-0.2869	-0.2648	-0.2593	-0.2553	-0.2537	-0.2526
-0.25	-0.2089	-0.2274	-0.2381	-0.2419	-0.2451	-0.2465	-0.2475

Table 3.2 Validating the fast sub-system model against Example 2, case 2

Orig	DPL=-1.25	DPL=-2.5	DPL=-5	DPL=-7.5	DPL=-12.5	DPL=-17.5	DPL=-25
	PR=5	PR=10	PR=20	PR=30	PR=50	PR=70	PR=100
	-2.3995	-3.9485	-6.8893	-9.7343	-15.2872	-20.7396	-28.8119
	-0.64	-1.5547	-3.6111	-5.7658	-10.2128	-14.7604	-21.6881
-0.25	-0.2303	-0.2484	-0.2498	-0.25	-0.25	-0.25	-0.25
0.25i	0.2723i	0.2561i	0.2514i	0.2506i	0.2502i	0.2501i	0.2501i

Table 3.3 Validating the fast sub-system model against Example 2, case 3

In addition to the results shown in the tables 3.1 to 3.3, Figure 3.1 shows a summary of the error in the fast poles locations compared with the DPL; and shows the value of  $R$ , both against the normalized fast poles location (PR); notice that  $R = \frac{1}{\epsilon}$ . Every error shown in Figure 3.1 is the average of the errors of the two fast poles with respect to the DPL. The three different cases of the example are shown. The results of this example and of the next example will be examined and explained together.

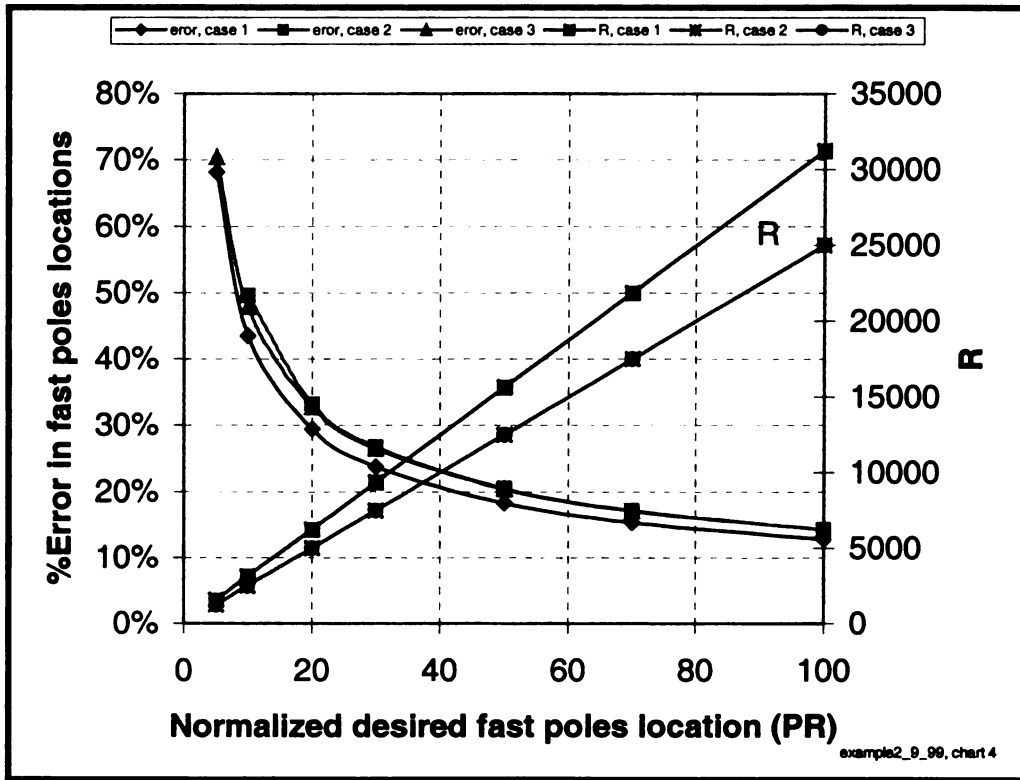


Figure 3.1. Effect of fast pole locations on the accuracy of the fast sub-system model for Example 2

The second example that is used to validate the fast sub-system model is the fluid pipe system (Example 3) that was introduced in CHAPTER 2. The homogeneous original system equations for this example was given in CHAPTER 2 as

$$\frac{dq_1}{dt} = -\frac{P_1}{I_1}$$

$$\frac{dq_2}{dt} = -\frac{P_2}{I_2}$$

$$\frac{dP_1}{dt} = \frac{1}{C_1}q_1 - R_1\frac{P_1}{I_1} - \frac{dP_5}{dt} - R_5\left(\frac{P_1}{I_1} + \frac{P_2}{I_2} - \frac{P_3}{I_3} - \frac{P_4}{I_4}\right)$$

$$\frac{dP_2}{dt} = \frac{1}{C_2}q_2 - R_2\frac{P_2}{I_2} - \frac{dP_5}{dt} - R_5\left(\frac{P_1}{I_1} + \frac{P_2}{I_2} - \frac{P_3}{I_3} - \frac{P_4}{I_4}\right)$$

$$\frac{dP_3}{dt} = \frac{dP_5}{dt} + R_5\left(\frac{P_1}{I_1} + \frac{P_2}{I_2} - \frac{P_3}{I_3} - \frac{P_4}{I_4}\right) - R_3\frac{P_3}{I_3}$$

$$\frac{dP_4}{dt} = \frac{dP_5}{dt} + R_5\left(\frac{P_1}{I_1} + \frac{P_2}{I_2} - \frac{P_3}{I_3} - \frac{P_4}{I_4}\right) - R_4\frac{P_4}{I_4}$$

$$\frac{P_5}{I_5} = \frac{P_1}{I_1} + \frac{P_2}{I_2} - \frac{P_3}{I_3} - \frac{P_4}{I_4}$$

And the modified system equations were given as

$$\frac{d}{dt} \begin{bmatrix} q_1 \\ q_2 \\ p_1 \\ p_2 \\ p_3 \\ p_4 \\ p_5 \\ q \end{bmatrix} = \begin{bmatrix} 0 & 0 & -\frac{1}{I_1} & 0 & 0 & 0 & 0 & 0 \\ 0 & 0 & 0 & -\frac{1}{I_2} & 0 & 0 & 0 & 0 \\ \frac{1}{C_1} & 0 & -\frac{R+R_1+R_5}{I_1} & -\frac{R+R_5}{I_2} & \frac{R+R_5}{I_3} & \frac{R+R_5}{I_4} & \frac{R}{I_5} & -\frac{1}{C} \\ 0 & \frac{1}{C_2} & -\frac{R+R_5}{I_1} & -\frac{R+R_2+R_5}{I_2} & \frac{R+R_5}{I_3} & \frac{R+R_5}{I_4} & \frac{R}{I_5} & -\frac{1}{C} \\ 0 & 0 & \frac{R+R_5}{I_1} & \frac{R+R_5}{I_2} & -\frac{R+R_3+R_5}{I_3} & -\frac{R+R_5}{I_4} & -\frac{R}{I_5} & \frac{1}{C} \\ 0 & 0 & \frac{R+R_5}{I_1} & \frac{R+R_5}{I_2} & -\frac{R+R_5}{I_3} & -\frac{R+R_4+R_5}{I_4} & -\frac{R}{I_5} & \frac{1}{C} \\ 0 & 0 & \frac{R+R_5}{I_1} & \frac{R+R_5}{I_2} & -\frac{R+R_5}{I_3} & -\frac{R+R_4+R_5}{I_4} & -\frac{R}{I_5} & \frac{1}{C} \\ 0 & 0 & \frac{R}{I_1} & \frac{R}{I_2} & -\frac{R}{I_3} & -\frac{R}{I_4} & -\frac{R}{I_5} & \frac{1}{C} \\ 0 & 0 & \frac{1}{I_1} & \frac{1}{I_2} & -\frac{1}{I_3} & -\frac{1}{I_4} & -\frac{1}{I_5} & 0 \end{bmatrix}$$

The following set of parameters values were used:

$$C1=0.001$$

$$C2=0.001$$

$$I1=1000$$

$$I2=200$$

$$I3=100$$

$$I4=100$$

$$I5=100$$

$$R1=3000$$

$$R2=1000$$

$$R3=1000$$

$$R4=1000$$

$$R5=1000$$

With the above given set of parameters, it can be shown that the original system eigenvalues are approximately the following:

-10.0            -10.0            -4.9042  
-2.6946        -0.96254       -0.32758

These slow eigenvalues were obtained by calculating the eigenvalues of the modified system with two very fast poles (-5012.57 & -4962.41; DPL = 5000) with respect to the original system. The same procedure described above in this subsection that was used with Example 2 was used with this example. Again equation (3.12) can be used to calculate the values of the parasitic parameters after obtaining  $I_{eq}$  that can be calculated using equation (3.10). Using equation (3.10),  $I_{eq}$  for this example is equal to

$$\frac{1}{\frac{1}{I_5} + \frac{1}{I_1} + \frac{1}{I_2} + \frac{1}{I_3} + \frac{1}{I_4}}$$

Table 3.4 shows the calculated eigenvalues from the modified system (as described above) for every desired pole location (DPL) that was used.

Orig	DPL=-50	DPL=-100	DPL=-200	DPL=-300	DPL=-500	DPL=-700	DPL=-1000
	PR=5	PR=10	PR=20	PR=30	PR=50	PR=70	PR=100
	-103.6	-166.68	-286.273	-401.678	-626.409	-846.66	-1172.3
	-18.46	-58.106	-138.77	-223.405	-398.692	-578.447	-852.8
-10	-13.039	-10.3186	-10.0675	-10.0287	-10.01	-10.005	-10
-10	-10	-10	-10	-10	-10	-10	-10
-4.9042	-4.9169	-4.9072	-4.9049	-4.9045	-4.9043	-4.9043	-4.9
-2.6946	-2.6946	-2.6946	-2.6946	-2.6946	-2.6946	-2.6946	-2.7
-0.96254	-0.9625	-0.9625	-0.9625	-0.9625	-0.9625	-0.9625	-1
-0.32758	-0.3276	-0.3276	-0.3276	-0.3276	-0.3276	-0.3276	-0.3

Table 3.4 Validating the fast sub-system model against Example 3

Figure 3.2 (similar to Figure 3.1) shows a summary of the error in the fast poles locations compared with the DPL; and shows the value of  $R$  both against the normalized fast poles location.

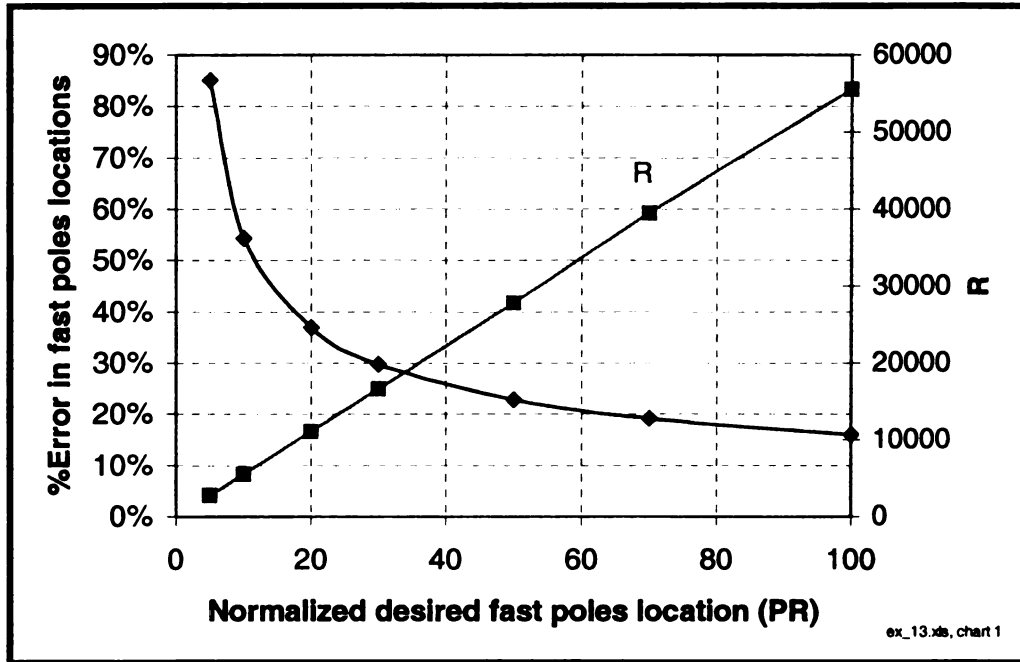


Figure 3.2. Effect of fast pole locations on the accuracy of the fast sub-system model for Example 3

Examining tables 3.1 to 3.4, it is noticeable that across the range of PR that is shown in the tables, the slow eigenvalues are very close to the original system eigenvalues except for one value in case two of Example 2 (1<sup>st</sup> column in table 3.2), where PR is equal to five and there is no obvious separation between the fast and the slow sub-systems. This should not be disappointing because, the rule of thumb is that there should be an order of magnitude separation (this corresponds to PR=10) so that the fast sub-system would not greatly affect the



slow one. On the other hand, it is apparent from tables 3.1 to 3.4 that the locations of the fast poles are somewhat different from the DPL that was used in equation (3.12) to calculate the parasitic elements parameters. Figure 3.1 and Figure 3.2 show that as the ratio PR (called normalized desired fast poles location in the figures) increases over ten the error rapidly decreases. It can also be noticed that for all cases shown in both figures, for a DPL that is an order of magnitude, or more, faster than the original system (this corresponds to PR bigger than or equal to ten) the following holds true:

- 1) The error in the fast poles locations are at or less than 55%.
- 2) The locations of the slow poles are very close to those of the original system (within 5%).

### 3.3.2 Conditions of Two Critically Damped Fast Poles

In this sub-section we examine the validity of the conditions, provided by the model under validation, for having two critically damped fast poles. These conditions are of particular interest; later it will be argued that a pair of two critically damped poles is the recommended choice for fast poles. The characteristic equation of the fast sub-system model was given in equation (3.12) as

$$\lambda^2 + \frac{R}{I_{eq}}\lambda + \frac{1}{CI_{eq}} = 0 \quad (3.12)$$

For the roots of this equation to be critically damped, the following relation must hold

$$\frac{R^2}{4I_{eq}^2} = \frac{1}{CI_{eq}}$$

This means that

$$R^2 C = 4I_{eq} \quad (3.13)$$

Substituting  $\frac{4}{R^2 C}$  for  $\frac{1}{I_{eq}}$  in equation (3.12) then, the characteristic equation of

the fast sub-system can be written as

$$\lambda^2 + \lambda \frac{4}{RC} + \frac{4}{R^2 C^2} = 0$$

which means that

$$P = \frac{-2}{RC}$$

Where P (identical to  $\lambda$ ) is the location of the two fast critically damped poles as  $\varepsilon$  becomes small. This result can be written as

$$P * RC = -2 \quad (3.14)$$

Equation (3.14) is a condition provided by the model for obtaining a pair of critically damped fast poles. To validate equation (3.14), different values of the product  $RC$  were chosen. For every value of  $RC$ , the values of  $R$  and  $C$  were changed until a pair of critically damped fast poles (P) were obtained from the modified system. For these values of  $R$  and  $C$  for which two critically damped fast poles occur, the location of the two critically damped poles (P) was recorded versus its corresponding  $R$  and  $RC$ . Figure 3.3 summarizes the results of this attempt for Example 2. The horizontal axis in Figure 3.3 is the value of  $R$

( $R = \frac{1}{\varepsilon}$ ); the first vertical axis shows the product  $P*RC$ . The second vertical axis shows the ratio between the critically damped fast poles location in the modified system and the real part of the fastest pole in the original system. This ratio is referred to as MO. The same procedure described in this sub-section was implemented for Example 3. Figure 3.4 (similar to Figure 3.3) summarizes the results of Example 3. Figure 3.3 and Figure 3.4 show that as  $R$  increase (i.e. as  $\varepsilon$  decreases) the product  $P*RC$  converges to minus two; this result confirms equation (3.14). They also show the product  $P*RC$  is close to minus two (within %15) for an MO ratio of ten or more (i.e. for fast poles that are an order of magnitude or more faster than the original system). It is also obvious that the product converges to minus two rapidly as MO gets bigger than ten.

Validation results shown in this sub-section and the last sub-section show that the model under validation (equation (3.11)) would be fairly accurate if the fast poles are an order of magnitude faster than the original system; and that the accuracy improves rapidly as the fast poles gets faster than an order of magnitude.

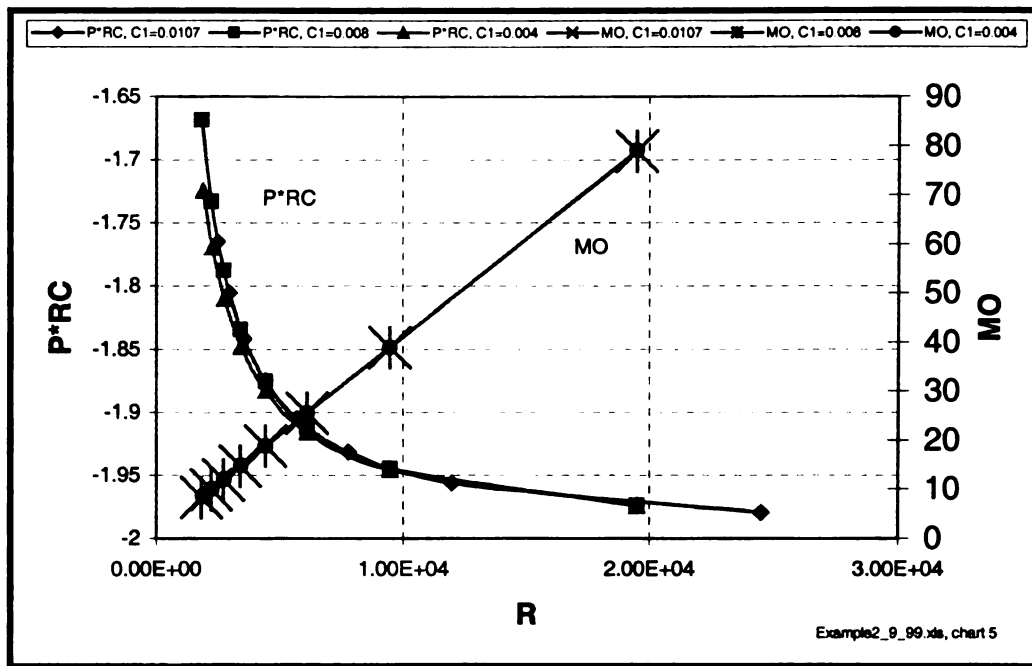


Figure 3.3. Conditions for two critically damped fast poles, Example 2

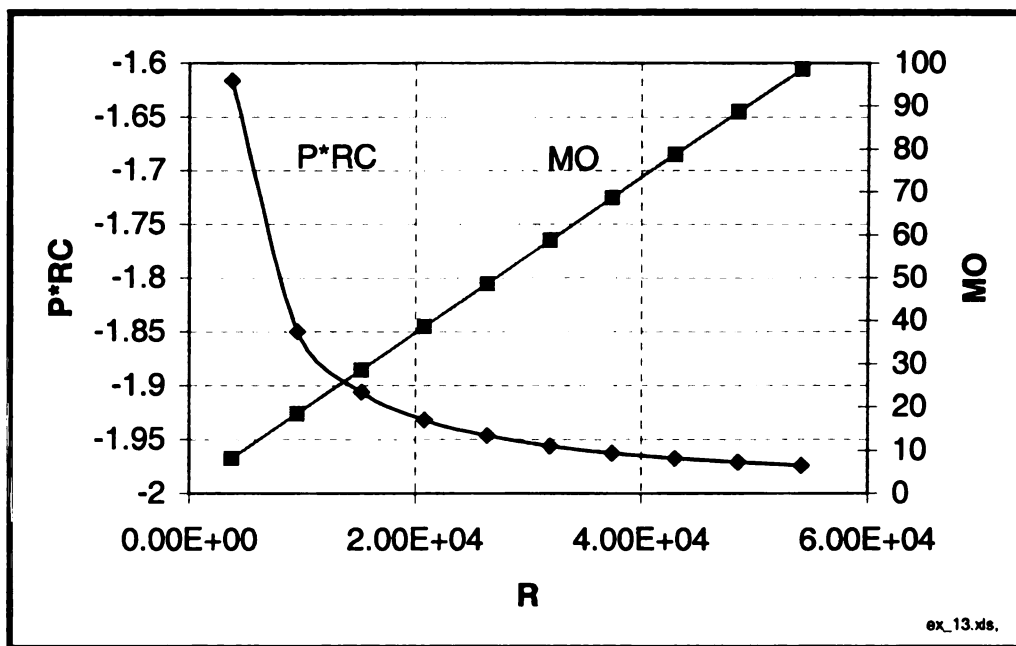


Figure 3.4. Conditions for two critically damped fast poles, Example 3

### **3.3.2.1 Advantages of Critically Damped Fast Poles**

The second order fast sub-system should be designed to be critically damped, to avoid unnecessary computational cost and potential excessive approximation errors. The reason is that if the fast sub-system is over damped, then it would contain two real poles; one of them is faster than the other. In this case the faster pole will determine the stiffness of modified system and, the less fast pole (of the two fast poles) will determine simulation accuracy. Consequently, there will be an un-necessary additional computational cost. On the other hand, if the fast subsystem is excessively under damped, there will be an overshoot and an oscillatory behavior, which is undesirable. To demonstrate this we simulate Example 1 that was introduced in CHAPTER 2. Figure 3.5 shows simulation results for calculating the state of the independent variable ( $i_1$ ) from Example 1 using three different systems: The original implicit system, the modified system with two excessively under damped fast pole, and the modified system with two critically damped poles. The product  $RC$  has the same value in the used two modified systems. It is obvious that the modified system with the two excessively under damped fast poles has oscillatory behavior that increases the approximation error introduced by the modified system. Figure 3.6 show the simulation results for the state ( $q$ ) of the dynamic parasitic element (the capacitor) using the above mentioned two modified systems. It is obvious that the case with two excessively under damped fast poles has an amplitude that is much bigger than that of the critically damped case.

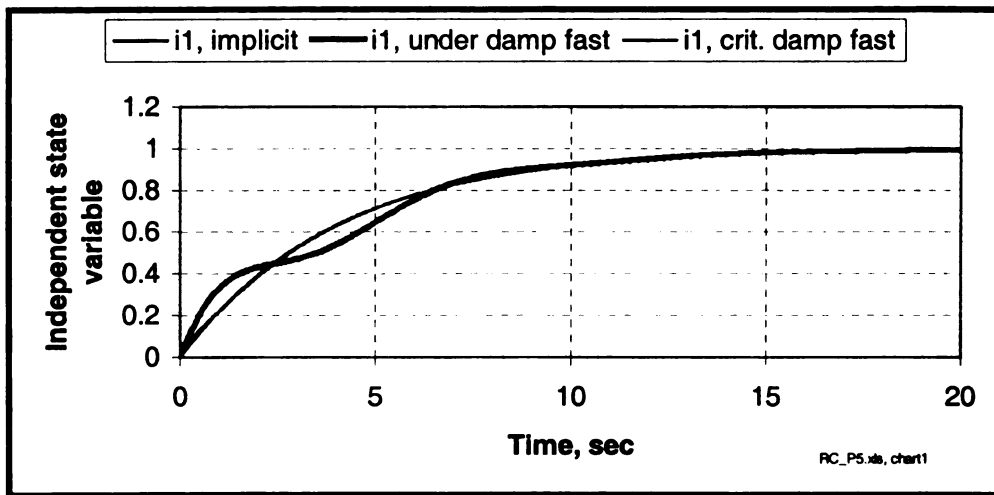


Figure 3.5. Approximation error for an excessively under damped and a critically damped fast sub-systems

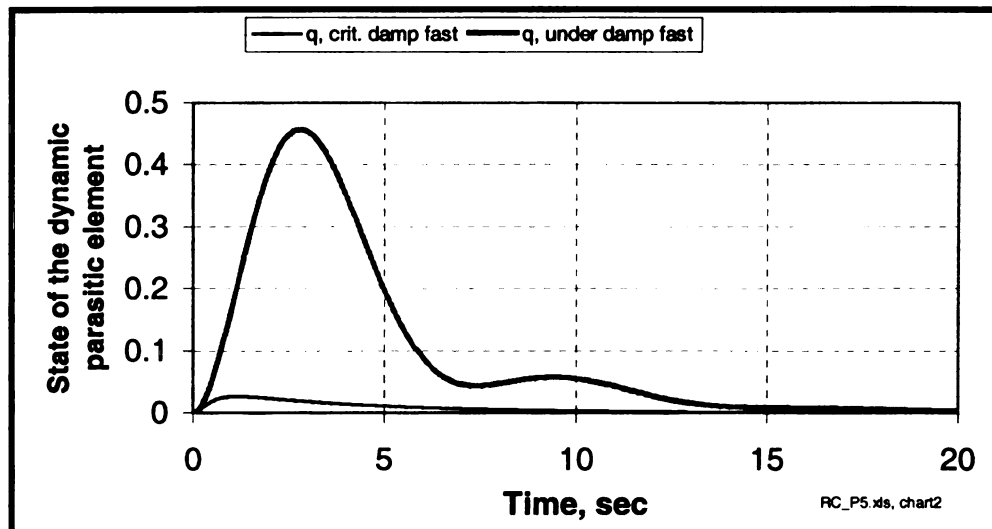


Figure 3.6. Behavior of the dynamic parasitic element for an excessively under damped and a critically damped fast sub-systems

### 3.3.3 Effect of Selected Dependent Element Value on Model Performance

If we have a storage field with a single instance of derivative causality, the choice of the dependent element is arbitrary. The fast sub-system model as given in equation (3.11) does not suggest which element one should choose as the dependent element. Therefore, we would like to answer the following questions. Suppose that we have a storage field whose elements have different values. Does the value of the selected dependent element (with respect to the independent ones) have an effect on the model performance? If there is an effect, what is the choice for which the model would perform best? This section addresses these questions through simulating Example 1 that has been introduced in CHAPTER 2.

Example 1 includes only two coupled inertances; its homogeneous original system was given in equations (2.27) to (2.28) and its homogeneous modified system was given in equations (2.29) to (2.31). These equations are rewritten here again for the reader's convenience.

$$\frac{dp1}{dt} = -m \left( mR1 \frac{p1}{I1} + \frac{dp2}{dt} \right) \quad (2.27)$$

$$\frac{p2}{I2} = m \frac{p1}{I1} \quad (2.28)$$

$$\frac{dp1}{dt} = -\frac{m^2(R + R1)}{I1} p1 + \frac{mR}{I2} p2 - \frac{m}{C} q \quad (2.29)$$

$$\frac{dp2}{dt} = \frac{mR}{I1} p1 - \frac{R}{I2} p2 + \frac{1}{C} q \quad (2.30)$$

$$\frac{dq}{dt} = \frac{m}{I1} p1 - \frac{1}{I2} p2 \quad (2.31)$$

To explore the effect of the value of the selected dependent element we simulate Example 1 with different combinations of the values of the inertances  $I1$  and  $I2$  and with both of them alternatively chosen as the dependent energy storing element. This is done for two different values of the transformer modulus ( $m$ ). The parameter  $R1$  of original system was held constant throughout these simulations at  $R1 = 1000$ . For every combination of  $I1$ ,  $I2$ , and  $m$ , we chose certain desired pole location (DPL) for a pair of critically damped fast poles. Based on this chosen location equation (3.12) was used to calculate the values of the parasitic elements  $R$  and  $C$ . These calculated values of  $R$  and  $C$  were then used in the modified model to calculate its eigenvalues. The fast eigenvalues of the modified model were then compared with the desired pole location (DPL) that was chosen and used in calculation. Figure 3.7 and Figure 3.8 summarize these simulation results for the two simulated cases,  $m = 1$  and  $m = 2$  respectively. The horizontal axis in both figures is the difference between the values of  $I1$  and  $I2$ . The two solid lines are the errors of the fast poles location for the two cases, when  $I1$  is the independent element and when  $I2$  is the independent element. Every calculated error is the average of the errors of the two fast poles with respect to the corresponding DPL. The dashed lines in



both figures shows the value  $\frac{I_2}{(I_1/m^2)}$ . It can be noticed from both figures that choosing either  $I_1$  or  $I_2$  as the independent element is not going to affect the model accuracy only at the point  $\frac{I_2}{(I_1/m^2)} = 1$ . Notice that  $(I_1/m^2)$  is the equivalent of  $I_1$  when reflected on  $I_2$ . Away from this special point the model will be more accurate if the dependent element value (or its equivalent) is smaller than that of the independent element.

It can be concluded from this sub-section that the dependent element should be chosen as the element of the least value. Notice that all element values should be evaluated at the same location.

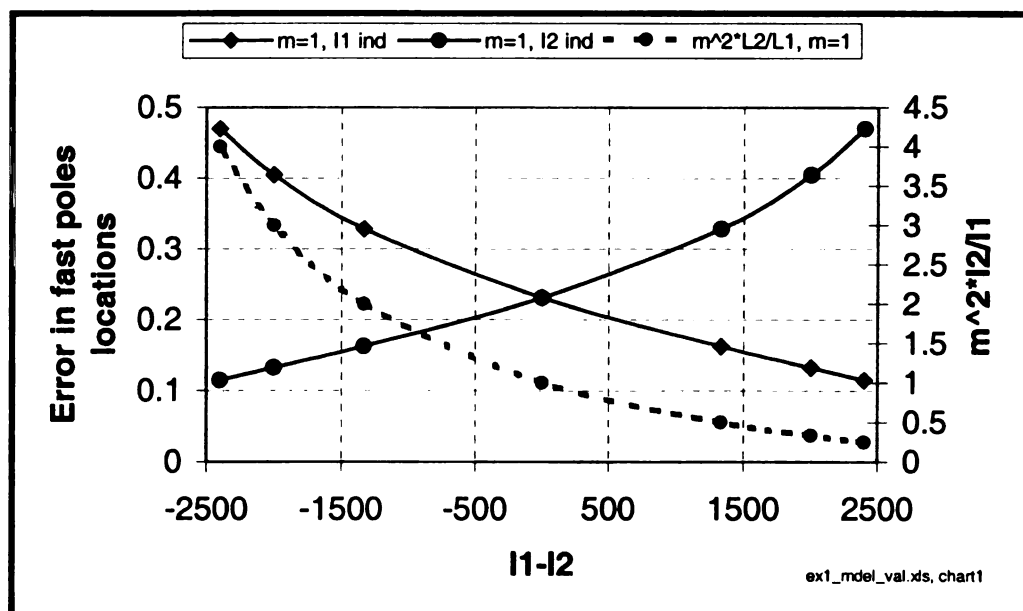


Figure 3.7. Effect of selecting the dependent element,  $m=1$

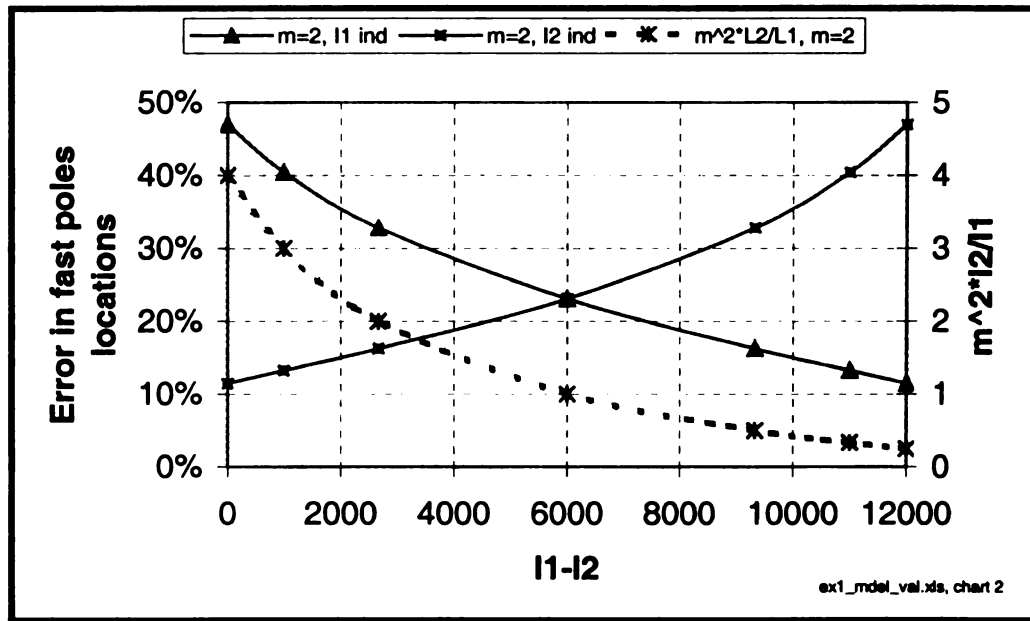


Figure 3.8. Effect of selecting the dependent element,  $m=2$

### 3.4 An Algorithm to Improve the Model Performance

Last section showed that the fast sub-system model (equation (3.11)) could be used to choose the value of the parasitic elements to locate the fast poles at certain user-defined location. Although, there would be some error in the poles locations, this error as shown above is negligible for the design objective of this work. However, this section shows an algorithm to improve the model results, in case this is of interest for other uses of the model.

The fast sub-system characteristic equation is rewritten here again for the reader's convenience.

$$I_{eq} = \frac{1}{(S_d + J_{id}^T S_i J_{id})} \quad (3.10)$$

$$\lambda^2 + \frac{R}{I_{eq}}\lambda + \frac{1}{CI_{eq}} = 0 \quad (3.12)$$

Before the algorithm is given some of the features of the characteristic equation (3.12) are demonstrated. For the roots of the characteristic equation (3.12) to have certain damping ratio  $\zeta_d$ , the following must hold true

$$4\zeta_d^2 = \frac{R^2}{I_{eq}^2} CI_{eq}, \text{ which means that}$$

$$R^2 C = 4I_{eq} \zeta_d^2 \quad (3.15)$$

Equation (3.15) means that the product  $R^2 C$  will always be a constant as  $\varepsilon$  become small. The real part of the roots of the characteristic equation (3.12) is

$$\frac{-R}{2I_{eq}} = \frac{-R^2 C}{2RC I_{eq}} = \frac{-R^2 C}{2I_{eq}} \frac{1}{RC} \quad (3.16)$$

As  $R^2 C$  is constant, equation (3.16) means that the location of the real part of the fast poles is inversely proportional to the product  $RC$ .

The method that is proposed here for improving the model results is based on successive improvements of the calculated  $I_{eq}$  using the calculated fast eigenvalues from the modified system. Assumes that the user has defined some specific locations  $\lambda_1$  and  $\lambda_2$  at which he/she would like to place the fast poles to separate them from the slow poles. Further assume that the two poles  $\lambda_1$  and  $\lambda_2$

have a real part that is referred to as  $\text{Re}(\lambda_1)$ , a damping ratio that is referred to as  $\zeta_d$ , and an undamped natural frequency that is referred to as  $\omega_{n,d}$ . The algorithm can be described as follows:

- 1) Use equation (3.10) to calculate  $I_{eq}$ , for convenience we will refer to it as

$$I_{eq,u}.$$

- 2) Calculate the values of the parasitic parameters  $R_c$  and  $C_c$  using the following equations

$$\frac{1}{I_{eq,u} C_c} = \omega_{n,d}^2 \quad (3.17)$$

$$\frac{R_c}{I_{eq,u}} = 2\zeta_d \omega_{n,d} \quad (3.18)$$

- 3) Use the calculated parasitic parameters ( $R_c$  and  $C_c$ ) from step two in the modified system model to calculate the eigenvalues of the modified system, and consequently identify the two fast poles. Let these two fast poles be  $\lambda_{1,c}$  and  $\lambda_{2,c}$ , let their corresponding damping ratio be  $\zeta_c$ , and let their natural frequency be  $\omega_{n,c}$ . If  $\zeta_c$  is "equal to"  $\zeta_d$  go to step six, otherwise proceed to step four.

- 4) Calculate an updated equivalent inertia ( $I_{eq,u}$ ) as follows

$$I_{eq,u} = \frac{R_c}{2\zeta_c \omega_{n,c}} \quad (3.19)$$

- 5) Go to step two above.

6) The final values of the parasitic elements parameters ( $R_f$  and  $C_f$ ) should be calculated from the following

$$R_f C_f = R_c C_c \frac{\text{Re}(\lambda_{1c})}{\text{Re}(\lambda_1)} \quad (3.20)$$

$$\frac{R_f}{2} \sqrt{\frac{C_f}{I_{eq\mu}}} = \zeta_d \quad (3.21)$$

The loop that includes steps two to five is used to improve the accuracy of the damping ratio of the placed poles and then step six is used to improve the accuracy of their real part. Equations (3.17) to (3.19) and (3.21) come directly from equation (3.12). Equation (3.20) is suggested by equation (3.16).

To demonstrate the effectiveness of the algorithm, we apply it to Example 3, the fluid pipe system. The desired fast poles were set to have real part of (-100) and a damping ratio of 0.7. Table 3.5 shows simulation results for implementing the algorithm with the loop involving steps two to five, repeated only five times. The first column in Table 3.5 has five labels, each one is used for its corresponding row; the next six cells are the original system's eigenvalues and the last two cells are the real part and the imaginary part of the desired poles locations respectively. The following six columns in Table 3.5 show the results for repeating the loop five times followed by the final result obtained from step six in the algorithm. It can be noticed from the table that the damping ratio of the placed fast poles converges monotonically to the desired one as we keep updating the value of the equivalent inertia. It is also remarkable that implementing step six has moved the fast poles very close to the two desired

values. It is also noticeable that in all the shown results the slow eigenvalues are very close to original system's eigenvalues.

One can repeat the loop involving steps two to five as many more times as needed; and further more can implement another loop involving steps 2 to 6 until the desired accuracy of pole placement is reached. However, as the purpose of this work does not need such accuracy; there will be no further demonstration to this idea.

	Loop, 1	Loop, 2	Loop, 3	Loop, 4	Loop, 5	Step 6
$I_{eq,u}$	24.5272	22.6945	21.6018	20.9271	20.5011	23.4986
$\zeta_c$	0.79277	0.75653	0.73541	0.72257	0.71455	0.69554
R	5555.278	4905.185	4538.673	4320.147	4185.213	4669.534
C	1.76E-06	2.00E-06	2.16E-06	2.27E-06	2.34E-06	1.84E-06
RC	0.009801	0.009801	0.009801	0.009801	0.009801	0.008605
-0.32758	-0.32758	-0.32758	-0.32758	-0.32758	-0.32758	-0.32758
-0.96254	-0.96253	-0.96253	-0.96253	-0.96253	-0.96253	-0.96253
-2.6946	-2.6946	-2.6946	-2.6946	-2.6946	-2.6946	-2.6946
-4.9042	-4.9056	-4.9058	-4.9059	-4.906	-4.906	-4.9056
-10	-10	-10	-10	-10	-10	-10
-10	-10.1335	-10.1517	-10.1643	-10.1729	-10.1786	-10.1377
-100	-112.483	-100.772	-94.1687	-90.2309	-87.7992	-96.5376
102.02	86.4819	87.1102	86.7695	86.3261	85.9614	99.7226

Table 3.5. Using the algorithm to Improve model results for Example 3

### 3.5 Design Procedure for the Fast Sub-System

It was demonstrated in the previous sections that the fast sub-system model could be used to place the fast poles at certain desired locations. This

section shows some design procedure whose objective is to achieve simulation efficiency while meeting certain accuracy bounds. As discussed earlier, the computational efforts needed to simulate the modified system increases as its stiffness increases. We have also discussed that the fast poles should be faster than the original system to avoid affecting the original system significantly. Therefore apparently, there is a need to know the location of the fastest pole in the original system. But the original system as we know is in the algebraic differential equation form, and it is not convenient to find exactly or directly its eigenvalues. This issue will be dealt with in the procedure to follow.

Assume that there is an original system whose modified system is required to be accurate to within certain specified bound, for some specified inputs. Assume that the error bounds are set for all the states of the original system and for the state of the dynamic parasitic element. The proposed algorithm can be summarized as follows:

- 1) Set  $j=0$ , where  $j$  is a counter; choose the smallest inertia as the dependent inertia. Make an initial estimate of the original system eigenvalues by omitting the dependent energy-storing element from the system. Consequently, one can determine an initial estimate of the radius of the original system's eigenvalues; let us refer to it as  $\rho_i$ .
- 2) Choose the two fast poles of the modified system to be critically damped; and choose a desired pole location for the two critically damped fast poles ( $DPL$ ) such that

$$DPL = 10 * \rho_i .$$

- 3) Use the fast sub-system model (equations (3.10) and (3.12)) to calculate the values of the parasitic parameters  $R$  and  $C$  needed to place the two fast poles at  $DPL$ . If  $j > 1$  go to step five directly
- 4) Use the calculated values for the parasitic parameters in step three in the modified explicit system and calculate the modified system eigenvalues. Assume that the real part of the two fast eigenvalues (or the slower one, if they are over damped) is  $Re_f$ ; and the calculated radius of the slow eigenvalues is  $\rho_c$ . If you can not distinguish two fast poles from the rest

of the poles, assume that  $\frac{Re_f}{\rho_c} = 1$ . If

$$\frac{Re_f}{\rho_c} < 5 , \text{ or } \frac{Re_f}{\rho_c} > 20 \text{ take}$$

$$DPL = DPL * 10 * \frac{\rho_c}{Re_f}$$

and go back to step three; otherwise proceed to step five. This will ensure enough separation between the fast and the slow sub-systems and prevent simulating an excessively stiff system during the design process unnecessarily.

- 5) Set  $j=j+1$ , and  $DPL_j = DPL$ .
- 6) Simulate the modified system and the original system and calculate the errors of the states for which the user requires bounds on their errors. Calculate the ratios between the calculated errors and the user-specified



error bounds; assume that these ratios are  $r_1, r_2, \dots, r_n$ . Find  $r_{\max}$  such that  $r_{\max, j} = \max \{r_1, r_2, \dots, r_n\}$ . Assume that the error whose ratio is  $r_{\max}$  is "e" and that its corresponding desired error is  $e_d$ .

7) If  $0.8 \leq r_{\max} \leq 1$ , go to step nine.

Otherwise;

if  $j > 1$ , calculate

$$\beta = \frac{e_j - e_{j-1}}{DPL_j - DPL_{j-1}},$$

$$DPL_{j+1} = DPL_j + \frac{e_d - e_j}{\beta}.$$

This assumes that the error is a linear function of the DPL.

If  $j=1$ , take

$$DPL = \frac{DPL_j}{fac}. \text{ Where } fac = 2, \text{ if } r_{\max} > 1, \text{ and } fac = 0.5 \text{ if } r_{\max} < 0.8$$

8) Go to step three.

9) End of design procedure.

Notice that, when the dependent energy-storing element is omitted from the original system, the system will become an explicit ODE system whose eigenvalues can easily be determined.

The procedure presented above assumes that the model of the original system is conveniently available. This assumption is true for several practical classes of systems. However, the user might prefer to deal only with the

modified explicit system. One possible reason for this preference could be avoiding deriving the implicit original model. In this case, there would be a need to find a reference other than the original implicit system to calculate the errors of the modified system with respect to. Since it is known from the singular perturbation theory that the errors of the modified system should decrease as  $\varepsilon$  decreases, we can choose this reference to be the modified system itself but with an excessively small  $\varepsilon$ . An excessively small  $\varepsilon$  means an excessively large  $R$ . To verify that certain  $\varepsilon$  is small enough for the modified system to be an “accuracy reference”, it is recommended to ensure that a further decrease (say an order of magnitude) of  $\varepsilon$  would not change the simulation results obtained from the modified system within the number of digits of accuracy required by the user. Figure 3.9 shows a flow chart for the main steps of the suggested design procedure.

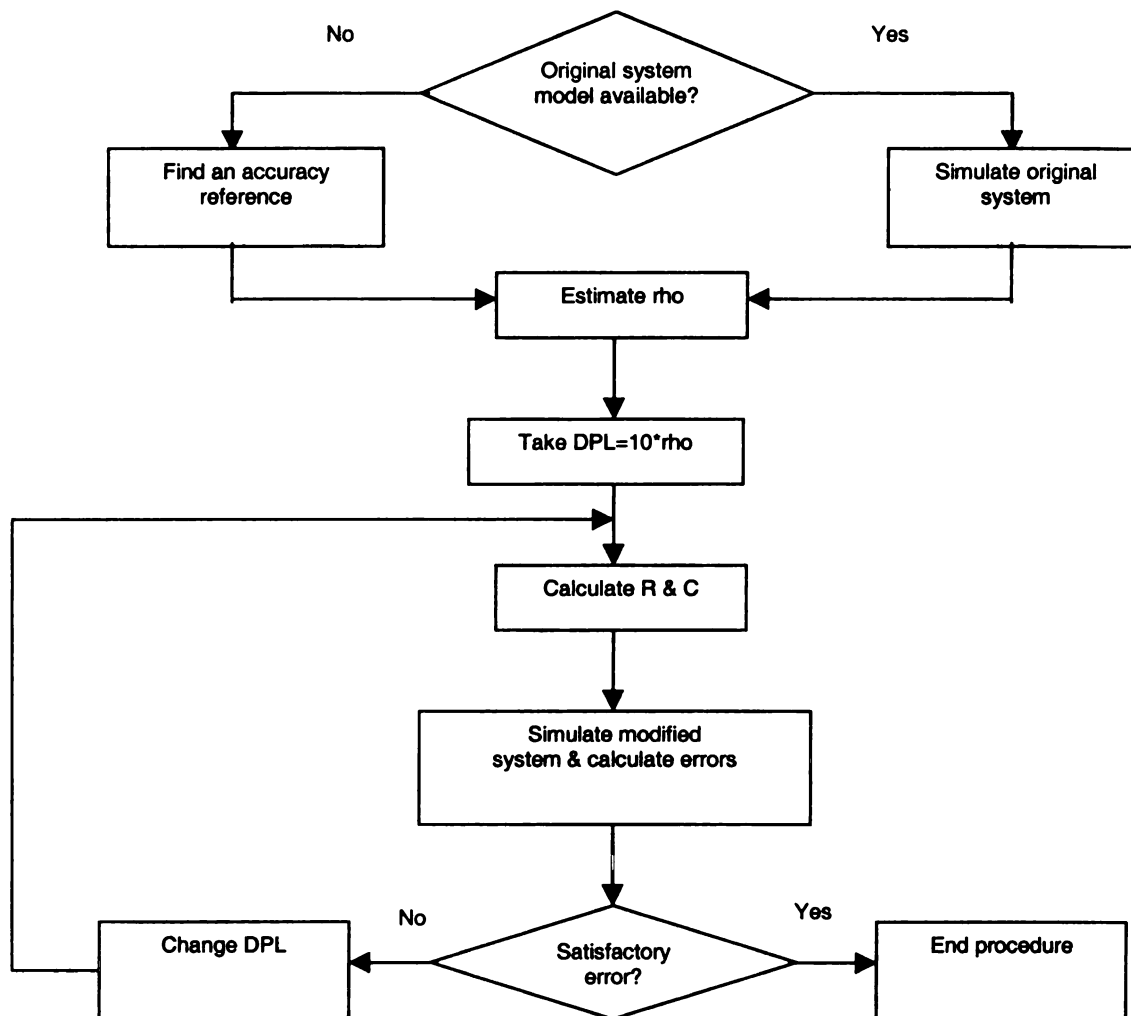


Figure 3.9. Flow chart for the proposed design procedure

### 3.5.1 An Example Using the Design Procedure

To demonstrate the usefulness of this procedure we apply it to design the fast sub-system for Example 3. The following set of parameters was used in this example:

$C1=0.0001;$        $C2=0.0001;$

$I1=100;$        $I2=100;$        $I3=100;$        $I4=100;$        $I5=100;$

$R1=300;$        $R2=300;$        $R3=100;$        $R4=100;$        $R5=100;$

Assume that the error bounds are set to be 1% for all the states of the original system for unit step inputs. Further assume that the error is defined as the ratio between the maximum absolute error value and the maximum absolute signal value.

All the inertia elements here have the same value, which is the most difficult situation to approximate; we will choose  $I5$  to be the dependent. To estimate the radius of the slow sub-system, omit  $I5$  and then calculate the eigenvalues of the original system. This will produce the following set of eigenvalues

-1.0000

-3.1331

-2.4334 - 9.4779i

-2.4334 + 9.4779i

-1.5000 - 9.8869i

-1.5000 + 9.8869i

The fastest pole in this set is (-3.1331). Therefore we will choose  $DPL=-31$ . Then we will use the fast sub-system model (equations (3.10) and (3.12)) to calculate the values of the parasitic parameters that are needed to obtain two critically damped fast poles at the chosen  $DPL$  (-31). This will result in the values

$$C = 5.2029e-005$$

$$R = 1240$$

Using these two values in the modified model, and subsequently calculating its eigenvalues produce the following set of eigenvalues for the modified system

$$-1.0000$$

$$-1.0037$$

$$-1.0920 - 7.5092i$$

$$-1.0920 + 7.5092i$$

$$-1.5000 - 9.8869i$$

$$-1.5000 + 9.8869i$$

$$-22.5286$$

$$-44.2837$$

It is obvious from this set that  $\text{Re}_f = -22.5286$ , and  $\rho_c = -1.5$ . Therefore,

$\frac{\text{Re}_f}{\rho_c} \approx 15$ , and we can proceed. Next we set  $DPL_1 = -31$  and  $j=1$ ; and simulate

the implicit original and the modified systems to calculate the errors. The errors calculated for the seven states of the original system are, in the order of the states, as follows:

	DPL=-31
e1	0.044539
e2	0.044539
e3	0.029023
e4	0.029023
e5	0.035824
e6	0.035824
e7	0.046535

Inspecting these errors show that some of them are larger than 1%. Therefore, there is a need to reduce the  $DPL$  used in the design. Since  $j$  is equal to one,  $DPL$  will be set to  $2 * DPL_1$ , which means that  $DPL_2 = -62$ . Using the new value for  $DPL$  in the fast sub-system model to calculate the values of the parasitic parameters produces

$$C = 1.3007e-005$$

$$R = 2480$$

Using these values of  $R$  and  $C$  in simulating the modified system, the obtained errors were as shown below

	DPL=-31	DPL=-62
e1	0.044539	0.012109
e2	0.044539	0.012109
e3	0.029023	0.007981
e4	0.029023	0.007981
e5	0.035824	0.009484
e6	0.035824	0.009484
e7	0.046535	0.01237

Again there are still some errors that are higher the set bounds. Therefore, there should be additional iterations as described in the design procedure. The results of all the iterations are summarized below.

	DPL=-31	DPL=-62	DPL=-64.2	DPL=-68.4
R	1240	2480	2568	2736
e1	0.044539	0.012109	0.011309	0.009988
e2	0.044539	0.012109	0.011309	0.009988
e3	0.029023	0.007981	0.007452	0.006579
e4	0.029023	0.007981	0.007452	0.006579
e5	0.035824	0.009484	0.008851	0.007818
e6	0.035824	0.009484	0.008851	0.007818
e7	0.046535	0.01237	0.011551	0.010199

MATLAB ode15s stiff integrator was used to simulate both the implicit and the modified systems. Simulation time for the original implicit system was 2.96 seconds and for the modified system whose errors satisfied the errors bounds was 3.63 seconds. One can notice that to double the value of DPL we needed to double the value of R. This is not a surprise because equation (3.14) shows that RC should be set equal to  $\frac{-2}{DPL}$  and it has also been shown that the product RRC converges to a constant as  $\epsilon$  gets small. It can be noticed also that the number of iterations that was needed to achieve the design objectives was not large.

## **CHAPTER 4**

### **ANALYSIS AND DESIGN OF A CLASS OF TWO-TIME-SCALE NONLINEAR MULTI-PORT MODELS**

#### **4.1 Introduction**

CHAPTER 2 and CHAPTER 3 demonstrated analysis and design of a class of two-time-scale linear systems. This chapter uses the results and insight obtained in CHAPTER 2 and CHAPTER 3 and further extends them to cover a class of nonlinear systems. Tools for analysis and design of a class of nonlinear systems are presented.

#### **4.2 Class of Nonlinear Systems Under Investigation**

The class of nonlinearity under investigation here is the displacement-modulated nonlinear junction structure. An example for this class of nonlinearity is a planar mechanism that has linear inertia field with displacement-modulated transformers. The general form of the homogeneous original system of this class of nonlinear systems is

$$\dot{X}_r = J_{rr}(X_r) * X_r + J_{ri}(X_r) * X_i \quad (4.1)$$

$$\dot{X}_i = J_{ir}(X_r) * X_r + J_{ii}(X_r) * X_i + J_{id}(X_r) * \dot{X}_d \quad (4.2)$$

$$Z_d = J_{di}(X_r) * X_i \quad (4.3)$$

$$Z_i = S_i X_i \quad (4.4)$$

$$X_d = S_d^{-1} Z_d \quad (4.5)$$



Where, the  $J$  matrices are the nonlinear constraints imposed by the junction structure;  $X_i$  is the independent energy variables vector in the coupled field;  $X_d$  is the dependent energy variables vector in the coupled field;  $Z_i$  and  $Z_d$  are the coenergy vectors for  $X_i$  and  $X_d$  respectively; and  $X_r$  is the state vector whose states are not among the coupled field and its dimension is  $r$ . As stated earlier, one way to recognize the elements of the coupled field is by the appearance of their parameters in  $J_{di}$ . The state vector of the corresponding modified explicit system is

$$X = \begin{bmatrix} X_r \\ X_i \\ X_d \\ q \end{bmatrix},$$

where  $q$  is the state of the inserted parasitic compliance. The explicit equations of the modified system will be in the general form

$$\dot{X}_r = J_{rr}(X_r) * X_r + J_{ri}(X_r) * X_i \quad (4.6)$$

$$\begin{aligned} \dot{X}_i = & J_{ir}(X_r) * X_r + J_{ii}(X_r) * S_i * X_i + \\ & J_{id}(X_r) * (R * (J_{di}(X_r) * S_i * X_i - S_d * X_d) + \frac{1}{C} q) \end{aligned} \quad (4.7)$$

$$\dot{X}_d = R * (J_{di}(X_r) * S_i * X_i - S_d * X_d) + \frac{1}{C} q \quad (4.8)$$

$$\dot{q} = J_{di}(X_r) * S_i * X_i - S_d * X_d \quad (4.9)$$

Where,  $C$  and  $R$  are the inserted parasitic compliance and resistance respectively. Throughout this chapter the junction matrices are functions of the

vector  $X_r$ ; however, sometimes this will not be written explicitly for the sake of clarity.

### 4.3 Obtaining the PSSPF

CHAPTER 2 showed how to use some general transformation procedure to obtain the PSSPF for the modified models of the class of linear systems that was under investigation. Kokotovic et al. (1986) gives some other general procedure to transform nonlinear systems to the standard singular perturbation form. This procedure is analogous to the above-mentioned procedure for linear systems. Therefore, the effort of applying the nonlinear procedure to get the PSSPF will directly benefit from the results and insight gained while discussing how to use the linear procedure. This section shows how to use the general procedure for nonlinear systems to obtain the PSSPF for the general modified nonlinear systems in the form (4.6) to (4.9). This procedure can be summarized as follows:

- 1) Put the system in the form

$$\varepsilon \dot{v} = h(v, \varepsilon), \quad v \in R^{n+m} \quad (4.10)$$

- 2) The fast variables are  $\eta = \Theta(v)$ , where  $\Theta(v)$  is the  $m$  independent equations that the  $n + m$  equations  $h(v, 0) = 0$  reduce to, knowing that

$$\text{rank } \frac{\partial \Theta}{\partial v} = m.$$

- 3) The slow variables are  $x = \sigma(v)$ . Find  $\sigma(v)$  from

$$\frac{\partial \sigma}{\partial \nu} h(\nu, 0) = 0 \quad (4.11)$$

The assumption is made that

$$\text{rank} \begin{bmatrix} \frac{\partial \sigma}{\partial \nu} \\ \frac{\partial \nu}{\partial \Theta} \\ \frac{\partial \nu}{\partial \nu} \end{bmatrix} = n + m \quad (4.12)$$

Next, this general procedure will be applied to the class of nonlinear modified systems expressed in equations (4.6) to (4.9). While doing so, the insight gained from CHAPTER 2 will be used.

We start by doing the scaling (change of variables)  $Rq$  for  $q$  in the equations (4.6) to (4.9); the usefulness of this scaling was demonstrated in CHAPTER 2. Doing this scaling produces

$$\dot{X}_r = J_{ri} * X_i + J_{rr} * X_r \quad (4.13)$$

$$\dot{X}_i = J_{ir} * X_r + J_{ii} * S_i * X_i + J_{id} * (R * (J_{di} * S_i * X_i - S_d * X_d) + \frac{R}{\alpha} Rq) \quad (4.14)$$

$$\dot{X}_d = R * (J_{di} * S_i * X_i - S_d * X_d) + \frac{R}{\alpha} Rq \quad (4.15)$$

$$R\dot{q} = RJ_{di} * S_i * X_i - RS_d * X_d \quad (4.16)$$

After this scaling the system is ready to be put in the form

$$\varepsilon \dot{\nu} = h(\nu, \varepsilon)$$

Based on what was demonstrated in CHAPTER 2, we will take  $\varepsilon = \frac{1}{R}$  and

$R^2 C = \alpha$ , where  $\alpha$  is a constant, which will produce the following equations:

$$\varepsilon \dot{X}_r = \varepsilon J_{ri} * X_i + \varepsilon J_{rr} * X_r \quad (4.17)$$

$$\varepsilon \dot{X}_i = \varepsilon J_{ir} * X_r + \varepsilon J_{ii} * S_i * X_i + J_{id} * ((J_{di} * S_i * X_i - S_d * X_d) + \frac{1}{\alpha} Rq) \quad (4.18)$$

$$\varepsilon \dot{X}_d = (J_{di} * S_i * X_i - S_d * X_d) + \frac{1}{\alpha} Rq \quad (4.19)$$

$$\varepsilon R\dot{q} = J_{di} * S_i * X_i - S_d * X_d \quad (4.20)$$

Following step two in the procedure above we obtain

$$h_r(v,0) = 0 \quad (4.21)$$

$$h_i(v,0) = J_{id} * ((J_{di} * S_i * X_i - S_d * X_d) + \frac{1}{\alpha} Rq) = 0 \quad (4.22)$$

$$h_d(v,0) = (J_{di} * S_i * X_i - S_d * X_d) + \frac{1}{\alpha} Rq = 0 \quad (4.23)$$

$$h_q(v,0) = J_{di} * S_i * X_i - S_d * X_d = 0 \quad (4.24)$$

Where  $h = \begin{bmatrix} h_r \\ h_i \\ h_d \\ h_q \end{bmatrix}$  and  $v = \begin{bmatrix} X_r \\ X_i \\ X_d \\ Rq \end{bmatrix}$ .

It is noticeable that either equation (4.22) or equation (4.23) is redundant.

Therefore,  $h(v,0) = 0$  reduces to two independent equations and the vector of the two fast variables  $\eta$  is:

$$\eta = \begin{bmatrix} J_{di}(X_r) * S_i * X_i - S_d * X_d \\ Rq \end{bmatrix} \quad (4.25)$$

The rank of  $\frac{\partial \eta}{\partial v}$  is the rank of

$$\begin{bmatrix} \frac{\partial J_{di} S_i X_i}{\partial X_r} & J_{di} S_i & -S_d & 0 \\ 0 & 0 & 0 & 1 \end{bmatrix},$$

which has the rank of

$$\begin{bmatrix} -S_d & 0 \\ 0 & 1 \end{bmatrix}.$$

This rank is two because  $S_d \neq 0$ . The slow variables vector is  $x = \sigma(v)$ , where

$$\sigma(v) \text{ can be found from equation (4.11). Assuming that } \sigma = \begin{bmatrix} \sigma_R \\ \sigma_I \end{bmatrix} = \begin{bmatrix} \sigma_1 \\ \cdot \\ \sigma_r \\ \sigma_{r+1} \\ \cdot \\ \sigma_{r+i} \end{bmatrix},$$

equation (4.11) can be written as

$$\begin{bmatrix} \frac{\partial \sigma_1}{\partial X_r} & \frac{\partial \sigma_1}{\partial X_i} & \frac{\partial \sigma_1}{\partial X_d} & \frac{\partial \sigma_1}{\partial Rq} \\ \cdot & \cdot & \cdot & \cdot \\ \cdot & \cdot & \cdot & \cdot \\ \frac{\partial \sigma_{r+i}}{\partial X_r} & \frac{\partial \sigma_{r+i}}{\partial X_i} & \frac{\partial \sigma_{r+i}}{\partial X_d} & \frac{\partial \sigma_{r+i}}{\partial Rq} \end{bmatrix} \begin{bmatrix} h_r(v,0) \\ h_i(v,0) \\ h_d(v,0) \\ h_q(v,0) \end{bmatrix} = 0.$$

Examining equations (4.21) to (4.24) shows that

$$h_r(v,0) = 0, \text{ and}$$

$$h_i(v,0) = J_{id} h_d(v,0)$$

Consequently, we can make the following choices

$$\frac{\partial \sigma_R}{\partial X_r} = I_r, \quad \frac{\partial \sigma_R}{\partial X_i} = 0, \quad \frac{\partial \sigma_R}{\partial X_d} = 0, \quad \frac{\partial \sigma_R}{\partial Rq} = 0,$$

$$\frac{\partial \sigma_l}{\partial X_r} = -\frac{\partial J_{id} X_d}{\partial X_r}, \quad \frac{\partial \sigma_l}{\partial X_i} = I_i, \quad \frac{\partial \sigma_l}{\partial X_d} = -J_{id}, \quad \frac{\partial \sigma_l}{\partial Rq} = 0.$$

Therefore, the slow variables vector can be written as

$$\sigma = \begin{bmatrix} X_r \\ X_i - J_{id}(X_r)X_d \end{bmatrix} \quad (4.26)$$

and

$$\frac{\partial \sigma}{\partial v} = \begin{bmatrix} I_r & 0 & 0 & 0 \\ -\frac{\partial J_{id} X_d}{\partial X_r} & I_i & -J_{id} & 0 \end{bmatrix} \quad (4.27)$$

has a rank of  $r + i$ .

#### 4.4. A Model for the Fast Sub-System and Proof of Stability

This section will define a model for the fast sub-systems for the class of nonlinear systems under investigation. To do that, the general form of the two fast variables that was obtained above will be used to derive a general form for the dynamics of the fast sub-system. The general form of the two fast variables was given in equation (4.25) as

$$\eta = \begin{bmatrix} \eta_1 \\ \eta_2 \end{bmatrix} = \begin{bmatrix} J_{di}(X_r) * S_i * X_i - S_d * X_d \\ Rq \end{bmatrix} \quad (4.25)$$

Therefore, we can obtain

$$\frac{d\eta_1}{dt} = \frac{dJ_{di}(X_r)}{dt} * S_i * X_i + J_{di}(X_r) * S_i * \dot{X}_i - S_d * \dot{X}_d \quad (4.28)$$

$$\frac{d\eta_2}{dt} = R\dot{q} \quad (4.29)$$

Using the general form of the modified system as given in equations (4.13) to (4.14) we can obtain

$$\begin{aligned} \frac{d\eta_1}{dt} = & f(X_r, X_i) + J_{di} S_i J_{id}^* (R^* (J_{di} S_i X_i - S_d X_d) + \frac{R}{\alpha} Rq) - \\ & S_d \left[ R^* (J_{di} S_i X_i - S_d X_d) + \frac{R}{\alpha} Rq \right] \end{aligned} \quad (4.30)$$

$$\frac{d\eta_2}{dt} = R J_{di} S_i X_i - R S_d X_d \quad (4.31)$$

Where,

$$f(X_r, X_i) = \frac{dJ_{di}}{dt} S_i X_i + J_{di} S_i^* (J_{ir} X_r + J_{ii} S_i X_i) \quad (4.32)$$

is, in general, a nonlinear function that does not include the parasitic parameter  $R$ . Notice that  $f(X_r, X_i)$  includes the term  $(\frac{dJ_{di}(X_r)}{dt} S_i X_i)$ , which is the part of the dynamics that results from the dependency of the junction structure on the state vector  $X_r$ . As  $\varepsilon$  gets small,  $R$  gets large and equation (4.30) can be approximated as

$$\begin{aligned} \frac{d\eta_1}{dt} = & J_{di} S_i J_{id}^* (R^* (J_{di} S_i X_i - S_d X_d) + \frac{R}{\alpha} Rq) - \\ & S_d \left[ R^* (J_{di} S_i X_i - S_d X_d) + \frac{R}{\alpha} Rq \right] \end{aligned} \quad (4.33)$$

The approximation given in equation (4.33) is an  $O(\varepsilon)$  approximation. It shows that the additional dynamics term  $(\frac{dJ_{di}(X_r)}{dt} S_i X_i)$  that results from the junction nonlinearity has a secondary effect that can be neglected for a small enough  $\varepsilon$ .

If the junction structure matrix  $J_{di}$  were a function of  $X_i$ , then its derivative with respect to time would have included  $\dot{X}_i$ . But, equation (4.14) shows that  $\dot{X}_i$  includes the parasitic parameter  $R$  as a factor for some of its terms. Therefore, if  $J_{di}$  were a function of  $X_i$  we would not have been able to neglect the term  $\frac{dJ_{di}}{dt} S_i X_i$  as an  $O(\varepsilon)$  approximation. Terms in equation (4.33) can be rearranged to write the equation as

$$\frac{d\eta_1}{dt} = -R^* (S_d + J_{id}^T S_i J_{id})^* (J_{di} S_i X_i - S_d X_d) - \frac{R}{\alpha} (S_d + J_{id}^T S_i J_{id}) R q \quad (4.34)$$

Equations (4.34) and (4.31) are the equations of the fast dynamics; they can be written as follows

$$\frac{d\eta_1}{dt} = \frac{-R}{I_{eq}} \eta_1 - \frac{R}{\alpha I_{eq}} \eta_2 \quad (4.35)$$

$$\frac{d\eta_2}{dt} = R \eta_1 \quad (4.36)$$

$$I_{eq} = \frac{1}{(S_d + J_{id}^T(X_r)^* S_i^* J_{id}(X_r))} \quad (4.37)$$

Equations (4.35) to (4.37) represent the fast sub-system model for a small enough  $\varepsilon$ .

Examining the fast sub-system model shown in equations (4.35) to (4.37) shows that the model is a function of the slow variable(s) ( $X_r$ ). Equation (4.26) shows that the variables of  $X_r$  are among the slow variables. Because of the



time-scale difference in a two-time-scale system, the slow variables will change only slightly during the dynamic behavior of the fast variables. Therefore, when solving for the fast variables that are dependent on the slow variables in a two-time-scale system, the slow variables are taken as constants at their initial conditions (Kokotovic et al. 1986). In fact, two-time-scale systems are solved by solving the fast sub-system as just described, and then solving the slow sub-system. This is true even for frequency excitation as long as the frequency of excitation is slower than the fast dynamics. Based on this understanding the equivalent inertia term  $I_{eq}$  in equation (4.37) needs to be evaluated only once at the initial conditions of the slow variables  $X_r$ . As a result, the fast sub-system model shown here is the same as the fast sub-system model (equations (3.10) and (3.11)) that was derived in CHAPTER 3 for the linear case, except that the matrix  $J_{id}$  here has to be evaluated at the initial conditions of  $X_r$ , instead of being totally independent of all variables.

$$\frac{1}{(S_d + J_{id}^T S_i J_{id})} \equiv I_{eq} \quad (3.10)$$

$$A_f = \begin{bmatrix} -\frac{R}{I_{eq}} & \frac{-R}{R^2 C I_{eq}} \\ R & 0 \end{bmatrix} \quad (3.11)$$

Consequently, the bond graph model and the physical interpretations of the fast sub-system for this class of nonlinear systems are the same as those for the linear systems studied in CHAPTER 2 and CHAPTER 3.

The only nonlinearity that appears in the fast sub-system model is in the term  $I_{eq}$  due the dependency of  $J_{id}$  on the slow variables  $X_r$ . Therefore, if the fast sub-system is stable as a linear system over the entire range of the values of  $I_{eq}$ , this proves that the fast sub-system is stable (Kokotovic et al. 1986). Consequently, if we prove that  $I_{eq}$  is always positive, this will prove that the second order fast sub-system, expressed in equations (4.35) to (4.37), is stable. As  $S_d$  and  $S_i$  are inverse inertia matrices,  $S_d$  must always be positive definite and  $J_{id}^T S_i J_{id}$  must always be positive semi definite. Consequently,  $I_{eq}$  is always positive and the fast sub-system is always stable for a small  $\varepsilon$ . If the fast sub-system is stable the entire two-time-scale system is stable if the slow (here the original) system is stable (Kokotovic et al. 1986). This proves that the entire modified system is stable for a small enough  $\varepsilon$  if the original system is stable.

#### 4.5 Effect of Inaccurate Effective Field Value on Model Performance

To use the fast sub-system model (4.35) to (4.37) to design the fast sub-system,  $I_{eq}$  has to be evaluated. As explained above,  $I_{eq}$  can be closely approximated by evaluating it at the initial conditions of  $X_r$ . This sub-section will investigate the effect of using an erroneous value for  $I_{eq}$  on the fast sub-system model performance. To investigate that, we will simulate Example 3 (the fluid pipe system) that was used in section 3.5. It is a linear system whose  $I_{eq}$  is a

known constant. We will use the linear fast sub-system model (3.12) to place the fast eigenvalues of the modified system of this example at certain locations while using some erroneous values for  $I_{eq}$ . The effect of different percentages of errors in the value used for  $I_{eq}$  on the model performance will be evaluated.

The same set of parameters that was used in section 3.5 is used here.

Tables 4.1 to 4.4 summarize the results of simulation carried out in this section. Every table presents simulation results for a different PR ratio. The PR ratio was defined previously as the ratio between the desired location of the two critically damped poles (DPL) that is used in calculations, and the fastest real part in the original system's poles. The first column in every table includes two labels (in the first two cells, they label their corresponding rows); the DPL value used in the whole table; and the eigenvalues of the original system. The two labels are  $\%I_{eq}$ , which refers to the percentage of the correct  $I_{eq}$  that is used; and Zeta-fast, which refers to the damping ratio of the two fast poles. Every column from the remaining columns in the tables shows, on its top, the percentage of the correct  $I_{eq}$  used in that column, the damping ratio of the two fast poles that are obtained from the modified model after using that percentage of  $I_{eq}$ , and the eigenvalues calculated from the modified system after using the percentage  $I_{eq}$  that is shown on the top of the column. When the two fast poles are complex conjugate, the real part is shown in one cell followed by the

imaginary part in the following cell. Notice that these situations (complex conjugate fast poles) will correspond to Zeta-fast (damping ratio of the two fast poles) that is less than one. It can be noticed from tables 4.1 to 4.4, that in all the presented cases, the original system's eigenvalues were affected only slightly (less than 5%). That is true over the entire range of the used  $\%I_{eq}$  (150% to 50%) and over the entire range of the used PR ratio (10 to 40). It can also be noticed that when the correct  $I_{eq}$  (100%  $I_{eq}$ ) is used, there are still some errors in the fast poles locations; these errors decrease as the ratio PR increases. Using an erroneous value for  $I_{eq}$  could increase or decrease this error; depending on whether this error in  $I_{eq}$  is going to counter affect or add to the approximation error of the model. The result will be obtaining fast poles that are (or one of them is, if they are over damped) slower than the desired fast poles location. Figure 4.1 shows the percentage error in the location of the slower of the two fast poles vs. the error in the value that is used for  $I_{eq}$ . When the two fast poles are under damped, their real part is used in the error calculations and the mark that identifies their location in Figure 4.1 has no background color. Figure 4.1 presents the four different cases for the PR ratio. It shows that in general equation, (3.10) slightly overestimates  $I_{eq}$ , and that its estimate improves as  $\epsilon$  gets small (means PR gets bigger). It can be noticed also, that in all cases for errors in  $I_{eq}$  within 50%, the additional errors in the pole location due to using the erroneous value for  $I_{eq}$  is always less than the percentage error

in the value that is used for  $I_{eq}$ . This suggests that if we are designing the fast sub-system to set the fast poles no slower than certain location and approximating the calculation of  $I_{eq}$ , we should increase the used PR ratio, than what we would use if we had accurate calculation for  $I_{eq}$ , with a percentage that is similar to the expected error in  $I_{eq}$ . Results shown here show that, in the worst case, when the inaccuracy in  $I_{eq}$  adds to the model approximation error, this can be counter affected by increasing the PR ratio; therefore, the price in the worst case will be slightly additional computational efforts compared to what would have been required if  $I_{eq}$  were known exactly.

$\% I_{eq}$	150%	140%	120%	100%	80%	60%	50%
Zeta-fast	1.340	1.303	1.225	1.142	1.054	0.959	0.910
DPL=-100	-270.626	-250.171	-208.902	-166.683	-121.432	-72.276	-62.212
DPL=-100	-54.275	-54.714	-55.944	-58.107	-63.271	21.3394i	28.3816i
-4.9	-4.906	-4.906	-4.907	-4.907	-4.908	-4.909	-4.910
-2.7	-2.695	-2.695	-2.695	-2.695	-2.695	-2.695	-2.695
-0.327	-0.328	-0.328	-0.328	-0.328	-0.328	-0.328	-0.328
-1	-0.963	-0.963	-0.963	-0.963	-0.963	-0.963	-0.963
-10	-10.208	-10.224	-10.263	-10.319	-10.405	-10.554	-10.680
-10	-10	-10	-10	-10	-10	-10	-10

Table 4.1. Effect of erroneous  $I_{eq}$  on model performance, PR=10

$\% I_{eq}$	150%	140%	120%	100%	80%	60%	50%
Zeta-fast	1.279	1.239	1.156	1.066	0.969	0.860	0.801
DPL=-200	<b>-507.341</b>	-465.297	-379.191	-286.273	-172.513	-132.498	<b>-112.487</b>
DPL=-200	<b>-117.725</b>	-119.766	-125.864	-138.770	44.32992i	78.54582i	84.09254i
-4.9	-4.905	-4.905	-4.905	-4.905	-4.905	-4.905	-4.906
-2.7	-2.695	-2.695	-2.695	-2.695	-2.695	-2.695	-2.695
-0.327	-0.328	-0.328	-0.328	-0.328	-0.328	-0.328	-0.328
-1	-0.963	-0.963	-0.963	-0.963	-0.963	-0.963	-0.963
-10	-10.045	-10.048	-10.056	-10.068	-10.085	-10.113	-10.137
-10	-10	-10	-10	-10	-10	-10	-10

Table 4.2. Effect of erroneous  $I_{eq}$  on model performance, PR=20

$\% I_{eq}$	150%	140%	120%	100%	80%	60%	50%
Zeta-fast	1.260	1.220	1.135	1.043	0.943	0.831	0.768
DPL=-300	-743.992	-680.252	-548.759	-401.678	-252.537	-192.531	-162.526
DPL=-300	-181.100	-184.839	-196.328	-223.405	89.22632i	129.1044i	135.356i
-4.9	-4.904	-4.904	-4.905	-4.905	-4.905	-4.905	-4.905
-2.7	-2.695	-2.695	-2.695	-2.695	-2.695	-2.695	-2.695
-0.327	-0.328	-0.328	-0.328	-0.328	-0.328	-0.328	-0.328
-1	-0.963	-0.963	-0.963	-0.963	-0.963	-0.963	-0.963
-10	-10.019	-10.021	-10.024	-10.029	-10.036	-10.048	-10.058
-10	-10	-10	-10	-10	-10	-10	-10

Table 4.3. Effect of erroneous  $I_{eq}$  on model performance, PR=30

$\% I_{eq}$	150%	140%	120%	100%	80%	60%	50%
Zeta-fast	1.251	1.210	1.125	1.032	0.930	0.816	0.753
DPL=-400	-980.621	-895.152	-718.077	-514.793	-332.546	-252.542	-212.540
DPL=-400	-244.479	-249.948	-267.021	-310.302	130.9763i	178.7838i	185.925i
-4.9	-4.904	-4.904	-4.904	-4.904	-4.904	-4.905	-4.905
-2.7	-2.695	-2.695	-2.695	-2.695	-2.695	-2.695	-2.695
-0.327	-0.328	-0.328	-0.328	-0.328	-0.328	-0.328	-0.328
-1	-0.963	-0.963	-0.963	-0.963	-0.963	-0.963	-0.963
-10	-10.011	-10.011	-10.013	-10.016	-10.020	-10.026	-10.032
-10	-10	-10	-10	-10	-10	-10	-10

Table 4.4. Effect of erroneous  $I_{eq}$  on model performance, PR=40

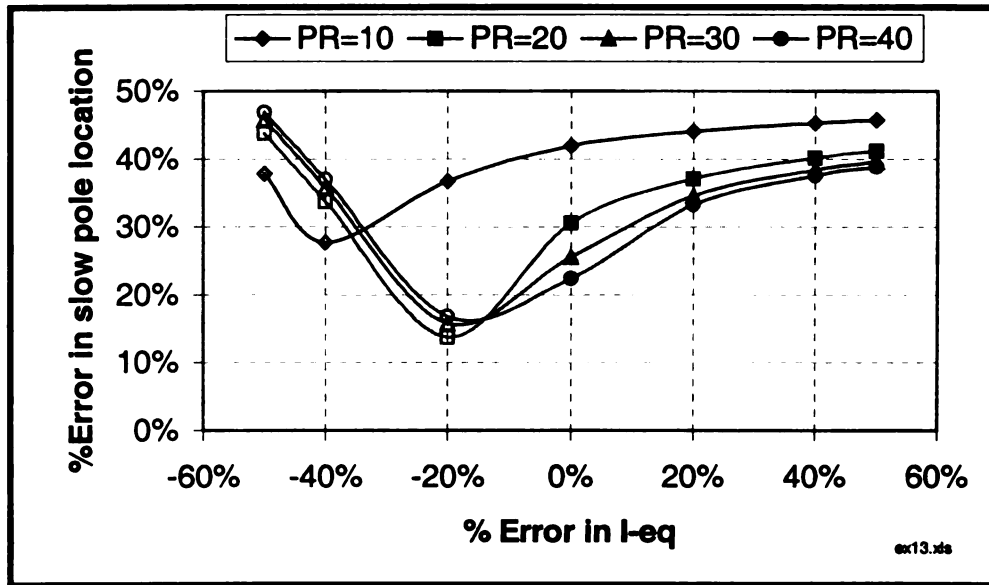


Figure 4.1. Effect of errors in I-eq on fast poles location errors

#### 4.6 Design Procedure for the Fast Sub-System

This section gives a procedure for designing a fast sub-system, from the class of nonlinear systems under investigation, to achieve simulation efficiency while meeting certain accuracy bounds. As discussed earlier, the computational efforts needed to simulate the modified system increases as its stiffness increases. The design procedure presented here are very similar to those presented in CHAPTER 3 except that we linearize the original and the modified systems to estimate the linearized systems eigenvalues. The linearization is done by evaluating the junction structure matrices at the initial conditions. As explained earlier, the slow variables change only slightly during the dynamic

behavior of the fast variables. Therefore, for fast sub-system design it would be sufficient to evaluate its slow-variables-dependent parameters at the initial conditions of these slow variables.

Assume that there is an original system whose modified system is required to be accurate to within certain specified bound for some specific inputs. Assume that the accuracy bounds are specified for all the states whose accuracy are of concern to the user. The design procedure can be stated as follows:

- 1) Set  $j=0$ , where  $j$  is a counter. Linearize the original system around its initial conditions by evaluating the junction matrices at the initial conditions of  $X_r$ . Choose the smallest inertia as the dependent inertia. If you can calculate the eigenvalues of the linearized system do so. If you cannot due to some cumbersome algebra, omit the smallest inertia and then calculate the eigenvalues for the linearized approximated system. Consequently, one can determine an estimate of the spectral radius of the linearized original system's eigenvalues; let us refer to it as  $\rho_i$ .
- 2) Choose the two fast poles of the linearized modified system to be critically damped; and choose a desired pole location for the two critically damped fast poles ( $DPL$ ) such that

$$DPL = 10 * \rho_i.$$

- 3) Use the fast sub-system model (equations (4.35) to (4.37)) to calculate the values of the parasitic parameters  $R$  and  $C$  needed to place the two fast poles at  $DPL$ .



- 4) Set  $j=j+1$ , and  $DPL_j = DPL$ .
- 5) Simulate the modified nonlinear system and the original nonlinear system and calculate the errors of the states for which the user requires bounds on their errors. Calculate the ratios between the calculated errors and the user-specified error bounds; assume that these ratios are  $r_1, r_2, \dots, r_n$ . Find  $r_{\max}$  such that  $r_{\max, j} = \max \{r_1, r_2, \dots, r_n\}$ . Assume that the error whose ratio is  $r_{\max}$  is "e" and that its corresponding desired error is  $e_d$ .
- 6) If  $0.8 \leq r_{\max} \leq 1$ , go to step eight.

Otherwise;

if  $j>1$ , calculate

$$\beta = \frac{e_j - e_{j-1}}{DPL_j - DPL_{j-1}},$$

$$DPL_{j+1} = DPL_j + \frac{e_d - e_j}{\beta}.$$

This assumes that the error is a linear function of the DPL.

If  $j=1$ , take

$$DPL = \frac{DPL_j}{fac}. \text{ Where } fac = 2, \text{ if } r_{\max} > 1, \text{ and } fac = 0.5 \text{ if } r_{\max} < 0.8$$

- 7) Go to step three.
- 8) End of design procedure.

If the user prefers to deal only with the modified system, the same method described in CHAPTER 3 can be used to find an "accuracy reference."

## 4.7 An Example

The slider crank mechanism shown in Figure 4.2 is taken from Rosenberg et al. (1983). It has a nonlinear junction structure manifested in its nonlinear modulated transformer ( $m$ ). The equations of the original system of the slider crank mechanism can be written as

$$\frac{d\theta}{dt} = \frac{p_\theta}{J} \quad (4.38)$$

$$\frac{dp_\theta}{dt} = T - m \left( R_1 m \frac{p_\theta}{J} + \frac{dp_x}{dt} \right) \quad (4.39)$$

$$\frac{p_x}{M} = m \frac{p_\theta}{J} \quad (4.40)$$

This means that

$$J_{id} = -m, \quad X_r = \theta, \quad X_i = p_\theta, \quad X_d = p_x \quad (4.41)$$

The transformer modulus  $m$  is function of  $\theta$  and can be calculated as follows

$$\begin{aligned} \frac{dx}{dt} &= \frac{dx}{d\theta} \frac{d\theta}{dt} = m \frac{d\theta}{dt}, & m &= \frac{dx}{d\theta} \\ x(\theta) &= r \cos \theta + \sqrt{l^2 - r^2 \sin^2 \theta} \\ m &= -r \sin \theta - r^2 \frac{\sin \theta \cos \theta}{\sqrt{l^2 - r^2 \sin^2 \theta}} \end{aligned} \quad (4.42)$$

Where  $\theta$  is the crank angle,  $M$  is the cylinder mass,  $J$  is the crank inertia,  $l$  is the length of the massless rod, and  $r$  is the radius of the crank. A bond graph

model for the modified system is shown in Figure 4.3; the modified model of this example can be written as

$$\frac{d\theta}{dt} = \frac{p_\theta}{J} \quad (4.43)$$

$$\frac{dp_\theta}{dt} = -m^2 \frac{(R_1 + R)}{J} p_\theta + m \frac{R}{M} p_x - m \frac{1}{C} q \quad (4.44)$$

$$\frac{dp_x}{dt} = m \frac{R}{J} p_\theta - \frac{R}{M} p_x + \frac{1}{C} q \quad (4.45)$$

$$\frac{dq}{dt} = m \frac{1}{J} p_\theta - \frac{1}{M} p_x \quad (4.46)$$

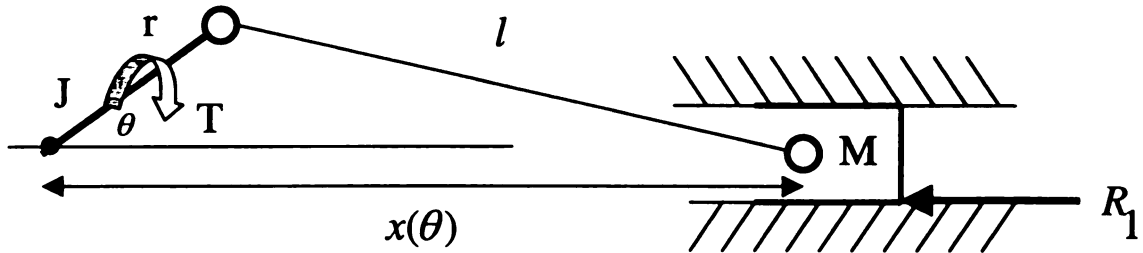


Figure 4.2 (a) Schematic diagram for the slider crank mechanism

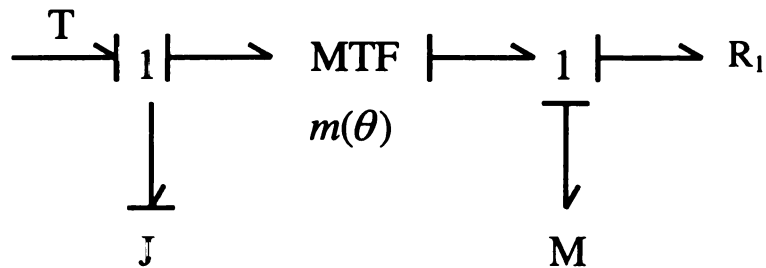


Figure 4.2 (b) Bond graph model for the slider crank mechanism

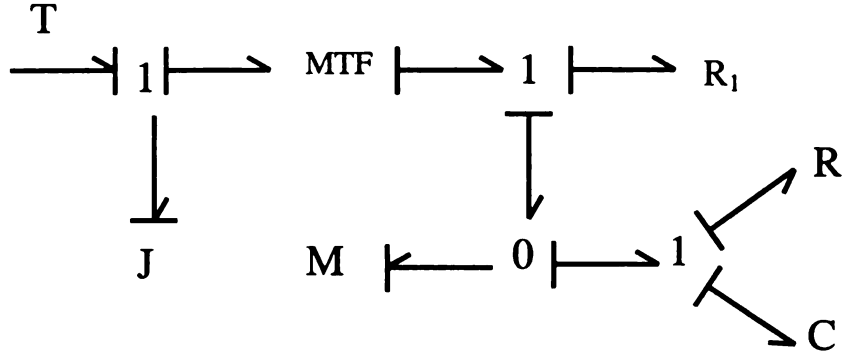


Figure 4.3. Bond graph model of the modified slider crank mechanism

First we put the modified model in the PSSPF. To do that, start by changing  $q$  to  $Rq$  and then follow the above-outlined procedure. Changing  $q$  to  $Rq$  produces

$$\frac{d\theta}{dt} = \frac{p_\theta}{J} \quad (4.47)$$

$$\frac{dp_\theta}{dt} = -m^2 \frac{(R_1 + R)}{J} p_\theta + m \frac{R}{M} p_x - m \frac{R}{\alpha} Rq \quad (4.48)$$

$$\frac{dp_x}{dt} = m \frac{R}{J} p_\theta - \frac{R}{M} p_x + \frac{R}{\alpha} Rq \quad (4.49)$$

$$\frac{dRq}{dt} = m \frac{R}{J} p_\theta - \frac{R}{M} p_x \quad (4.50)$$

1) Put the system in the form  $\varepsilon \dot{v} = h(v, \varepsilon)$

$$\varepsilon \frac{d\theta}{dt} = \varepsilon \frac{p_\theta}{J} = h_1$$

$$\varepsilon \frac{dp_\theta}{dt} = -m^2 \frac{(\varepsilon R_1 + 1)}{J} p_\theta + m \frac{1}{M} p_x - m \frac{1}{\alpha} Rq = h_2$$

$$\varepsilon \frac{dp_x}{dt} = m \frac{1}{J} p_\theta - \frac{1}{M} p_x + \frac{1}{\alpha} Rq = h_3$$

$$\varepsilon \frac{dRq}{dt} = m \frac{1}{J} p_\theta - \frac{1}{M} p_x = h_4$$

$$h = \begin{bmatrix} h_1 \\ h_2 \\ h_3 \\ h_4 \end{bmatrix}$$

$$v = \begin{bmatrix} \theta \\ p_\theta \\ p_x \\ Rq \end{bmatrix}$$

$$2) h(v, 0) = 0 \Rightarrow$$

$$-m^2 \frac{1}{J} p_\theta + m \frac{1}{M} p_x - m \frac{1}{\alpha} Rq = 0$$

$$m \frac{1}{J} p_\theta - \frac{1}{M} p_x + \frac{1}{\alpha} Rq = 0$$

$$m \frac{1}{J} p_\theta - \frac{1}{M} p_x = 0$$

This means that

$$m \frac{1}{J} p_\theta - \frac{1}{M} p_x = 0$$

$$Rq = 0$$

and the fast variables are

$$\eta = \begin{bmatrix} m \frac{1}{J} p_\theta - \frac{1}{M} p_x \\ Rq \end{bmatrix} \quad (4.51)$$

$$\frac{\partial \eta}{\partial \nu} = \begin{bmatrix} \frac{p_\theta}{J} \frac{\partial m}{\partial \theta} & \frac{m}{J} & \frac{-1}{M} & 0 \\ 0 & 0 & 0 & 1 \end{bmatrix}, \text{ has rank two.}$$

3) Find the slow variables  $x = \sigma(\nu)$ ,  $\frac{\partial \sigma}{\partial \nu} h(\nu, 0) = 0$

$$\begin{bmatrix} \frac{\partial \sigma_1}{\partial \theta} & \frac{\partial \sigma_1}{\partial p_\theta} & \frac{\partial \sigma_1}{\partial p_x} & \frac{\partial \sigma_1}{\partial Rq} \\ \frac{\partial \sigma_2}{\partial \theta} & \frac{\partial \sigma_2}{\partial p_\theta} & \frac{\partial \sigma_2}{\partial p_x} & \frac{\partial \sigma_2}{\partial Rq} \end{bmatrix} h(\nu, 0) = 0, \text{ leads to}$$

$$\frac{\partial \sigma_1}{\partial \theta} h_1(\nu, 0) + \frac{\partial \sigma_1}{\partial p_\theta} h_2(\nu, 0) + \frac{\partial \sigma_1}{\partial p_x} h_3(\nu, 0) + \frac{\partial \sigma_1}{\partial Rq} h_4(\nu, 0) = 0$$

$$\frac{\partial \sigma_2}{\partial \theta} h_1(\nu, 0) + \frac{\partial \sigma_2}{\partial p_\theta} h_2(\nu, 0) + \frac{\partial \sigma_2}{\partial p_x} h_3(\nu, 0) + \frac{\partial \sigma_2}{\partial Rq} h_4(\nu, 0) = 0$$

To obtain the slow variables vector

$$\sigma = \begin{bmatrix} \theta \\ p_\theta + m p_x \end{bmatrix}, \quad (4.52)$$

make the following selections

$$\frac{\partial \sigma_1}{\partial \theta} = 1, \quad \frac{\partial \sigma_1}{\partial p_\theta} = 0, \quad \frac{\partial \sigma_1}{\partial p_x} = 0, \quad \frac{\partial \sigma_1}{\partial Rq} = 0$$

$$\frac{\partial \sigma_2}{\partial \theta} = \frac{\partial m}{\partial \theta} p_x, \quad \frac{\partial \sigma_2}{\partial p_\theta} = 1, \quad \frac{\partial \sigma_2}{\partial p_x} = m, \quad \frac{\partial \sigma_2}{\partial Rq} = 0$$

Consequently,

$$\frac{\partial \sigma}{\partial \nu} = \begin{bmatrix} 1 & 0 & 0 & 0 \\ \frac{\partial m}{\partial \theta} p_x & 1 & m & 0 \end{bmatrix}, \text{ has rank two.}$$

Assume that the example has the following set of parameters

$$J=2, \quad M=10, \quad R1=100, \quad \theta(t=0) = \frac{\pi}{4}$$

$$r=0.2, \quad l=3*r$$

Where, all units are SI units. Further assume that the rest of the initial conditions are zeros and that, the input torque is

$$T = 2, t \leq 2; T = 0 \text{ otherwise.}$$

Assume that error bounds are specified for both the speeds that are coupled in the inertia fields in the original system; and whose coupling is broken in the modified system by inserting the parasitic elements. Those two speeds are the angular velocity and the piston velocity. Assume that the errors are specified such that the ratio between the maximum absolute value of error and the maximum absolute value of the signal should be less than or equal to 1%. We will call the error in angular velocity  $e_1$ , and the error of piston velocity  $e_2$ .

The value of the transformer modulus at time zero is

$$m\left(\frac{\pi}{4}\right) = 0.17577$$

This is the value that will be used for the fast sub-system design. Substituting this value in the original model and calculating the eigenvalues of the associated linearized model shows that the fastest calculated eigenvalue is about -1.34. Therefore we will start our design iterations by choosing  $DPL=-13.4$ . Using this value to design the fast sub-system in the linearized modified model, gives the following values for the parasitic parameters

$$R = 232.14 \quad C = 6.4295e-004$$

Using these two values in the linearized modified model gives the following eigenvalues for the linearized modified model

$$-15.2594$$

$$-11.7448$$

$$-1.3406$$

Proceeding to step five in the algorithm to simulate the modified and the original systems (both nonlinear) and calculate the errors, we find that

$$e1 = 0.0090$$

$$e2 = 0.0457$$

As the  $e2$  is still larger than the desired bound (0.01) and  $j=1$ , we will take DPL equal to twice its current value and go to step three. The results of this iteration and the rest of the iterations are summarized in table 4.5.

DPL	-13.4	-26.8	-36.9	-48.4	-60.3
R	232.1401	464.2801	639.25	838.47	1044.6
e1	0.009	0.007	0.0067	0.0066	.0065
e 2	0.0457	0.0234	0.0164	0.0129	.010

Table 4.5. Summary of results of design procedure

It is noticeable that the algorithm converges quickly. It can also be realized that  $e2$ , which is the error in the speed of the dependent inertia is larger than that of the independent inertia and also more responsive and consistent to changes in  $\varepsilon$ . Analysis presented in this work did not investigate this issue. Figure 4.4 and Figure 4.5 compare simulation results of both the original and the modified



systems resulting from the previous design. Comparisons are shown for the two velocities that were coupled in the original system and whose coupling was broken in the modified system. The modified system is seen to follow the original system closely. It is interesting also that simulation time for the original implicit system was 5.49 seconds while it was 2.86 seconds for the modified stiff system with the parasitic parameters values corresponding to  $DPL=-60.3$ ; same integrator (MATLAB ode15s) was used in both cases. This indicates that following the design procedure prescribed here can lead to computational savings even as compared with the effort required for the original implicit system.

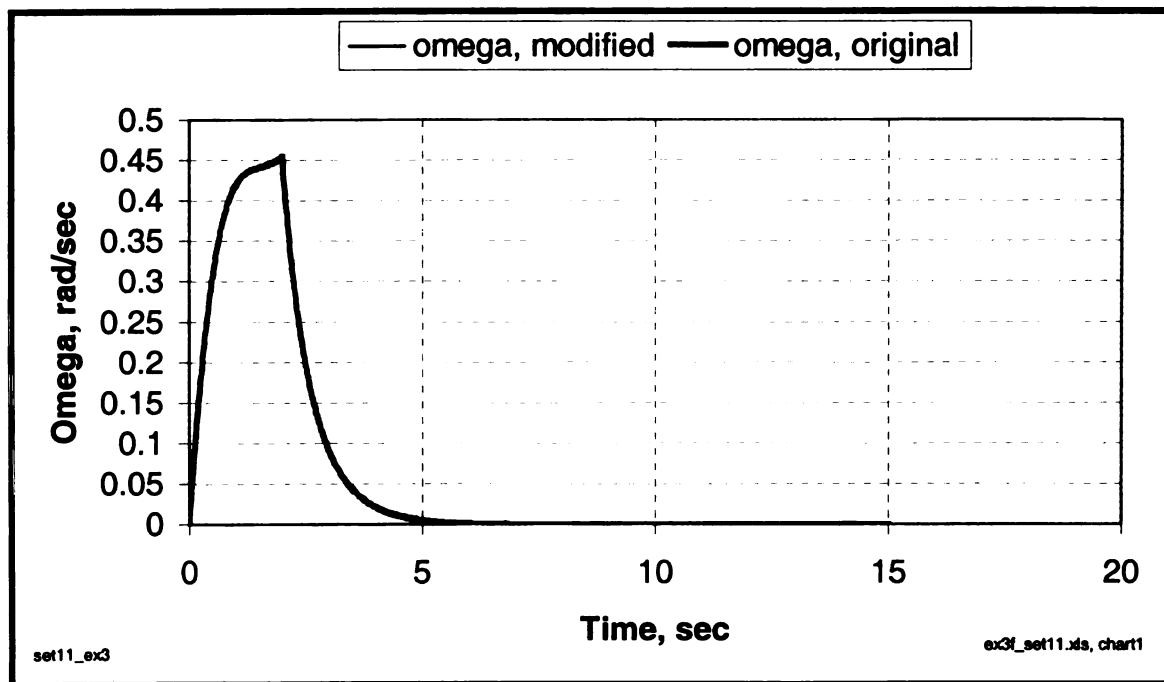


Figure 4.4. Comparing omega from the original and modified systems

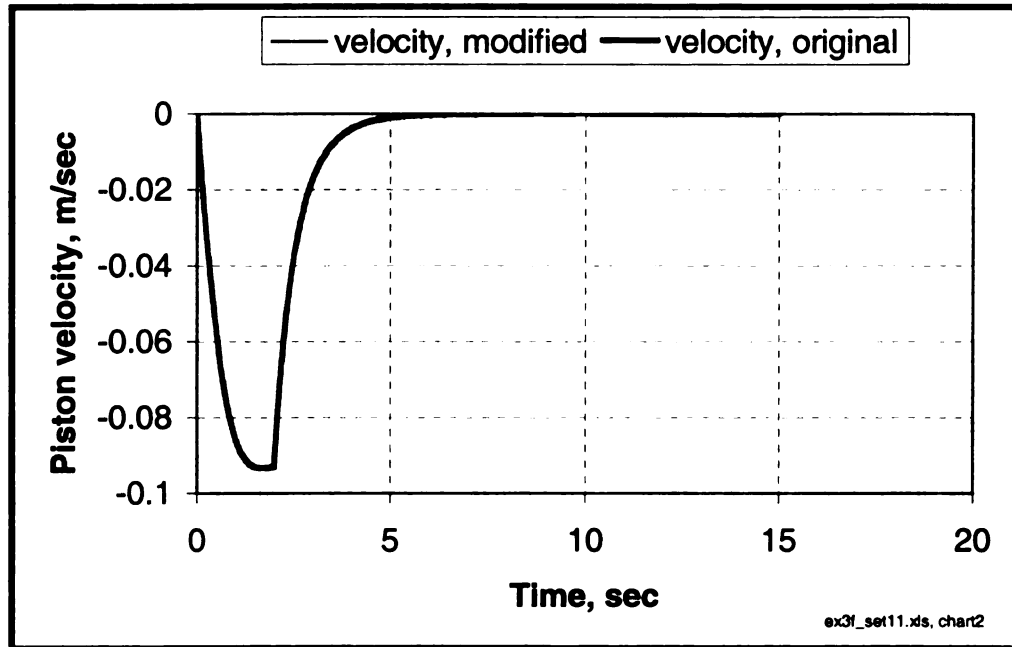


Figure 4.5. Comparing velocities from the original and modified systems

## **CHAPTER 5 CONCLUSIONS**

### **5.1 Summary of Main Contributions**

This research work had two main objectives:

- 1) Analyze the class of two-time-scale modified systems that results from using parasitic elements in a specified structure to eliminate derivative causality. The purpose of this analysis is to better understand the important two-time-scale properties of that class of two-time-scale systems.
- 2) Formalize the above-mentioned approach of using parasitic elements to eliminate derivative causality in a design context. The purpose of this formalization was to enable the user to achieve the greatest possible simulation efficiency for specified approximation accuracy, by making the appropriate choices for the values of the parasitic element parameters.

These two main objectives have been met. Analysis shown in this document revealed some important aspects of the time-scale properties of the modified problem under investigation, which greatly improved our understanding of the systems under investigation. The design procedure presented in this document serves to meet the second objective.

Several contributions have been made toward achieving these objectives.

The following gives a brief description and comments on these contributions:

- 1) Determining the choices of  $\varepsilon$  and variables scaling ( $\varepsilon = \frac{1}{R}$ ,  $R^2C$  is constant, and  $Rq$  for  $q$ ) that help formulate the modified systems in the standard singular perturbation form and reveal its time-scale properties.
- 2) Formulating the modified system in a physically meaningful standard singular perturbation form (PSSPF). The states of this PSSPF are related directly to the states of the original system and other physically meaningful quantities that are of particular interest in the study of these systems. Using the general procedures outlined in Kokotovic et al. (1986) could lead to a standard singular perturbation form whose state variables are not physically meaningful and not of special interest. Methods to systematically obtain this PSSPF were shown for classes of both linear and nonlinear systems.
- 3) Showing that the modified system can be divided into two distinct sub-systems and that each sub-system can have its own model. This is an enabler for any analysis and design work on the modified system, and offers great insight into it.
- 4) Showing that the fast sub-system can be closely approximated by an R-L-C model.
- 5) Showing that as  $\varepsilon$  gets small the only parameters from the original system that continue to affect the fast sub-system are the parameters of the coupled field; all other effects from the original system diminish.
- 6) Showing that the transient of the error introduced into the algebraic equation can be directly designed, which is a significant improvement on

what was known of taking  $R$  “very big” and  $C$  “very small” to obtain fast parasitic dynamics in prior published work.

- 7) Giving procedures to design the fast subsystem to achieve certain required accuracy at a highly efficient computational price. The design procedures used the results obtained from the analysis work. The key part of the procedures is the use of the fast sub-system model. In the case of linear models it was shown that the user could also place the fast poles as desired. It was suggested that the designer should target the two fast poles to be critically damped to provide for efficient computation. Examples of using the design procedures were given. These examples show that the proposed design procedures can effectively and efficiently select the appropriate values for the parasitic parameters, so that the modified system is just stiff enough to meet the accuracy bounds. They also showed that the typical number of iterations is small.

The results of these research efforts make the method of derivative causality elimination that was under investigation more understandable, more tractable, and much more rigorous as an option for eliminating the derivative causality. In addition they bring a new set of tools and a very useful mind-set for attacking certain classes of problems.

## **5.2 Suggested Directions for Future Research**

Research results that were presented herein point to some directions of further research efforts. This section briefly describes two such research directions.

### **5.2.1 More than One Dependent Storage Element**

Research efforts presented in this document addressed directly the case in which there is one dependent energy-storing element in the coupled field. However, there are situations in which there is more than one energy-storing element in a coupled field. In these situations, if the modified system is designed to be two-time-scale, then there will be couplings between the different parasitic fast dynamics. This observation is made based on some preliminary work done by the author. The nature, the effect, and the chances of manipulating and/or approximating these couplings are to be evaluated. Another possible solution to this case would be to design a multi-time-scale system. The number of time-scales would be equal to the number of the dependent energy storing elements plus one, for the original system. The process could be a successive design process in which the designer starts with the fastest time- scale sub-system and then does the second fastest sub-system, and so on. This solution might raise computational-efficiency-related concerns, especially as the number of time

scales increases. The proof of stability of the fast sub-systems also must be addressed.

### **5.2.2 Analysis and Design for Eliminating Algebraic Loops**

It was indicated in CHAPTER 1 that the presence of an algebraic coupling in a resistance field could also lead to an implicit set of differential equations. Algebraic loops could also occur in the junction structure. As explained earlier it is often desirable to obtain an explicit set of ODEs. One way to break these algebraic loops is to insert parasitic dynamic elements. As a result some parasitic dynamics occurs. It seems that this parasitic dynamics would share some similar aspects with the parasitic dynamics that was dealt with in the problem that was under investigation in these research efforts. Consequently, it is recommended to examine the possibility of treating this problem with the same techniques that were used in the derivative storage element.

## REFERENCES



## REFERENCES

Allen, R. R., "Dynamics of Mechanisms and Machine Systems in Accelerating Reference Frames," *Journal of Dynamic Systems, Measurement, and Control*, Vol. 103, pp. 395-403, Dec. 1981.

Auslander, D., Kempf, C., *Mechatronics Mechanical Systems Interface*, Prentice Hall, 1996.

Bennett, B.S., *Simulation Fundamentals*, Prentice Hall, 1995.

Borutzky, W., Cellier, F. E., "Tearing Algebraic Loops in Bond Graphs," *Trans. of SCS*, 13(2), 1996a, pp.102-115.

Borutzky, W., Cellier, F. E., "Tearing in Bond Graphs with Dependent Storage Elements," *Proc. CESA 96 IMACS Multiconference*, Lille, France, July 9-12, 1996b, pp. 1113-1119.

Bos, A., Tiernego, M., "Formula Manipulation in the Bond Graph Modeling and Simulation of Large Mechanical Systems," *Journal of The Franklin Institute*, Vol. 319, No. ½, pp. 51-65, February 1985.

Cellier, F. E., "Hierarchical Non-Linear Bond Graphs: A Unified Methodology for Modeling Complex Physical Systems," *Simulation*, Vol. 58, No. 4, pp. 230-248, April 1992.

Cellier, F. E., "Bond Graphs: The Right Choice for Educating Students in Modeling Continuous Physical Systems," *Simulation*, Vol. 64, No. 3, pp. 154-159, March, 1995.

Cellier, F. E., *Continuous System Modeling*, Springer-Verlag, 1991.

Chang, D. C., and Rohde, S.M., "The Role of Synthesis, Analysis, and Simulation in Engineering a Complex System: the Automotive Vehicle," *International Congress of Mechanical Engineers*, 1996, Atlanta.

Dauphin-Tanguy, G., and Borne, P., "Order Reduction of Multi-Time Scale Systems Using Bond Graphs, the Reciprocal System and the Singular Perturbation Method," J. Franklin Inst., Vol. 319, No. 1/2, pp. 157-171, 1985.

Edstrom, K., "Generating State Space Equations from A Bond Graph with Derivative Causality Using Singular Perturbation Theory," ICBGM, pp. 105-109, 1999.

Gordon, B., Liu, S., "A Singular Perturbation Approach for Modeling Differential-Algebraic Systems," ASME Journal of Dynamic systems, Measurement, and Control, Vol. 120, 1998, pp. 541-545

Granda, J., "Bond Graph Modeling Solutions of Algebraic Loops and Differential Causality in Mechanical and Electrical Systems," Proc. Applied Simulation and Modeling, IASTED Conference, SF,CA,1984, pp.183-193.

Joseph, B. J., Martens, H. R., "The Method of Relaxed Causality in The Bond Graph Analysis of Nonlinear Systems," Journal of Dynamic Systems, Measurements, and Control, March 1974, pp. 95-99.

Karnopp, D and Margolis, D., "Analysis and Simulation of Planar Mechanism Systems Using Bond Graphs," Journal of Mechanical Design, Vol. 101, April 1979, pp.187-191.

Karnopp, D. C., Margolis, D. L., Rosenberg, R. C., *System Dynamics: Modeling and Simulation of Mechatronic Systems*, John Wiley & Sons, 2000.

Karnopp, D., "Alternative Bond Graph Causal Patterns and Equation Formulations for Dynamic Systems," Transactions of the ASME, Vol. 105, June 1983, pp. 58-63.

Karnopp, D., "An Approach to Derivative Causality in Bond Graph Models of Mechanical Systems," J. Franklin Institute 329 (1), 1992, pp. 65-75.

Karnopp, D.C., "Lagrange's Equations for Complex Systems," Trans. ASME, J. Dynamic Systems, Measurement, and Control, December 1977, pp. 300-306.

Karnopp, D.C., "Power-Conserving Transformations: Physical Interpretations and Applications using Bond Graphs," J. Franklin Institute 288 (3), Sep. 1969, pp. 175-201.

Karnopp, D.C., "The Energetic Structure of Multibody Dynamic Systems," J. Franklin Institute, V. 306, No. 2, 1978, pp. 165-181.

Khalil, Hassan K., *Nonlinear Systems*, New York MacMillan 1992.

Kokotovic, V., Khalil, Hassan K., O'Malley, R. E., *Singular Perturbation Methods in Control. Analysis and Design*, Academic Press, London, 1986.

Kokotovic, V., O'Malley, R. E., Sannuti, P., "Singular Perturbation and Order Reduction in Control Theory- An Overview," Automatica, Vol. 12, pp. 123-132, 1976.

Margolis, D., "Bond Graph Causality and the Derivation of Analytical Transfer Functions," ICBGM, 1993.

Ogata, K., *Modern Control Engineering*, Prentice Hall, 1990.

Paynter, H. M., 1961, *Analysis and Design of Engineering Systems*, MIT Press, Cambridge, MA.

R. C. Rosenberg, "Exploiting Bond Graph Causality in Physical System Models," *ASME Journal of Dynamic Systems, Measurements, and Control*, Vol. 109, pp. 378-383, 1987.

Rosenberg, R. C., "State Space Formulation for Bond Graph Models of Multiport Systems," *Transactions ASME Journal Dynamic Systems, Measurements and Control*, Vol. 93 Series G, March 1971, pp. 35-40.

Rosenberg, R. C., *The Enport Reference Manual*. 1987, Rosencode Associates Inc., Lansing, MI.

Rosenberg, R.C. and D. C. Karnopp, *Introduction to Physical System Dynamics*, McGraw-Hill Book Co., Inc., New York, 1983.

Rosenberg, R.C. and J. McCalla, "Power to the User in Formulating Model Equations," ASME 1991, DSC-Vol. 34, Automated Modeling.

Rosenberg, R.C., "Exploiting Bond Graph Causality in Physical System Models," ASME Journal of Dynamic Systems, Measurements, and Control, Vol. 109, pp. 378-383, 1987.

Rosenberg, R.C., and Andry, A.N., Jr., "Solvability of Bond Graph Junction Structures with Loops," IEEE Trans. Circuits Syst., Vol. CAS-26, No. 2, pp. 130-137, 1979.

Rosenberg, R.C., and Zhou, T., "Power-Based Model Insight," Proceedings of the 1988 ASME Winter Annual Meeting, Symposium on Automated Modeling for Design, pp. 61-67.

Stein, Jeffrey L., Yih-Tun Tseng, "Strategies for Automating the Modeling Process," Proceedings of the 1991 ASME Winter Annual Meeting, Symposium on *Automated Modeling*, pp. 69-87.

Sueur, C., "Bond Graph Approach to Multi-time Scale Systems Analysis," J. Franklin Inst., Vol. 329, No. 5/6, pp. 1005-1026, 1991.

Sueur, C., and Dauphin-Tanguy, G., "Bond-graph Approach for Structural Analysis of MIMO Linear Systems," J. Franklin Inst., Vol. 328, No. 1, pp. 55-70, 1991.

Sueur, C., and Dauphin-Tanguy, G., "Structural Controllability/Observability of Linear Systems Represented by Bond Graphs," J. Franklin Inst., Vol. 326, No. 6, pp. 869-883, 1989.

Tomkinson, D., and Horne, J., *Mechatronics Engineering*, McGraw-Hill Book Co., Inc., New York, 1996.

Van Dijk, Johannes, *On the Role of Bond Graph Causality in Modeling Mechatronic Systems*, Ph. D. dissertation, University of Twente, Netherlands, 1994.

Zeid, A, "An Algorithm for Eliminating Derivative Causality," Proc. ASME Winter Annual Meeting, Vol. 8, Automated Modeling for Design, 1988, pp. 15-21.

Zeid, A. And Rosenberg, R., "Eigenvalue Spectra and Bounds for Certain Classes of Dynamic Systems Having Tree Bond Graphs," IEEE Transactions on Circuits and Systems, Vol. 33, No. 12, Dec. 1986, pp. 1232-1240.

MICHIGAN STATE UNIVERSITY LIBRARIES



3 1293 02088 0922